Aus der

Medizinischen Klinik und Poliklinik III

Klinikum der Ludwig-Maximilians-Universität München

With a little help from a friend:

Enhancing immunotherapy in acute myeloid leukemia

Dissertation

zum Erwerb des Doctor of Philosophy (Ph.D.)

an der Medizinischen Fakultät der

Ludwig-Maximilians-Universität zu München

vorgelegt von:

Anetta Paulina Marcinek

aus:

Vilshofen, Deutschland

Jahr:

2023

Mit Genehmigung der Medizinischen Fakultät der

Ludwig-Maximilians-Universität zu München

Erstes Gutachten:	Prof. Dr. Marion Subklewe
Zweites Gutachten:	Prof. Dr. Karsten Spiekermann
Drittes Gutachten:	Prof. Dr. Max Schnurr
Viertes Gutachten:	Prof. Dr. Carole Bourquin

Dekan: Prof. Dr. med. Thomas Gudermann

Tag der mündlichen Prüfung: 21.12.2023

Affidavit

Affidavit

Marcinek, Anetta
Surname, first name

Feodor-Lynen-Strasse 25
Street

81377 München, Germany
Zip code, town, country

I hereby declare, that the submitted thesis entitled:

With a little help from a friend:

Enhancing immunotherapy in acute myeloid leukemia

is my own work. I have only used the sources indicated and have not made unauthorised use of services of a third party. Where the work of others has been quoted or reproduced, the source is always given.

I further declare that the submitted thesis or parts thereof have not been presented as part of an examination degree to any other university.

München, 09.01.2024 — Anetta Marcinek

place, date — Signature doctoral candidate

Confirmation of congruency

LMU LUDWIG-MAXIMILIANS-UNIVERSITÄT MÜNCHEN

Promotionsbüro Medizinische Fakultät

MMRS

Confirmation of congruency between printed and electronic version of the doctoral thesis

Marcinek, Anetta

Surname, first name

Feodor-Lynen-Strasse 25

Street

81377 München, Germany

Zip code, town, country

I hereby declare, that the submitted thesis entitled:

With a little help from a friend:

Enhancing immunotherapy in acute myeloid leukemia

is congruent with the printed version both in content and format.

München, 09.01.2024

place, date

Anetta Marcinek

Signature doctoral candidate

Table of content

List of abbreviations

ADC	Antibody-drug conjugate
ADCC	Antibody-dependent cellular cytotoxicity
ADCP	Antibody-dependent phagocytosis
Allo-HSCT	Allogeneic hematopoietic stem cell transplantation
AML	Acute myeloid leukemia
BiTE	Bispecific T-cell engager
CAR	Chimeric antigen receptor
CiTE	Checkpoint inhibitory T-cell engaging
CPI	Checkpoint inhibition
CR	Complete remission
CRi	Complete remission with incomplete hematologic recovery
FL	Follicular lymphoma
FLT-3	Fms like tyrosine kinase 3
GO	Gemtuzumab ozogamicin
GvHD	Graft versus host disease
GvL	Graft versus leukemia
HD	Healthy donor
HMA	Hypomethylating agents
IC	Induction chemotherapy
IMiD	Immunmodulatory imide drug
LAA	Leukemia-associated antigen
LIC	Leukemia-initiating cells
LRA	Lineage-restricted antigen
LSA	Leukemia-specific antigen
LSC	Leukemic stem cell
MM	Multiple myeloma
moAB	Monoclonal antibody

NK	Natural killer
OS	Overall survival
PD-L1	Programmed-cell-death ligand-1
r/r	Relapsed/refractory
scFv	Single chain variable fragment
TA	Target antigen
TCR	T-cell receptor
TME	Tumor microenvironment
TRAE	Treatment-related adverse events
Treg	Regulatory T cell
WT-1	Wilm’s tumor 1

List of publications

This thesis includes two publications that have been accepted for publication in peer-reviewed journals. The contribution to each paper is stated under 1.4.1 and 1.4.2:

"CD33 BiTE® molecule-mediated immune synapse formation and subsequent T-cell activation is determined by the expression profile of activating and inhibitory checkpoint molecules on AML cells"

Anetta Marcinek, Bettina Brauchle, Lisa Rohrbacher, Gerulf Hänel, Nora Philipp, Florian Märkl, Thaddäus Strzalkowski, Sonja M. Lacher, Dragica Udiljak, Karsten Spiekermann, Sebastian Theurich, Sebastian Kobold, Roman Kischel, John R. James, Veit L. Bücklein, Marion Subklewe

Cancer Immunol Immunother (2023); *https://doi.org/10.1007/s00262-023-03439-x*

"SIRPα-αCD123 fusion antibodies targeting CD123 in conjunction with CD47 blockade enhance the clearance of AML-initiating cells"

Siret Tahk, Binje Vick, Björn Hiller, Saskia Schmitt, **Anetta Marcinek**, Enrico D. Perini, Alexandra Leutbecher, Christian Augsberger, Anna Reischer, Benjamin Tast, Andreas Humpe, Irmela Jeremias, Marion Subklewe, Nadja C. Fenn and Karl-Peter Hopfner

J Hematol Oncol (2021) 14:155; https://doi.org/10.1186/s13045-021-01163-6

Further I have contributed to the following publications, which have been accepted in peer-reviewed journals and are not part of this thesis:

"WT1 and DNMT3A play essential roles in the growth of certain patient AML cells in mice"

Maryam Ghalandary, Yuqiao Gao, Diana Amend, Ginte Kutkaite, Binje Vick, Karsten Spiekermann, Maja Rothenberg-Thurley, Klaus H. Metzeler, **Anetta Marcinek**, Marion Subklewe, Michael P. Menden, Vindi Jurinovic, Ehsan Bahrami, Irmela Jeremias

Blood (2023) 141 (8): 955–960. https://doi.org/10.1182/blood.2022016411

“T-cell exhaustion induced by continuous bispecific molecule exposure is ameliorated by treatment-free intervals”

Nora Philipp, Maryam Kazerani, Alyssa Nicholls, Binje Vick, Jan Wulf, Tobias Straub, Michaela Scheurer, Amelie Muth, Gerulf Hänel, Daniel Nixdorf, Monika Sponheimer, Malte Ohlmeyer, Sonja M Lacher, Bettina Brauchle, **Anetta Marcinek**, Lisa Rohrbacher, Alexandra Leutbecher, Kai Rejeski, Oliver Weigert, Michael von Bergwelt-Baildon, Sebastian Theurich, Roman Kischel, Irmela Jeremias, Veit L Bücklein, Marion Subklewe

Blood, 2022 Jul 25:blood.2022015956. https://doi.orgi/10.1182/blood.2022015956

“Bifunctional PD-1 × αCD3 × αCD33 fusion protein reverses adaptive immune escape in acute myeloid leukemia”

Monika Herrmann, Christina Krupka, Katrin Deiser, Bettina Brauchle, **Anetta Marcinek**, Ana Ogrinc Wagner, Felicitas Rataj, Ralph Mocikat, Klaus H. Metzeler, Karsten Spiekermann, Sebastian Kobold, Nadja C. Fenn, Karl-Peter Hopfner, Marion Subklewe

Blood (2018) 132 (23): 2484–2494. https://doi.org/10.1182/blood-2018-05-849802

1. Introductory summary

1.1 Acute myeloid leukemia

Acute myeloid leukemia (AML) is the most common acute leukemia in the adult population. It is characterized by the high proliferation of undifferentiated hematopoietic cells, which primarily populate the bone marrow leading to a displacement of the normal hematopoiesis. Consequently, patients may present with anemia, neutropenia, and thrombocytopenia. For decades, induction chemotherapy (IC), consisting of continuous infusion of cytarabine (7 days) and short time infusion of daunorubicin or idarubicin (3 days) ("7+3" scheme) has been the golden standard in the treatment of AML [1].

Based on the advances in genomic diagnostics, deeper insights into the molecular pathogenesis of the disease were gained, and targeted treatment options have evolved. Accordingly, nowadays the choice of induction therapy is integrating the genetic markers of the AML cells. Therefore, the combination of the development of targeted therapies and a better understanding of the impact of mutations on the survival and treatment of AML patients has reshaped the landscape of therapeutic options [2, 3]. In patients harboring a mutation in the fms like tyrosine kinase 3 (FLT-3) gene prolonged overall survival (OS) has been observed, when protein kinase inhibitors like Midostaurin, Quizartinib, or Sorafenib were combined with standard chemotherapy. For non-adverse AML patients, the antibody-drug conjugate gemtuzumab ozogamicin (GO) has been approved by the FDA in 2017 and by the EMA in 2018 and is now available as a combination therapy in addition to 7+3 [3–5].

Long-term remission rates of around 35 to 50 % are achieved in younger and fit patients with a favorable genetic risk profile. However, most patients with AML present with a median age of 68 years, a variable number of comorbidities, and, importantly, an unfavorable genetic risk profile. In this subgroup, the cure rate is below 15 % and most of the patients are not suitable for IC or allogeneic hematopoietic stem cell transplantation (allo-HSCT) [2, 6, 7]. In the past, mainly low-dose cytarabine or hypomethylating agents (HMAs) like azacytidine and decitabine were available as less-intensive therapy options. However, these monotherapies are not curative, and the median survival did not reach more than 10 months [8, 9]. Recently, the combinatorial therapy of azacytidine and venetoclax has shown to be well-tolerated, to induce high complete response rates (73 % vs. 10-50 %) and prolonged OS with up to 17 months, now being the standard medical care for this subgroup[10, 11].

Albeit great importance has been placed on the improvement of IC regimens for newly diagnosed AML patients to reduce the leukemic burden and to achieve complete remission (CR), relapse rates remain high due to surviving chemo-resistant cells. In case of relapse, treatment options are rather limited and allo-HSCT has proven to be the dominant curative option for relapsed patients, harnessing the potential of T cells to induce a graft-versus-leukemia (GvL) effect. However, this approach is only applicable in < 10% of patients and the success of allo-HSCT is hampered by infectious complications and treatment-related adverse events (TRAE) including graft-versus-host disease (GvHD) [12, 13]. Therefore, effective post-remission therapies and novel treatment options for chemorefractory patients are of high medical need, either as a stand-alone therapy or a bridge to transplant.

1.2 Antibody-based immunotherapy in AML

Empowered by the success of immunotherapies in solid cancers, innovative immunotherapeutic strategies have also been developed in the field of hematological malignancies. These approaches mainly rely on the immune system's effector cells to induce antileukemic activity and research led to a broad spectrum of available tools ranging from dendritic cell vaccination and adoptive cell therapy to antibody therapy. Furthermore, the availability of a suitable target antigen as well as its recognition by effector cells is crucial for the success of immunotherapies. The ideal target antigen (TA) that is exclusively expressed on the cancerous cells while being absent on healthy tissue, has not been found yet in AML. However, several lineage-restricted antigens (LRAs) as well as leukemia-associated and -specific antigens (LAAs and LSAs) have been identified (Figure 1), which are being investigated in clinical trials utilizing several immunotherapeutic platforms [14–16].

1.2.1 Target antigens in AML

Target antigens that are mainly expressed on the cell surface of leukemic blasts and that share the expression with cells from the myeloid lineage are so called lineage-restricted antigens (LRA). As surface antigens, they are practical targets for antibody-based approaches or chimeric antigen receptor (CAR) T-cells. However, due to the expression of LRAs on HSCs, targeted therapies could potentially lead to aplasia and on-target off-tumor toxicities. Unlike to B-cell malignancies, in which the eradication of healthy $CD19^+$ and $CD20^+$ can be well-managed, LRAs in AML like CD33, CD123, CLL-1, or FLT-3 do not meet these favorable criteria. Nonetheless, targeting combined antigen pairings

seem to be a promising attempt in reducing on-target off-tumor toxicities and increasing selectivity [17, 18].

An alternative approach is to target LAAs, which are also overexpressed in leukemic blasts compared to healthy tissue, but the expression is either comparably low or tissue-specific. In AML surface expressed LAAs like MUC1, CD44v6, and CD174 are mainly studied in CAR-T trials [19–23]. However, LAAs are frequently expressed intracellularly, requiring the ability to be presented within the HLA complex [24]. Therefore, intracellular target antigens like hTERT, survivin, and PRAME are potentially attractive to be the subject of vaccination strategies, like dendritic cell or peptide vaccines [25, 26]. Interestingly, novel bispecific developments also enable targeting intracellular target antigens presented in the context of defined HLA molecules. The first of this kind has recently been approved in the setting of advanced uveal melanoma (tebentafusp) [27]. In the context of AML, early phase I trials are currently evaluating an HLA-A2/WT-1 targeting T-cell bispecific based on encouraging preclinical investigations [28].

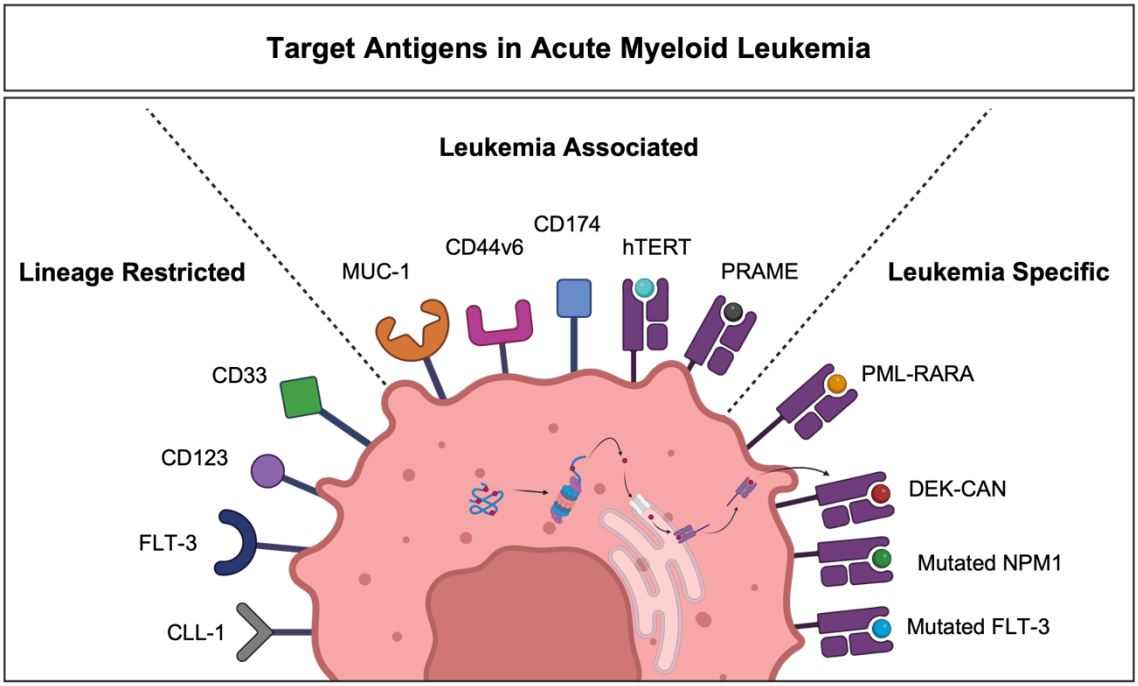

Figure 1: Target antigens in acute myeloid leukemia. Figure modified from [29]. Created with BioRender.com

In contrast to LRAs and LAAs, the properties of LSAs nearly fit the requirements for an ideal target as the expression is uniquely linked to the leukemic compartment. LSAs arise from leukemia-specific mutations or protein fusions caused by leukemia-specific chromosomal translocations, which need to be presented within the HLA complex as peptide fragments [14, 16]. Although the mutational burden in AML is known to be low compared to other cancers, immunogenic mutations that could serve as “neoantigens” have been identified. Mutated NPM1 and FLT-3 were able to induce T-cell responses *in*

vitro and *ex vivo.* For PML-RARA and DEK-CAN no spontaneous immune responses could be observed, likely due to a lack of presentation on the cell surface [30–32]. Clinical evaluation of LSA-targeted therapy is yet to be conducted.

1.2.2 Monoclonal antibodies

Unconjugated monoclonal antibodies

A straightforward approach to target an antigen is the use of monoclonal antibodies (moAB). In that way, effector cells can be recruited by the FC domain of the antibody and mediate immune effector mechanisms like antibody-dependent cellular cytotoxicity (ADCC) or antibody-dependent phagocytosis (ADCP) [33]. The first of its kind was the CD20-targeting antibody Rituximab, which has become the standard of care in the treatment of non-Hodgkin lymphoma and follicular lymphoma [34, 35]. For now, clinical trials investigating moABs as monotherapy or in combination with chemotherapy or HMAs have been conducted. However, translation to AML is challenging and trials with mABs targeting, for example, CD33 (Lintuzumab; NCT00006045) [36, 37], CD123 (Talacotuzumab; NCT02992860 and NCT02472145) [38, 39] and FLT-3 (LY3012218; NCT00887926) [40] had to be terminated due to lack of efficacy. The unconjugated moAB cusatuzumab directed against CD70 has shown promising results in the dose-escalation phase I study in combination with azacytidine achieving CR and CR with incomplete hematologic recovery (CRi) rates of 83 %. Though, in the phase II study, with more patients included, CR/CRi rate dropped to around 50 % [41–43].

Another promising candidate is the CD47-directed moAB magrolimab. The blockade of the “don’t eat me” signal induces phagocytosis mediated by macrophages, which together with azacytidine and venetoclax could be further enhanced [44–46]. The synergistic elimination of leukemic blasts with encouraging overall response rates (65 %; CR/CRi of 56 %), especially in TP53 mutated patients (CR/CRi in 67 %) led to the initiation of a phase III trial [47, 48].

Conjugated monoclonal antibodies

Although unconjugated moABs often show high preclinical efficacy *in vitro* against AML cell lines and primary cells as well as in *in vivo* mouse models, clinical translation often lacks benefit. A further approach to make use of moAB after engagement to the target antigen, is the delivery of radioisotopes or toxins to the tumor site, therefore, enabling the killing of the tumor by internalization of the antibody-drug conjugate (ADC). The only approved immunotherapy in AML is the ADC gemtuzumab ozogamicin (GO) [5, 49]. The humanized CD33-targeting antibody is conjugated with calicheamicin and has gotten its first FDA approval in 2000. However, it was withdrawn voluntarily due to safety concerns

and lack of verification to be beneficial for the selected patient population of elderly, who have relapsed. After re-evaluating the dosing regimen, it regained approval in 2017 for the treatment of newly diagnosed AML [50]. Furthermore, it is now available for relapsed/refractory (r/r) pediatric patients [51]. The success of GO encouraged further clinical trials with ADCs directed against CD33, CD123, and FLT-3, for example (NCT02674763, NCT04086264, NCT02864290) [52, 53].

1.2.3 T-cell redirecting bispecific antibodies

The potency of moABs is predominately mediated by phagocytic or natural killer (NK) cells. However, the GvL effect after allo-HSCT has demonstrated that T cells also harbor a great anti-leukemic potential [12]. Given the fact, that only a minority of patients is eligible for allo-HSCT, strategies have been investigated to specifically redirect T cells to the tumor site, while minimizing undesired toxicity against healthy tissue.

According to their name, T-cell redirecting bispecific antibodies, are built up of two paratopes, which are directed against a TA and (a part of) the T-cell receptor (TCR) bridging the effector and the tumor cell to build an immunological synapse independent of TCR-specificity (Figure 2). With the development of blinatumomab, a CD19xCD3 bispecific T-cell engaging (BiTE) molecule, the concept of T-cell redirection has been demonstrated to be successful in hematological malignancies [54]. It is the first FDA-approved T-cell redirecting bispecific antibody and is now available for the treatment of r/r and minimal residual disease-positive B-cell precursor acute lymphoblastic leukemia [55–58]. Since then, the idea of T-cell redirection has been translated into other bispecific antibody formats and malignancies. Consequently, more clinical trials have followed and led to the approval of mosunetuzumab in the setting of r/r B-cell lymphoma, teclistamab in multiple myeloma, and tebentafusp for the treatment of uveal melanoma [27, 59, 60]. Still, no immunotherapy of this kind has been approved in AML and the translation remains challenging, mainly accounted for the absence of an appropriate target antigen. However, preclinical studies and results from early clinical trials indicate that T-cell redirecting bispecific antibodies could be a promising immunotherapeutic treatment strategy in AML.

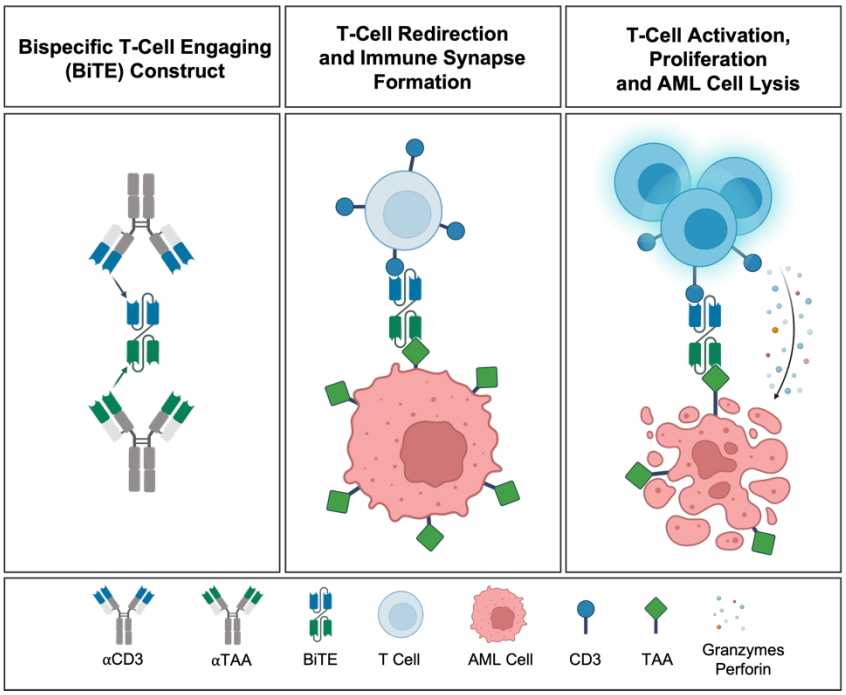

Figure 2: Mechanisms of action of a bispecific T-cell engaging (BiTE) molecule against a tumor-associated antigen (TAA). Figure modified from [61]. Created with BioRender.com

Based on the success of GO, a CD33 targeting BiTE molecule, AMG 330, has been developed [62]. Equivalent to blinatumomab, AMG 330 is comprised of two single-chain variable fragments (scFv) of conventional antibodies connected by a linker resulting in a recombinant protein of around 55 kDa. Consequently, it has a relatively short serum half-life of only a few hours, necessitating a continuous intravenous infusion for the patients. Therefore, a half-life extended version (AMG 673) has been developed by fusing an FC domain to AMG 330 making the infusion schedule more compliant for patients [63]. AMG 330 has shown high efficacy against primary AML samples *ex vivo* and promising preclinical studies led to the initiation of phase I clinical trials with both, AMG 330 and AMG 673, for the treatment of r/r AML patients [62–65]. During dose-escalation, 17 % of patients achieved CR/CRi with the minimal efficacious dose of ≥120 µg/day for AMG 330. AMG 673 treatment was able to induce CRi in one out of 27 evaluable patients. Although, both constructs showed antileukemic activity and had acceptable safety profiles with manageable TRAEs like cytokine release syndrome (CRS; around 65 %; ≥ grade 3 in around 15 % for both constructs), nausea (20 % for AMG 330) and elevated liver tests (25 % for AMG 330; 32 % for AMG 673), both trials were terminated based on company's prioritization decision. Further CD33 targeting T-cell redirecting bispecific antibodies including JNJ-67571244 (NCT03915379) and AMV564 (NCT03144245) are currently being evaluated for r/r AML patients in clinical trials and study updates are awaited [66–68].

Another prominent LRA in AML is CD123, which is not only over-expressed on AML blast but also on leukemic stem cells (LSCs) [69]. Additionally, high expression is associated with a poor prognosis making it an attractive target antigen [70–72]. Among other clinically investigated CD123 targeting bispecific antibodies, flotetuzumab, a dual-affinity retargeting (DART) antibody has shown potent antileukemic activity, safety, and tolerability, especially in primary induction failure and early relapse patients [73]. Further T-cell redirecting bispecific antibodies that are under preclinical or early clinical investigation target common AML-associated antigens like CLL-1, FLT-3, and WT-1 [28, 74–76].

1.3 Resistance mechanisms to immunotherapy

A deeper understanding of the interaction of the immune system and AML blasts is crucial for the development of novel immunotherapeutic strategies. It has been progressively demonstrated that the changes in the tumor microenvironment (TME) shape the hematopoietic niche, leading to immune evasion, disease adaption, and progression [14, 77].

1.3.1 Immune evasion

The recognition of AML blasts for immune cells plays a pivotal role in combating the leukemic burden with immunotherapeutic strategies. In patients relapsing after allo-HSCT, it has been observed that HLA class II genes were epigenetically downregulated and genomic loss of HLA occurred, circumventing T-cell recognition by lack of antigen presentation [78–80]. Furthermore, AML blasts demonstrate immune editing properties by secretion of soluble factors, which promote the development of cellular components of an immune suppressive TME and alter T-cell and NK-cell immune responses [81]. The secretion of extracellular vesicles, that contain the oncoprotein MUC1, by AML blasts is known to be a driver of myeloid-derived suppressor cell expansion [82–85]. In addition, the differentiation of monocytes into tumor-associated macrophages of the M2 type can be promoted by the secretion of certain enzymes like arginase II [86, 87]. Other soluble factors secreted by AML blasts namely TGF-β, IDO1, and IL-10 negatively impact T-cell functions like proliferation and are known to induce T-cell apoptosis [88]. Furthermore, enrichment of immunosuppressive regulatory T cells (Treg) has been linked to the altered cytokine milieu within the bone marrow niche and patients with a high frequency of Tregs tend to have a poorer prognosis [89–91].

Besides the secretion of soluble factors and the concomitant alteration of the TME, the expression of inhibitory ligands on AML blasts contribute to immune evasion leading to

T-cell and NK-cell dysfunction. One of the most prominent inhibitory ligands in AML is the programmed-cell-death ligand-1 (PD-L1). Upregulation of PD-L1 was observed in patients treated with HMAs and is linked to a lower OS. Further, PD-L1 upregulation was observed on AML blasts in patients relapsing after allo-HSCT emphasizing the PD-1/PD-L1 axis as an immune escape mechanism [92–94]. The interaction of PD-L1 on the leukemic blasts with its corresponding receptor PD-1 on T cells serves as an inhibitory signal and hampers T-cell activation. A higher frequency of PD-1$^+$ effector T cells was observed for AML patients compared to healthy controls suggesting a dysfunctional T-cell state in AML patients [95, 96]. In addition, gene-expression profiling of AML patients' T cells demonstrated an altered phenotype linked to an impaired actin cytoskeleton and defective immune synapse formation, consequently [97].

Further, the co-expression of PD-1 with other inhibitory receptors is associated with T-cell dysfunctionality like T-cell exhaustion and senescence. In AML, co-expression with TIM-3 and/or LAG-3 was connected to poor response to IC and a lower likelihood of senescent-like T-cells responding to BiTE molecule stimulation *in vitro* [98, 99]. Other T-cell and NK-cell inhibitory pathways that contribute to immune evasion in AML are the galectin-9/TIM-3, CD155/TIGIT, CD112/TIGIT, and the NKG2D/(s)NKG2DL axes [77].

The advancements in the field of spatially-resolved immunohistochemistry, mass spectrometry, and transcriptomics have contributed to more detailed insights into immune evasion in AML, therefore, conceiving novel possibilities to interfere with immunotherapeutic strategies. Checkpoint blockade has already entered daily clinical practice in solid tumors with the approval of checkpoint inhibitors (CPIs) against PD-1 (nivolumab, pembrolizumab), PD-L1 (atezolizumab, avelumab, durvalumab), CTLA-4 (ipilimumab) or LAG-3 (relatlimab). However, the clinical benefit as monotherapy or in conjunction with HMA appears to be limited, and possibly, CPIs are of greater benefit when combined with other immunotherapy approaches, like bispecific antibodies or CAR-T cells.

1.3.2 Targeting checkpoint molecules with novel antibody formats

T-cell redirecting strategies are accompanied by the release of inflammatory cytokines, leading to the upregulation of PD-L1 on AML blasts. *Ex vivo* evaluation of AMG 330 combined with PD-1/PD-L1 blockade showed enhanced cytotoxic potential of T cells against primary AML cells [100]. However, the clinical evaluation of AMG 330 in combination with pembrolizumab was terminated after phase I (NCT04478695).

One major hurdle in the clinical application of PD-1 and PD-L1 blocking antibodies is the occurrence of TRAEs like hepatitis, skin disorders, or myocarditis. To reduce TRAEs and

benefit from the properties of a BiTE at the same time, Hermann et al developed a bifunctional checkpoint inhibitory T-cell engaging (CiTE) antibody [101]. The CiTE is composed of two scFvs directed against CD33 with high-affinity binding properties and CD3ε within the TCR complex. Furthermore, the extracellular domain of PD-1 ($PD\text{-}1_{ex}$) with low binding affinities to PD-L1 has been fused to the antibody construct (Figure 3). The combination of high-affinity αCD33 and low-affinity αPD-L1 mediated high and selective cytolytic properties of T cells *in vitro* against $CD33^{+}PD\text{-}L1^{+}$ cell lines and *ex vivo* against AML cells. *In vivo* the CiTE antibody had a safe toxicity profile with no TRAEs and induced eradication of the leukemic burden in a xenograft mouse model, making it a promising candidate for early clinical studies.

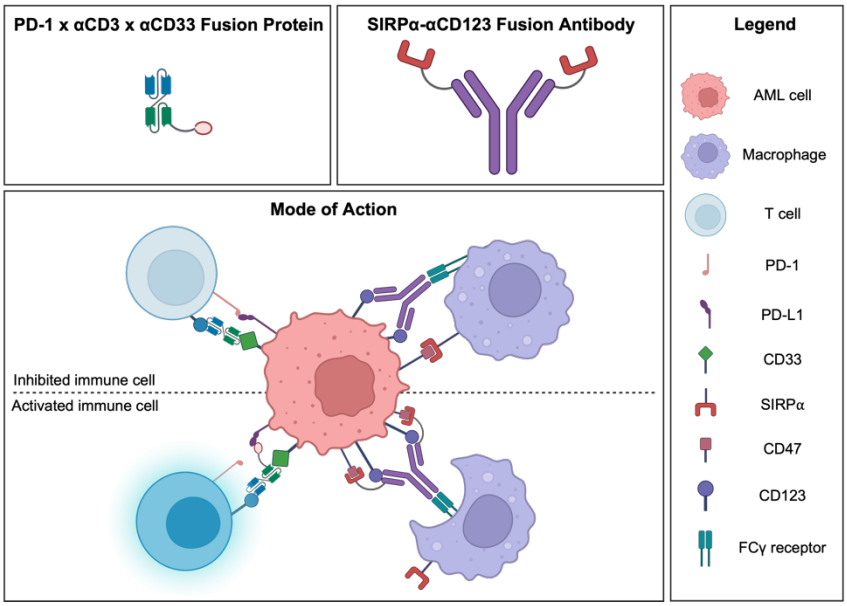

Figure 3: Mode of action of novel antibody formats targeting checkpoint molecules on AML cells. Figure modified from [101, 102]. Created with BioRender.com.

Another novel antibody format combining checkpoint molecule blockade with targeted NK-cell and macrophage-mediated lysis of AML cells has been developed by Tahk et. al [102]. In this approach, a conventional αCD123 IgG1 antibody has served as a backbone to which either one or two SIRPα domains were fused. Due to the low affinity binding properties of the SIRPα domains to CD47, the fusion antibody preferentially binds to $CD123^{+}CD47^{+}$ double-positive cells, while sparing healthy tissue ($CD123^{-}CD47^{+}$). Therefore, AML blasts and LSCs were selectively targeted enabling phagocytosis by blocking the “don’t eat me signal” CD47. Furthermore, the fusion antibody redirected NK-cell mediated cytotoxicity against cell lines *in vitro* and *ex vivo* against primary AML blasts. *In vivo* Tahk et. al could show, that NSG mice, who received patient-derived xenograft cells, that were previously treated in a co-culture with NK cells and the SIRPα fusion antibody did not develop leukemia, conversely to their counterparts treated with a conventional αCD123 antibody or an isotype control.

Taken together, several novel combinatorial strategies are under development demonstrating high efficacy in preclinical studies. Especially, designing antibody constructs that aim to increase selective targeting of cancerous cells with a dual-targeting approach seem to be promising.

1.3.3 Combination with the immunomodulatory drug lenalidomide

Functional immune cells are the linchpin for the success of immunotherapeutic strategies. Therefore, T-cell redirecting approaches rely on the formation of a stable immune synapse to achieve the full cytotoxic potential of T cells [103, 104]. However, it is known that hematologic and solid cancers can induce impairment of T-cell actin dynamics by inhibitory ligands as an immunosuppressive strategy hampering the success of immunotherapies [97, 105].

Looking at its mode of action, the immunomodulatory imide drug (IMiD) lenalidomide has a high potential to reverse immune evasion and to serve as a drug for combinatorial immunotherapeutic options. On the one hand, lenalidomide promotes antitumor effects like apoptosis and inhibition of tumor cell proliferation. Furthermore, it has been observed that *ex vivo* exposure of CLL cells to lenalidomide enhanced their function as antigen-presenting cells by upregulation of CD95 (FasL) as well as costimulatory molecules CD80, CD86 and CD40 [106, 107]. On the other hand, exposure to the IMiD markedly increased proliferative capacities and effector function of T- and NK cells as seen by enhanced killing of tumor cells, high IL-2 secretion, and improved immune synapse formation. Also, preclinical studies have demonstrated an even higher cytotoxic potential of T and NK cells when lenalidomide and CPI were combined [108, 109].

Clinically, lenalidomide is now a well-established IMiD for the treatment of various myeloid and lymphoid malignancies, especially in combinatorial strategies. It has been approved by the FDA for the treatment of multiple myeloma (MM) and follicular lymphoma (FL). In MM the present standard of care for newly diagnosed MM patients is the combination of lenalidomide with dexamethasone and bortezomib or daratumumab, a CD38-targeting moAB [110]. In FL, the AUGMENT trial (NCT01938001) demonstrated that the combination of lenalidomide with rituximab significantly prolonged progression-free survival (39.4 vs 14.1 months) compared to rituximab alone, which also led to an FDA approval of this combinatorial approach [111].

Interestingly, in AML the combination of lenalidomide with a WT-1-specific T-cell bispecific antibody increased cytotoxic potential against primary AML blasts *ex vivo* [28]. However, no clinical trials in AML have been initiated yet investigating the combination of lenalidomide with T- or NK-cell redirected immunotherapies.

1.4 Summary of publications and contribution

1.4.1 Publication I: CD33 BiTE® molecule-mediated immune synapse formation and subsequent T-cell activation is determined by the expression profile of activating and inhibitory checkpoint molecules on AML cells

Bispecific T-cell engaging (BiTE®) molecules are comprised of two single-chain variable fragments (scfv) derived from conventional antibodies. Those scfvs are directed against a target antigen expressed on the leukemic blasts and against CD3zeta expressed within the T-cell receptor complex. However, physiologically, T-cells require at least two signals (signal 1: engagement of the TCR; and signal 2: engagement of costimulatory molecules and/or cytokines) to become fully activated. Given the fact, that BiTE molecules lack the provision of signal 2, we investigated the modulatory capacity of the expression profile of costimulatory and -inhibitory antigens on target cells on BiTE molecule-mediated T-cell function in this publication. As a first step, we demonstrated that the CD33xCD3 BiTE molecule AMG 330, in general, was able to induce TCR-triggering using a reconstituted T-cell system. Next, we have developed a cell-based model system by transducing the murine pro-B-cell line with CD33 (target antigen), CD86 (costimulation), and/or PD-L1 (co-inhibition). In co-cultures with the different Ba/F3 sublines and healthy donor (HD) T-cells, we observed that expression of CD86 significantly enhanced AMG 330 mediated T-cell function reflected by cytotoxic potential, T-cell proliferation, granzyme B expression, cytokine secretion, downstream signaling and metabolic fitness of T cells. Additionally, these observations were validated in an orthotopic mouse model. Furthermore, the number of formed Ba/F3 cell-T cell conjugates was significantly increased when CD86 was expressed on Ba/F3 sublines, accompanied by a more stable immune synapse. Oppositely, additional expression of PD-L1 on Ba/F3 sublines diminished previously observed enhancement in T-cell function.

We confirmed our findings with primary AML samples and investigated strategies to overcome PD-L1-mediated resistance to AMG 330 treatment *in vitro.* In line with our previous findings, AMG 330 mediated T-cell cytotoxicity, granzyme B expression, and cytokine secretion, as well as immune synapse formation were decreased when primary AML samples expressed PD-L1. However, when combining either a PD-1 blocking antibody (nivolumab) and/or the immunomodulatory drug lenalidomide with AMG 330 in co-cultures of primary AML samples and HD T cells the negative impact of PD-L1 could be reversed. Compared to nivolumab, which only led to a minor enhancement, lenalidomide significantly increased AMG 330 mediated granzyme B expression, IFNy,

and IL-2 secretion. The strongest effect on specific lysis, as well as IL-2 secretion, was obtained when nivolumab and lenalidomide were combined.

I contributed to this publication by designing, planning, performing, analyzing, and interpreting all *in vitro* experiments. In addition, I performed flow cytometric staining, analysis, and interpretation of *in vivo* experiments and analyzed patient samples for antigen expression. Moreover, I designed all figures, wrote the manuscript draft, and went along with the revision process until final publication.

1.4.2 Publication II: SIRPα-αCD123 fusion antibodies targeting CD123 in conjunction with CD47 blockade enhance the clearance of AML-initiating cells

In this study, published by Tahk et. al, novel immunotherapeutic antibodies were investigated, comprising a dual-targeting approach to treat AML. AML-initiating leukemic stem cells (LSCs) upregulate the inhibitory immune checkpoint CD47 which leads to the inhibition of phagocytosis by interaction with SIRPα, which is expressed on phagocytic cells. Blockade of the CD47/SIRPα axis renders a promising strategy to overcome immune evasion. However, due to the ubiquitous expression of CD47 on healthy tissue antigen sink and potential on-target off-tumor toxicities may arise. On the other hand, CD123 is a well-known therapeutic target antigen, expressed on LSCs and AML blasts. Therefore, we have generated SIRPα-αCD123 fusion antibodies and investigated their potential to eliminate AML cells. The fusion antibodies either contained one (1x) or two (2x) extracellular SIRPα domains fused to each light chain of an αCD123 antibody. In the first step, several binding studies were performed highlighting that the fusion antibodies preferentially bind to $CD123^{+}CD47^{+}$ cells than to $CD123^{-}CD47^{+}$ cells. Due to the weaker binding affinity of the SIRPα domains to CD47 compared to the high affinity of the αCD123 antibody to CD123, potential antigen sink generated by e.g., red blood cells ($CD123^{-}CD47^{+}$) can be avoided. Additionally, we could show that our fusion antibodies didn't induce platelet aggregation and we observed lower binding to PBMCs compared to clinically tested high-affinity αCD47 binding antibody (Hu5F9-G4) or commercially available antibody (B6H12 clone). Next, functional properties of SIRPα-αCD123 fusion antibodies to induce phagocytosis and NK-cell mediated cell lysis were investigated. Indeed, both 1× and 2×SIRPα-αCD123 fusion antibodies induced ADCP and ADCC against MOLM-13 cell line as well as against primary AML cells to a higher extent than Hu5F9-G4 or B6H12. Interestingly, SIRPα-αCD123 fusion antibodies showed higher potency in NK-cell mediated cytotoxicity compared to analog fusion antibodies directed against CD33. This was especially pronounced in NK-cell activation depicted as CD69 expression on NK cells. Lastly, we addressed the question of whether

the SIRPα-αCD123 fusion antibody could eliminate LSCs. Hence, patient-derived xenograft cells were co-cultured *ex vivo* with HD NK cells in the presence of αCD123 antibody, 2×SIRPα-αCD123, or an isotype control. The remaining live AML cells from the ADCC assay were sorted and re-transplanted into NSG mice, defining that the leukemia-initiating cells (LICs) served as a surrogate for LSCs. In NSG mice receiving LICs from the isotype or αCD123 antibody condition engraftment of the leukemia was observed. In mice receiving 2×SIRPα-αCD123 treated LICs the outgrowth of leukemia was prevented.

I contributed to this publication by conducting the AML long-term ADCC experiments, which led to the results displayed in Figure 5 B, C, D, and E.

2. Publications

2.1 Publication I

Cancer Immunology, Immunotherapy
https://doi.org/10.1007/s00262-023-03439-x

RESEARCH

CD33 BiTE® molecule-mediated immune synapse formation and subsequent T-cell activation is determined by the expression profile of activating and inhibitory checkpoint molecules on AML cells

Anetta Marcinek[1,2] · Bettina Brauchle[1,2] · Lisa Rohrbacher[1,2] · Gerulf Hänel[1,2] · Nora Philipp[1,2] · Florian Märkl[6] · Thaddäus Strzalkowski[6] · Sonja M. Lacher[1,2] · Dragica Udiljak[1,2] · Karsten Spiekermann[1,3,4] · Sebastian Theurich[1,3,5] · Sebastian Kobold[3,6] · Roman Kischel[7,8] · John R. James[9] · Veit L. Bücklein[1,2] · Marion Subklewe[1,2,3]

Received: 18 December 2022 / Accepted: 27 March 2023

Abstract
Bispecific T-cell engager (BiTE®) molecules recruit T cells to cancer cells through CD3ε binding, independently of T-cell receptor (TCR) specificity. Whereas physiological T-cell activation is dependent on signal 1 (TCR engagement) and signal 2 (co-stimulation), BiTE molecule-mediated T-cell activation occurs without additional co-stimulation. As co-stimulatory and inhibitory molecules modulate the strength and nature of T-cell responses, we studied the impact of the expression profile of those molecules on target cells for BiTE molecule-mediated T-cell activation in the context of acute myeloid leukemia (AML). Accordingly, we created a novel in vitro model system using murine Ba/F3 cells transduced with human CD33 ± CD86 ± PD-L1. T-cell fitness was assessed by T-cell function assays in co-cultures and immune synapse formation by applying a CD33 BiTE molecule (AMG 330). Using our cell-based model platform, we found that the expression of positive co-stimulatory molecules on target cells markedly enhanced BiTE molecule-mediated T-cell activation. The initiation and stability of the immune synapse between T cells and target cells were significantly increased through the expression of CD86 on target cells. By contrast, the co-inhibitory molecule PD-L1 impaired the stability of BiTE molecule-induced immune synapses and subsequent T-cell responses. We validated our findings in primary T-cell-AML co-cultures, demonstrating a PD-L1-mediated reduction in redirected T-cell activation. The addition of the immunomodulatory drug (IMiD) lenalidomide to co-cultures led to stabilization of immune synapses and improved subsequent T-cell responses. We conclude that target cells modulate CD33 BiTE molecule-dependent T-cell activation and hence, combinatorial strategies might contribute to enhanced efficacy.

Keywords Acute myeloid leukemia · Bispecific antibodies · Immune synapse · Costimulation (CD86) · Checkpoint molecule (PD-L1)

✉ Marion Subklewe
Marion.Subklewe@med.uni-muenchen.de

[1] Department of Medicine III, University Hospital, LMU Munich, Munich, Germany

[2] Laboratory for Translational Cancer Immunology, LMU Gene Center, Munich, Germany

[3] German Cancer Consortium (DKTK) and German Cancer Research Center (DKFZ), Heidelberg, Germany

[4] Experimental Leukemia and Lymphoma Research (ELLF), Department of Medicine III, University Hospital, LMU Munich, Munich, Germany

[5] Cancer-and Immunometabolism Research Group, LMU Gene Center, Munich, Germany

[6] Division of Clinical Pharmacology, Department of Medicine IV; Member of the German Center for Lung Research (DZL), University Hospital, LMU, Munich, Germany

[7] AMGEN Research Munich GmbH, Munich, Germany

[8] AMGEN Inc., Thousand Oaks, CA, USA

[9] Division of Biomedical Sciences, Warwick Medical School, University of Warwick, Coventry, UK

Published online: 11 April 2023

Abbreviations

AML	Acute myeloid leukemia
APC	Antigen presenting cell
BCP-ALL	B-cell precursor acute lymphoblastic leukemia
BM	Bone marrow
BMMC	Bone marrow mononuclear cell
(c)BiTE	(Control) bispecific T-cell engager
cSMAC/dSMAC/pSMAC	Central/distal/peripheral supramolecular activation cluster
ECAR	Extracellular acidification rate
FACS	Fluorescence-activated cell sorting
HD	Healthy donor
IMiD	Immunomodulatory drug
MFI	Median fluorescence intensity
MRD^+	Minimal residual disease-positive
OCR	Oxygen consumption rate
OS	Overall survival
PB	Peripheral blood
PBMC	Peripheral blood mononuclear cell
PSG	Penicillin–streptomycin–glutamine
r/r	Relapsed/refractory
SRC	Spare respiratory capacity
TCR	T-cell receptor

Introduction

Within the last 5 years, several novel agents have been approved for use against acute myeloid leukemia (AML), changing the treatment landscape [1–3]. Despite these advances, overall survival rate is poor and high relapse rates remain a challenge. Nevertheless, allogeneic stem cell transplantation is still the most potent anti-leukemic treatment strategy, with donor lymphocyte infusions demonstrating the power of T cells to eliminate chemo-refractory AML cells [4].

The success of blinatumomab, a CD19xCD3 bispecific T-cell-engager ($BiTE^®$) molecule for treating relapsed/refractory (r/r) and minimal residual disease-positive (MRD^+) B-cell precursor acute lymphoblastic leukemia (BCP-ALL), has shown that alternative T-cell-recruiting strategies are also able to eliminate leukemias [5, 6]. The results of further trials utilizing CD20-directed bispecific antibodies in mature B-cell malignancies underline the potential of T-cell engagers in combating hematological malignancies [7, 8]. Translating this success to AML has proved to be challenging, and the response rates reported to date have not met expectations. Currently, various formats of T-cell-redirecting antibodies against tumor-associated antigens in AML are undergoing (pre-)clinical investigation. These investigations include phase I/II trials with a WT-1 T-cell bispecific antibody (RO7283420) and studies on CD3-engaging BiTE molecules directed against CD33 (CD33*CD3 BsAb and AMG 330) and CD135/FLT-3 (CLN-049) (NCT04580121, NCT05077423, NCT02520427, NCT05143996, respectively) [9–16].

Bispecific T-cell antibodies recruit T cells against cancer cells only through CD3ε binding and independently of T-cell receptor (TCR) specificity and expression of major histocompatibility complex molecules [17]. In contrast to our physiological understanding of T-cell activation, which is dependent on signal 1 (TCR engagement) and signal 2 (co-stimulation), BiTE molecule-mediated T-cell triggering is devoid of extrinsic co-stimulation. Previous studies have shown that T-cell co-signaling ligands on target cells, such as CD80, CD86 and PD-L1, modulate the function and activity of T cells redirected by bispecific T-cell antibodies in vitro [18–20]. However, their relevance to the formation and stabilization of immune synapses (the interface between two conjugating cells) induced by BiTE molecules is poorly understood. In physiological antigen-presenting cell (APC)–T-cell conjugates, immune synapses are well-organized and tightly regulated three-dimensional structures composed of different regions called the central, peripheral, and distal supramolecular activation clusters (cSMAC, pSMAC and dSMAC, respectively) [21]. In the context of BiTE molecules and other T-cell-dependent bispecific antibodies, it has been shown that induced immune synapses show hallmarks of maturity such as characteristic LFA-1 ring structures in the pSMAC and exclusion of CD45 from the cSMAC [17, 22].

In this study, we set out to investigate CD33 BiTE molecule-mediated interplay between T cells and target cells. Firstly, we focused on the influence of co-stimulatory and -inhibitory molecules on BiTE molecule-induced formation of immune synapses and their stability, the subsequent T-cell responses, and intracellular downstream signaling in T cells. For this, we established a cell-based model system using the murine pro-B-cell line Ba/F3, which is devoid of human cross-reactive checkpoint molecules, and integrated different sets of co-stimulatory and -inhibitory molecules in addition to the target antigen CD33. Secondly, we translated our findings to primary AML cells for which we modified the expression profile to mimic different clinically relevant phenotypes. Finally, using the immunomodulatory drug (IMiD) lenalidomide, we developed strategies to reverse the impairment of BiTE molecule-mediated T-cell responses that are modulated by the expression profile of AML cells.

Methods

Patient and healthy donor material

Peripheral blood mononuclear cells (PBMCs) and bone marrow mononuclear cells (BMMCs) were isolated from peripheral blood (PB) and bone marrow (BM), respectively, using density gradient centrifugation over Histopaque (Sigma-Aldrich, St. Louis, MO, USA). Cell surface expression of CD80, CD86 and PD-L1 was assessed in the Laboratory of Leukemia Diagnostics, University Hospital, LMU Munich, by flow-cytometry (Navios, Beckman Coulter) from > 300 PB and BM samples obtained at the time of first diagnosis or relapse.

Cell lines

Ba/F3 cells were purchased from the Deutsche Sammlung von Mikroorganismen und Zellkulturen (Leibniz-Institut DSMZ, Braunschweig, Germany) and cultivated under standard conditions in RPMI 1640 supplemented with 10% FBS, 0.5 mg/ml penicillin–streptomycin–glutamine (PSG; Thermo Fisher Scientific, 10,378,016, Waltham, MA, USA), 10 mM HEPES (Carl Roth, HN78.1), and 10% WEHI-conditioned medium. Phoenix-Eco cells were kindly provided by K. Spiekermann (University Hospital, LMU Munich). Phoenix-Eco cells were cultivated in DMEM (Thermo Fisher Scientific, 21,969,035, Waltham, MA, USA) containing 10% FBS and 0.5 mg/ml PSG.

Primary AML samples

Cryo-preserved patient samples were thawed and cultivated with irradiated MS-5 cells as previously described [9]. Samples were cultivated in α-MEM (PAN Biotech, P04-21500, Aidenbach, Germany) supplemented with 12.5% FBS, 12.5% horse serum (Sigma-Aldrich, H1270, St. Louis, MO, USA), and 0.5 mg/ml PSG. The medium was additionally supplemented with 20 ng/ml recombinant human (rhu) granulocyte colony-stimulating factor (Peprotech, 300–23, Hamburg, Germany), rhu interleukin 3 (Peprotech, 200–03, Hamburg, Germany), rhu thrombopoietin (Peprotech, 300–18, Hamburg, Germany), and 57.2 µM 2-mercaptoethanol (Sigma-Aldrich, 63,689, St. Louis, MO, USA).

For some experiments, 25 ng/ml IFNγ and 50 ng/ml TNFα (both Peprotech, Hamburg, Germany) were added to AML cells after 24 h. After a total pre-culture time of 72 h, T cells were magnetically depleted from the cell suspension (Stemcell Technologies, Vancouver, Canada) and AML cells were used as described in the following sections. Detailed patient characteristics obtained for ex vivo evaluation is summarized in supplementary Table S2.

DNA constructs and vectors

Human cDNA encoding CD80, CD86 and PD-L1 was purchased from R&D Systems (RDC1086, RDC0693 and RDC1087, respectively) and subcloned into the retroviral expression vector MSCV-neo. Human CD33 cDNA was subcloned into the MSCV-IRES-GFP vector (both kindly gifted by K. Spiekermann).

Transfection of Phoenix-Eco cells

Phoenix-Eco cells (6.5×10^6) were seeded in a 10 mm Petri dish 1 day prior to transfection. Subcloned plasmid DNA was transiently transfected using calcium phosphate co-precipitation. Medium was replenished after incubation for 18 h, and after another 30 h retroviral supernatant was collected.

Transduction of Ba/F3 cells

Ba/F3 cells (1.5 ml) were seeded at a density of 5×10^5/ml in six-well plates. Transduction was performed by adding 1.5 ml of retroviral supernatant in presence of polybrene (8 µg/ml). Cells were spun (90 min, 1565 rcf), then cultivated for 72 h, and positive cell fractions were sorted using fluorescence-activated cell sorting (FACS). Quantification of antigen expression was determined using QuantiBRITE PE Beads (BD Biosciences, Franklin Lakes, NJ, USA) according to manufacturer's instructions. All antibodies used for flow cytometry and FACS staining are listed in supplementary Table S1.

T-cell-mediated cytotoxicity assay

Redirected cytotoxicity was evaluated in co-cultures of Ba/F3 sublines or primary AML samples and different T-cell subsets in the presence of AMG 330 (0.5–5 ng/ml) or a control construct (c BiTE; specificity against an herbicide. Provided by AMGEN) with an effector to target cell ratio (E:T) of 1:4–1:1. T-cell subsets were either sorted by FACS ($CD3^+$, $CCR7^+CD45RA^+$ and $CCR7^+CD45RA^-$) or isolated magnetically and untouched (pan T cells, $CD4^+$, $CD8^+$) according to the manufacturer's recommendations (Stemcell Technologies, Vancouver, Canada). In some experiments, T-cells were labeled with CellTrace Far Red (Thermo Fisher Scientific, Waltham, MA, USA) according to the manufacturer's recommendations. After 3 days, cytotoxicity, T-cell proliferation, granzyme B expression and cytokine secretion were determined using multiparameter flow cytometry (MPFC) (CytoFLEX, Beckman

Coulter). Specific lysis was calculated as follows: % specific lysis = 100–[number of viable $CD33^+$ target cells (AMG 330 condition)]/[number of viable $CD33^+$ target cells (c BiTE condition)] × 100. T-cell proliferation was determined by dilution of membrane dye (% proliferation in AMG 330 condition set to c BiTE condition as baseline) or calculation of relative T-cell numbers on day 3 compared to day 0. Granzyme B expression was assessed by intracellular cytokine staining. IFNγ, TNFα and IL-2 secretion was measured by analyzing co-culture's supernatant by cytometric bead array according to the manufacturer's instructions (BD Biosciences, Franklin Lakes, NJ, USA).

In vivo mouse studies

Ba/F3 $CD33^+$ or Ba/F3 $CD33^+$ $CD86^+$ sublines (1×10^7) were injected with T cells (1×10^7) intravenously into the tail vain of 8–12-weeks-old female and male NSG mice (own breeding or Janvier Labs, Le Genest-Saint-Isle, France). Mice were treated either with AMG 330 or c BiTE (200 µg/kg) and sacrificed after 24 h. Samples from bone marrow and spleen were collected and analyzed by MPFC. Specific lysis was calculated as follows: % specific lysis = 100–[mean of number of viable $CD33^+$ target cells (AMG 330 condition)]/[mean of number of viable $CD33^+$ target cells (c BiTE condition)] × 100. All animal experiments were approved by the local regulatory agency (Regierung von Oberbayern).

Phospho-flow and imaging flow cytometry

Cell conjugates were formed by seeding $0.5–2 \times 10^6$ cells/ml (100–200 µl) with an E:T ratio of 1:1. For phospho-flow analysis, cells were spun (30 s, 550 rcf) immediately after adding AMG 330 (5 ng/ml) to the cell suspension. Cells were gently resuspended by flicking the tube, and reactions were stopped with the addition of fixation buffer (BD Biosciences, Franklin Lakes, NJ, USA) after a total of 1, 3, 5, 10 or 20 min. Cells were fixed for 15 min at 37 °C, spun (5 min, 550 rcf) and permeabilized with methanol (BD Biosciences, Franklin Lakes, NJ, USA) for 30 min on ice. Afterwards, cell conjugates were stained against CD45, pERK1/2, pAkt, and pZAP70 and analyzed by flow cytometry. For imaging flow cytometry (Amnis ImageStream Mk II, Luminex) cell conjugation was stopped after 1 h. Twenty minutes before fixation, LFA-1 staining antibody was added to the reaction. Fixed cells were spun (5 min, 550 rcf), stained for CD45, and Hoechst 33,342 (Thermo Fisher Scientific, Waltham, MA, USA) was added. In the case of primary AML samples, target cells were labeled with CellTrace CFSE (Thermo Fisher Scientific, Waltham, MA, USA) before conjugate formation.

Spinning disc confocal microscopy

To study TCR triggering, we used a reconstituted T-cell system previously described by James et al. [23]. Briefly, for these experiments, HEK-T cells are non-immune HEK293T cells expressing the TCR complex and CD45 genetically fused to eGFP. HEK-T cells (1×10^5 cells) were conjugated for 20 min with CD33-transduced Raji B cells (2×10^5 cells) in the presence of either AMG 330 (1.25 µg/ml) or a c BiTE construct, which had been fluorescently labeled with Alexa Fluor 647. The Raji B cells expressed mTagBFP for identification, and the transduced CD33 was tagged with mScarlet so its clustering could be directly visualized. Spinning disk confocal microscopy (Andor) was used to image the cell conjugates at 37 °C. All images were analyzed, and all presented images were manipulated in an equivalent manner using ImageJ. The level of protein clustering and segregation of denoted proteins was measured by manually defining the intensity of fluorescently labeled proteins in the plasma membrane within the cell–cell interface.

Metabolic analysis

$CD33^+$ cells were depleted from T cell–Ba/F3 cell co-cultures using a Human CD33 Positive Selection Kit (Stemcell Technologies, Vancouver, Canada) according to the manufacturer's instructions, and the remaining T cells (2.5×10^5 T cells/well) were plated on a poly-D-lysine-coated 96-well Seahorse utility plate (Agilent, Santa Clara, CA, USA). Metabolic functions were analyzed in standard mitochondrial and glycolysis stress tests on a Seahorse XFe96 Analyzer using appropriate kits (Agilent, Santa Clara, CA, USA, respectively). Final concentration for the mitochondrial stress test for oligomycin, FCCP and rotenone/antimycin A were 1 µM, each. For the glycolysis stress test a final concentration of 10 mM glucose, 1 µM oligomycin and 50 mM 2-DG were used. Positive control was performed with pan T cells activated for 72 h with Human T-Activation CD3/CD28 Dynabeads (Thermo Fisher Scientific, Waltham, MA, USA) at a 1:2 beads:cell ratio. Untreated pan T cells served as a negative control.

Data analysis

Flow cytometry data were analyzed using FlowJo software (BD Biosciences, version 10) and imaging flow cytometry data were analyzed with IDEAS 3.0 (Amnis). GraphPad Prism was used to perform statistical evaluations (GraphPad, version 9.3). ImageJ was used to analyze spinning disc confocal microscopy images. TIMER2.0 was used to perform analysis between gene expression and clinical outcome [24].

Results

T-cell co-signaling ligands are expressed on leukemic cells

Cell surface expression of the T-cell co-signaling ligands CD80, CD86 and PD-L1 was assessed on leukemic bulk cells ($CD45^{dim}SSC^{low}$) from peripheral blood (PB) and bone marrow (BM) samples obtained at the time of first diagnosis or relapse. All analyzed samples were negative for cell surface expression of CD80 (Fig. 1A). We observed CD86 expression in 61 of 333 (18.32% with an MFI ratio > 1.5; Fig. 1A) and PD-L1 expression in 21 of 377 (5.57% with an MFI ratio > 1.5; Fig. 1A) primary AML samples. Patient samples showed a variability in their expression levels, and we report these subdivided into the five groups defined by Tamura et al. [25]: < 5%, 5–10%, 10–30%, 30–60% and > 60% (Fig. 1B, C).

Based on these findings, we decided to investigate the roles of CD86 and PD-L1 in a cell-based model system. For this, we generated a stable expression system by transducing the murine pro-B cell line Ba/F3 with human (hu) CD33 ($2.4–3.1 \times 10^8$ molecules/cell) ± huCD86 ($1.4–1.7 \times 10^8$ molecules/cell) ± huPD-L1 (4.8×10^7 molecules/cell) (Fig. 1D, E). Expression levels of CD86 and PD-L1 are higher on Ba/F3 sublines compared to primary AML samples. However, the CD86/PD-L1 ratio of mean expression (~ 1.7) were comparable.

AMG 330 induces TCR triggering characterized by CD45 exclusion from and CD33 clustering within the synapse

Using a reconstituted T-cell system previously described by James et al. [23], we characterized the immune synapse that forms upon AMG 330-induced TCR triggering. We observed exclusion of CD45 from the immune synapse and simultaneous CD33 clustering within the Raji B–HEK T-cell interface in the presence of AMG 330, but not in the presence of c BiTE (Fig. 2A). Quantification of the relative fluorescence signal intensities of CD45, CD33 and AMG 330 within the cell–cell interface revealed that CD33 clustering and AMG 330 binding were co-localized. In contrast, CD45 exclusion was spatially distinct and clearly anti-correlated (Fig. 2B). Next, we investigated AMG 330-mediated conjugation and stability of synapse formation after 20 and 60 min, respectively, with different Ba/F3 sublines. The total number of conjugates formed with $CD33^+$ $CD86^+$ Ba/F3 subline was approximately 1.3-fold higher than with those expressing either no co-stimulatory antigen or additional PD-L1 in the presence of AMG 330 (Fig. 4A). Furthermore, expression of CD86 without PD-L1 on Ba/F3 $CD33^+$ subline resulted in a remarkable increase of

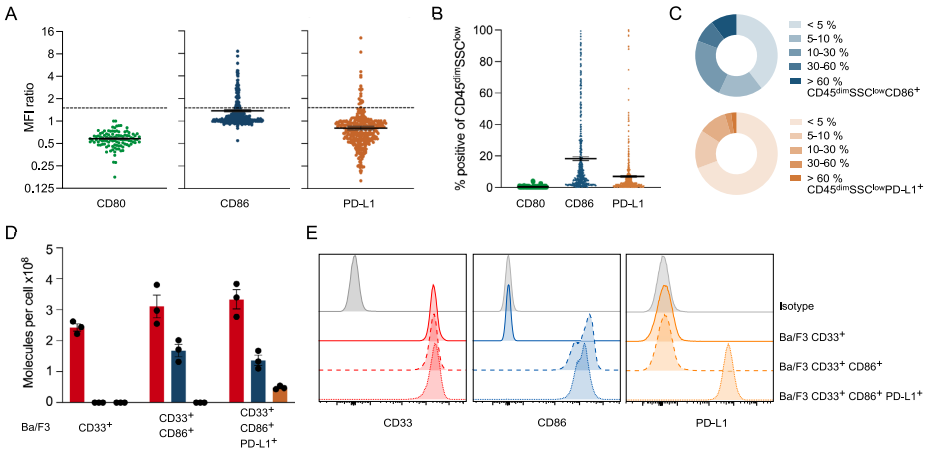

Fig. 1 T-cell co-signaling receptors are expressed on leukemic cells and transduced Ba/F3 sublines. **A** MFI ratio of cell surface expression of CD80 (green), CD86 (blue) and PD-L1 (orange) in $CD45^{dim}SSC^{low}$ primary AML samples ($n = 107–377$). MFI ratios ≥ 1.5 (dashed lines) indicate positivity. **B** Percentage of CD80-, CD86- and PD-L1-positive cells and **C** distribution of CD86 and PD-L1 expression intensities within primary AML samples ($n = 432–521$). **D** Antigen count of CD33 (red), CD86 (blue) and PD-L1 (orange) on transduced Ba/F3 sublines ($n = 3$) with **E** representative histograms

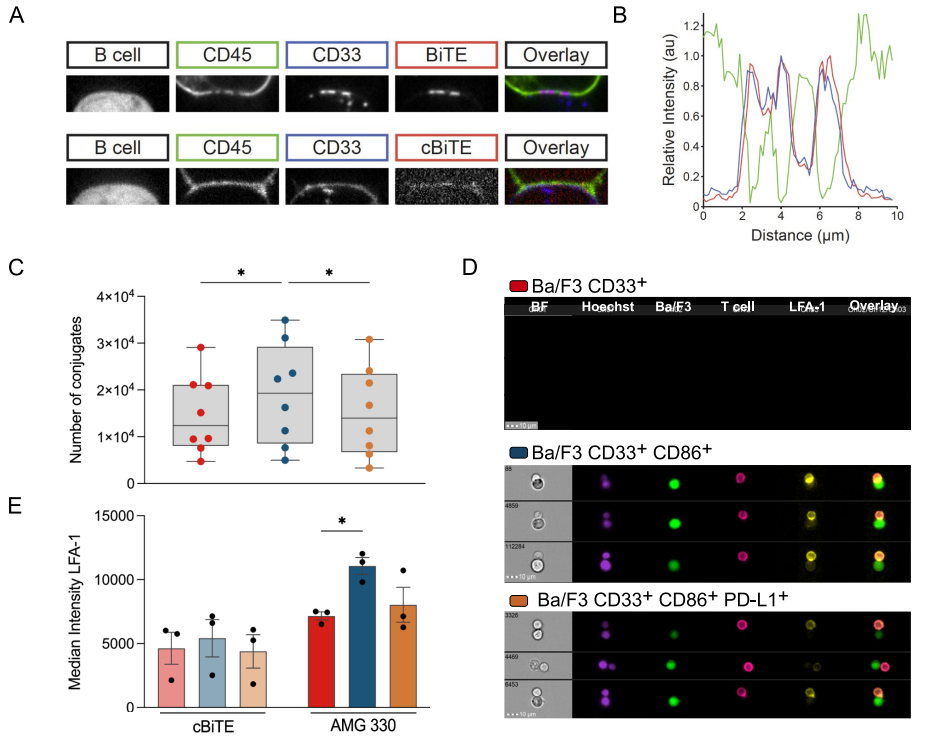

Fig. 2 AMG 330 induces TCR triggering characterized by CD45 exclusion from and CD33 clustering within the synapse. **A** Representative spinning disc confocal microscope images of AMG 330 (BiTE® molecule) and c BiTE molecule-mediated conjugates formed of a CD33-transduced Raji B cell and a reconstituted HEK-T cell. **B** Line profiles of CD45 (green), CD33 (blue), and AMG 330 (red) intensities across a conjugate interface equivalent to that shown in a representative image in panel A. **C** Total number of AMG 330-induced T-cell–CD33$^+$ CD86$^\pm$ PD-L1$^\pm$ Ba/F3 cell conjugates after 20 min, assessed by flow cytometry. **D** Representative imaging flow cytometric analysis of AMG 330-induced T-cell–CD33$^+$ CD86$^\pm$ PD-L1$^\pm$ Ba/F3 cell conjugation: brightfield (BF, gray), Hoechst staining (purple), Ba/F3 cell (GFP$^+$; green), T cell (CD45$^+$; magenta), LFA-1 (yellow), and overlay of Ba/F3, T-cell and LFA-1 channels. **E** Median intensity of LFA-1 accumulation at the interface of AMG 330-and c BiTE molecule-induced T-cell–CD33$^+$ CD86$^\pm$ PD-L1$^\pm$ Ba/F3 cell conjugates. Statistical analysis: One-way ANOVA with Dunnett's multiple comparisons test; ns $p > 0.05$, $^*p \leq 0.05$

LFA-1 accumulation at the cell–cell interface, determined by imaging flow cytometry (for gating strategy see supplementary Fig. S1). In contrast, LFA-1 expression intensity within Ba/F3 CD33$^+$ PD-L1$^\pm$–T cell conjugates was comparable to the control with c BiTE (Fig. 2C, D). Collectively, our results demonstrate that expression of the co-stimulatory molecule CD86 stabilizes immune synapses, as seen by the accumulation of LFA-1 at the cell–cell interface, whereas concomitant expression of PD-L1 had a negative impact on the formation of conjugates and synapses.

Checkpoint molecule expression on target cells modulates AMG 330-mediated cytotoxicity and T-cell function

In co-culture assays with different Ba/F3 sublines and healthy donor (HD) T cells the potential for CD86 and PD-L1 to modulate T-cell cytotoxicity and AMG 330-redirected T-cell function was evaluated. We observed that lysis of CD33 single-positive Ba/F3 cells upon addition of AMG 330 and HD T cells was < 25% after 3 days.

Cytotoxicity was significantly improved by co-expression of CD86 (Fig. 3A). Higher cytotoxicity against Ba/F3 CD33$^+$ CD86$^+$ was accompanied by significant increases in T-cell proliferation, expression of granzyme B, and secretion of IFNγ and TNFα (Fig. 3B, C). HD T cells did not induce lysis against Ba/F3 cells due to xenogeneic MHC recognition (Fig. S2C). Furthermore, we were able to translate our findings into an in vivo model system. Specifically, we observed higher clearance of the Ba/F3 CD33$^+$ CD86$^+$ subline compared to the Ba/F3 CD33$^+$ subline in the BM and spleen in an orthotopic mouse model (Fig. 3D). In line with these observations, T cells from Ba/F3 CD33$^+$ CD86$^+$ mice also showed higher CD69 expression levels (Fig. 3E). The influence of co-inhibition was investigated in co-cultures with the CD33$^+$ CD86$^+$ PD-L1$^+$ Ba/F3 subline. Although this resulted in an only marginal decrease of AMG 330-mediated cytotoxicity, T-cell proliferation and function were markedly reduced (Fig. 3A–C). These findings could be observed in bulk T cells and in CD4$^+$, CD8$^+$, naïve and memory T-cell subpopulations used for co-culture. Our findings underline the importance of co-stimulatory molecules in AMG 330-mediated cytotoxicity against CD33-expressing target cells.

AMG 330-induced downstream signaling in T cells is strongly enhanced by CD86 expression on target cells

In a next step, we aimed to characterize downstream signaling in T cells of various kinases that are involved in the regulation of TCR phosphorylation and subsequent T-cell proliferation and survival. Therefore, we measured the phosphorylation of Akt, ERK1/2 and ZAP70 after engagement between HD T cells and different Ba/F3 subline in the presence of AMG 330. The percentage of kinase phosphorylation after 1, 3, 5, 10, and 20 min was determined relative to unstimulated T cells as a background control. We observed time-dependent phosphorylation of Akt, ERK1/2 and ZAP70 within the T cells regardless of which Ba/F3 subline was engaging (Fig. 4A–C). The extent of phosphorylation varied between the T-cell HDs and also depended on the Ba/F3 subline, according to the trend Ba/F3 CD33$^+$ CD86$^+$ > > Ba/F3 CD33$^+$ CD86$^+$ PD-L1$^+$ > Ba/

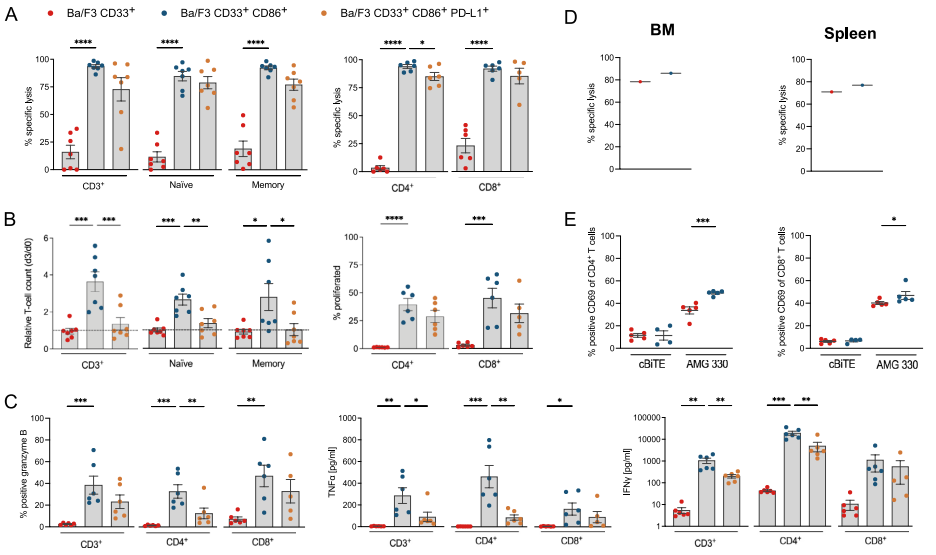

Fig. 3 Checkpoint molecule expression on target cells modulates AMG 330-mediated cytotoxicity and T-cell function. **A** AMG 330-mediated cytolytic capacity, **B** proliferation, **C** granzyme B expression and cytokine secretion of HD T-cell subsets after co-culture with CD33$^+$ CD86$^\pm$ PD-L1$^\pm$ Ba/F3 sublines for 72 h. **D** AMG 330-mediated cytolytic capacity in BM and spleen and **E** CD69 expression of HD T cells (from BM) against CD33$^+$ CD86$^\pm$ sublines in vivo. AMG 330 concentration = 0.5–5 ng/ml (in vitro) or 200 µg/kg (in vivo); E:T ratio = 1:1; n = 5–6; Error bars represent mean ± SEM; Statistical analysis: One-way ANOVA or Mixed-effects analysis with Dunnett's multiple comparisons test; ns $p > 0.05$, *$p \leq 0.05$, **$p \leq 0.01$, ***$p \leq 0.001$, **** $p \leq 0.0001$

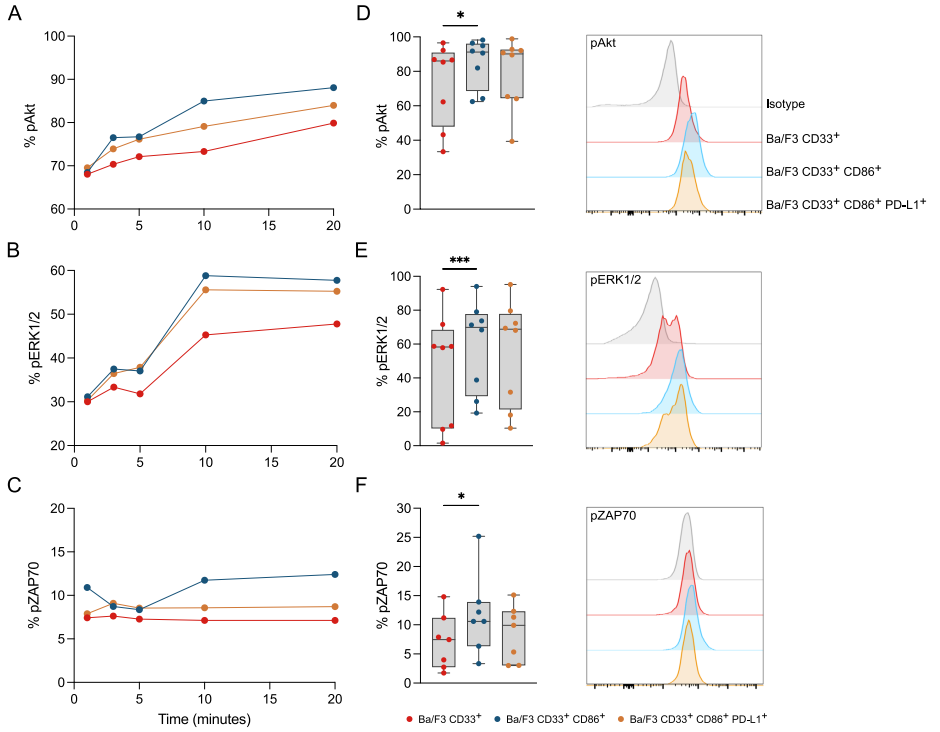

Fig. 4 AMG 330-induced downstream signaling in T cells is strongly enhanced by CD86 expression on target cells. Kinetics of phosphorylation (% positive) of **A** Akt, **B** ERK1/2, and **C** ZAP70 in T cells after 1, 3, 5, 10, and 20 min of AMG 330-mediated engagement with different Ba/F3 cell constructs. Percentage of phosphorylated **D** Akt, **E** ERK1/2, and **F** ZAP70 in T cells after 10 min of engagement. Overlays of representative flow cytometry histograms after 10 min of engagement are shown. AMG 330 concentration = 5 ng/ml; E:T ratio = 1:1; $n = 7–8$; Error bars represent mean ± SEM; Statistical analysis: One-way ANOVA or Mixed-effects analysis with Dunnett's multiple comparisons test; ns $p > 0.05$, *$p \leq 0.05$, **$p \leq 0.01$, ***$p \leq 0.001$

F3 CD33$^+$. This observation was most pronounced after 10 min of conjugate formation (Fig. 4D–F).

PD-L1 expression on target cells alters metabolic reprogramming of T cells

Activation of T cells is accompanied by a metabolic reprogramming and is further modulated by the engagement of ligands expressed on APCs [26]. T cells activated by AMG 330 in co-culture with the CD33$^+$ Ba/F3 subline, devoid of positive co-stimulatory molecules, showed very low metabolic activity with low oxygen consumption rates (OCRs; Fig. 5A) and extracellular acidification rates (ECARs; Fig. 5C). By contrast, T cells activated by AMG 330 in co-culture with the CD33$^+$ CD86$^+$ Ba/F3 subline, showed a significant increase of both glycolysis and oxidative phosphorylation, indicating high metabolic activity (Fig. 5A–D). T cells stimulated with the CD33$^+$ CD86$^+$ PD-L1$^+$ Ba/F3 subline showed an altered metabolic phenotype, preferring oxidative phosphorylation over glycolysis as the main pathway for energy production. In accordance with a comparable approach, PD-L1 stimulation led to an even higher spare respiratory capacity (SRC) in T cells than CD86 stimulation alone (Fig. 5B) [26]. These data underline that co-stimulation is a prerequisite for achieving a fully functional BiTE molecule-mediated T-cell response.

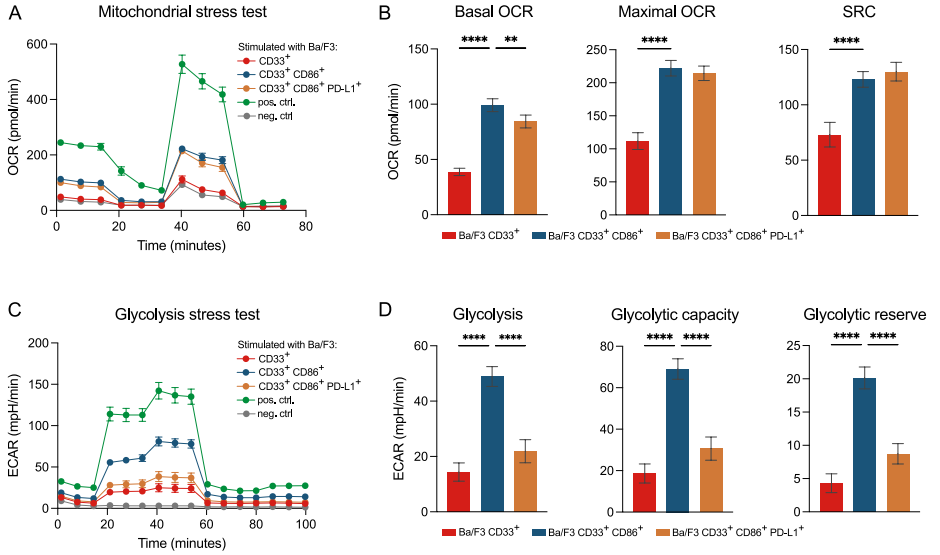

Fig. 5 PD-L1 expression on target cells alters metabolic reprogramming of T-cells. **A** OCR kinetics of T cells after 72 h of co-culture with different Ba/F3 sublines in the presence of AMG 330, after 72 h of stimulation with CD3/CD28 beads (pos. ctrl) or left unstimulated for 72 h (neg. ctrl); **B** corresponding bar graphs showing basal OCR, maximal OCR, and SRC in a mitochondrial stress test. **C** Kinetics of ECAR of T cells after 72 h of co-culture with different Ba/F3 sublines in the presence of AMG 330, after 72 h of stimulation with CD3/CD28 beads (pos. ctrl) or left unstimulated for 72 h (neg. ctrl); **D** corresponding bar graphs showing glycolysis, glycolytic capacity, and glycolytic reserve in a glycolysis stress test. AMG 330 concentration = 0.5 ng/ml; E:T ratio = 1:1; $n = 5$; Error bars represent mean ± SEM; Statistical analysis: Mixed-effects analysis with Dunnett's multiple comparisons test; ns $p > 0.05$, *$p \leq 0.05$, **$p \leq 0.01$, ***$p \leq 0.001$, ****$p \leq 0.0001$

IFNγ and TNFα modulate the profile of checkpoint molecule expression of primary AML cells

Having found that T-cell co-signaling ligands on target cells influence AMG 330-mediated T-cell function in our cell-based model system, we next aimed to translate our findings into primary patient material. To increase PD-L1 levels in primary AML samples, we pre-cultivated primary AML samples with IFNγ and TNFα to induce PD-L1 expression (PD-L1^{ind}). After 48 h we observed a significant upregulation of PD-L1, whereas expression of CD33 and CD86 was not significantly affected by cytokine treatment (Fig. 6A). This led to significantly reduced AMG 330-mediated cytotoxicity and granzyme B expression, together with a decrease in IFNγ and IL-2 secretion (Fig. 6B). Importantly, these observations were accompanied by reduced stability of the immune synapse, as indicated by lower levels of LFA-1 expression within AMG 330-induced cell–cell conjugates after IFNγ and TNFα pre-treatment (Fig. 6D).

Lenalidomide reversed the negative impact of IFNγ and TNFα on AMG 330-mediated T-cell function and synapse formation in co-cultures with primary AML samples

Pre-treatment of primary AML samples with IFNγ and TNFα led to PD-L1 upregulation and decreased AMG 330-mediated stability of immune synapses. Accordingly, we observed that the AMG 330-mediated function of T cells was diminished in co-cultures with pre-treated AML samples. In a next step, we aimed to reverse this functional impairment due to pro-inflammatory cytokines by using the IMiD lenalidomide (10 µM). Indeed, we could show that T-cell responses and the stability of immune synapses were significantly improved by adding lenalidomide to co-cultures. Interestingly, PD-1 blockade with nivolumab (10 µg/ml) could not abrogate the negative impact of the inflammatory stimuli to the same extent as lenalidomide. However, the combination of PD-1 blockade and lenalidomide mediated the highest specific lysis of primary AML cells and

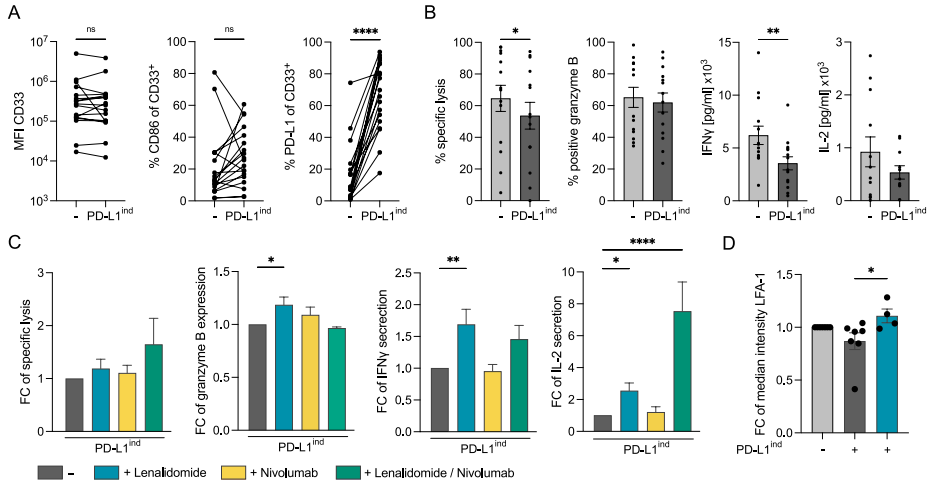

Fig. 6 Lenalidomide reverses negative impact of IFNγ and TNFα on AMG 330-mediated T-cell function and synapse formation in co-cultures with primary AML samples. **A** Expression of CD33 (MFI), CD86 (% CD33$^+$), and PD-L1 (% CD33$^+$) on primary AML samples after pretreatment ± IFNγ and TNFα (PD-L1^{ind}) for 48 h. **B** AMG 330-mediated cytolytic capacity, granzyme B expression, IFNγ and IL-2 secretion of HD T cells against non-pretreated and PD-L1^{ind} primary AML samples. **C** Fold change of AMG 330-mediated cytolytic capacity, granzyme B expression, IFNγ and IL-2 secretion of HD T cells against PD-L1^{ind} primary AML samples ± lenalidomide or/and nivolumab after 72 h of co-culture. **D** Fold change of median intensity of LFA-1 accumulation at the interface of AMG 330-induced T-cell–primary AML cell conjugates. Primary AML samples were pretreated ± IFNγ and TNFα for 48 h and HD T cells were pretreated ± lenalidomide for 24 h; AMG 330 concentration = 5 ng/ml; Lenalidomide = 10 µM; Nivolumab = 10 µg/ml; E:T ratio = 1:4 (panels B and C) or 1:1 (panel D); n = 4–14; Error bars represent mean ± SEM; Statistical analysis: Paired t-test (panel A and B) and One-way ANOVA with Dunnett's multiple comparisons test (Panels C and D); ns $p > 0.05$, *$p \leq 0.05$, **$p \leq 0.01$, ***$p \leq 0.001$, ****$p \leq 0.0001$

significantly enhanced IL-2 secretion (Fig. 6B–D; Fig. S3). Of note, expression levels of PD-L1 and CD86 on primary AML cells and PD-1 on T-cells remained unchanged through the exposure to lenalidomide (Fig. S3). Our results support the notion that lenalidomide can reverse the negative impact of IFNγ and TNFα on AMG 330-mediated T-cell responses by improving immune synapse formation and circumventing inhibitory signals on T cells by boosting their effector function, especially in combination with PD-1 blockade.

Discussion

Since the approval of blinatumomab—the first bispecific T-cell-redirecting antibody molecule—other bispecific constructs of different formats have been evaluated in several clinical trials. Antibodies including mosunetuzumab have entered clinical practice in the setting of r/r B-cell lymphoma. Tebentafusp, a bispecific fusion protein, was granted approval for treating uveal melanoma, and other bispecific T-cell-redirecting agents are expected to follow in hematological and solid malignancies [6–8, 27–30].

Despite these impressive developments, a significant number of patients do not respond to this type of therapy, or they eventually relapse. It is well known that the efficacy of bispecific T-cell-redirecting antibodies crucially depends on T-cell activation and proliferation, although the parameters determining these activities are poorly understood [31]. Therefore, it is of critical importance to better understand the contributors to an effective T-cell response for improving treatment strategies involving T-cell-redirecting antibodies.

Here, we present a unique model cellular platform based on the murine Ba/F3 cell line aimed at deepening our insight into the mechanistic aspects of T-cell activation mediated by CD33 BiTE molecules. This model system is free from interfering endogenous stimulatory or inhibitory checkpoint molecules (Fig. S4) and provides an ideal setup for understanding how selected surface molecules are involved in the formation of synapses and subsequent T-cell activation and downstream signaling.

Specifically, our cell-based platform integrates different T-cell co-signaling ligands in combination with an AML-associated target antigen to mimic the expression profile of primary AML samples. To achieve this, we screened the surface expression of > 300 primary AML samples for the T-cell co-signaling ligands CD80, CD86 and PD-L1 by MPFC. Furthermore, we correlated gene expression to overall survival (OS) for AML patients. PD-L1^{high} patients have worse OS than PD-L1^{low} patients (Fig. S4).

Based on this analysis, we integrated CD86 and PD-L1 into our model system. Notably, whereas the expression of CD80 and CD86 has been reported at varying levels, [25, 32, 33] our analysis showed a smaller proportion of patients with CD86 expression and, in line with the study by Maeda et al. [34], a lack of CD80 expression in primary AML samples.

Next, by using a reconstituted T-cell system, we demonstrated that AMG 330 induces TCR triggering, showing hallmarks of the formation of mature immune synapses, such as the exclusion of CD45 and enrichment of CD33 at the cell–cell interface [22, 23]. Another characteristic of maturation and stability of an immune synapse is the enrichment of LFA-1 within the cell–cell surface area of engagement [35, 36]. Importantly, human LFA-1 binds to murine ICAM-1 [37] enabling a cross-species assay setup to study human antigen-specific BiTE molecules and their impact on synapse stability. Indeed, LFA-1 expression intensities were highest in the Ba/F3 CD33$^+$ CD86$^+$ cell–T cell conjugates. As a consequence, target cell lines expressing CD86 elicited significantly higher BiTE molecule-mediated cytotoxicity, T-cell proliferation, granzyme B expression and cytokine secretion than those expressing only the target antigen or in combination with PD-L1. Surprisingly, CD4$^+$ T cells exhibited similar levels of cytotoxicity and T-cell proliferation in comparison to CD8$^+$ T cells against the Ba/F3 CD33$^+$ CD86$^+$ subline. In line with these observations, Melenhorst et. al. [38] reported on a dominance of CD4$^+$ CAR T-cells subsets in CLL patients with long lasting remission. Also, previous reports in antiviral immunity demonstrated cytolytic function within the CD4 T-cell compartment [39, 40].

It is well known that T cells undergo a reprogramming of different metabolic pathways depending on the stimulus they encounter during their activation, which shapes their long-term survival and persistence [41–43]. We provide evidence that the absence of co-stimulation leads to T cells entering a metabolically inactive state in the presence of BiTE molecules, whereas stimulation by CD86 promotes a switch to glycolysis to meet the nutritional demand of highly functional effector T cells. Consistent with a reduced effector function, T cells stimulated additionally with PD-L1 generate less energy by glycolysis, but remarkedly increased their oxidative phosphorylation with high SRC, as reported for physiological APC–T-cell interactions mediated by PD-1–PD-L1 ligation [26].

Our cell-based model system is devoid of interfering molecules, enabling the impact of CD86 and PD-L1 on BiTE molecule-mediated downstream signaling in T cells to be isolated. We tracked the phosphorylation of ZAP70, Akt and ERK1/2, the main contributors to the activation cascade, and demonstrated that T-cell co-signaling ligands predetermine CD33 BiTE molecule-mediated T-cell function. These observations underline the essential nature of signal 2 (co-stimulation) in CD33 BiTE molecule-mediated T-cell responses and suggest that the expression profiles of patient-derived samples contribute to the efficacy of bispecific T-cell-redirecting molecules.

Finally, we aimed to validate our findings from the cell-based model system in primary AML samples. In response to redirected T-cell activation and linked pro-inflammatory cytokine secretion, the expression of PD-L1, among others, is a mechanism of the adaptive immune response in various malignancies. We conditioned primary AML cells with IFNγ and TNFα, which resulted in the upregulation of PD-L1 accompanied by impaired T-cell-redirected cytotoxicity and immune synapse formation by the BiTE molecule AMG 330.

Our observations are consistent with other preclinical studies attempting to overcome the detrimental impact PD-L1 has on T-cell responses mediated by bispecific antibodies [18, 44, 45]. The concept of combining bispecific T-cell-redirecting antibodies with checkpoint inhibition in AML is currently being evaluated in early clinical trials, however, only limited data exists to assess its effectiveness. Therefore, we sought to implement a novel combinatorial approach for overcoming the loss of functionality of T-cells acquired during treatment with redirecting bispecific antibodies. Based on our findings, we hypothesized that we could improve BiTE molecule-mediated T-cell responses by modulating immune synapse formation.

In fact, by introducing lenalidomide into our *in vitro* model system with primary AML cells, we were able to significantly enhance CD33 BiTE molecule-mediated T-cell cytotoxicity and cytokine secretion. In accordance with reports on T-cell defects in chronic lymphocytic leukemia (CLL) due to impaired LFA-1 activation and motility, we observed an improvement in the stability of immune synapses through the addition of lenalidomide [46, 47]. Together, this supports the concept of combining bispecific T-cell-redirecting molecules with an IMiD to increase their efficacy.

Our study provides a unique and reliable cell-based model system with which to unravel the molecular mechanisms as redirected by CD33 BiTE molecules. This system is highly suitable for investigating and deciphering their mode of action as it can be modulated to express nearly any desired surface antigen in different combinations [48, 49]. Thereby, we were able to demonstrate the impact of

co-stimulatory and co-inhibitory molecules on synapse formation and subsequent T-cell responses. Furthermore, we translated our findings from the cell-based model to primary patient material, underlining the notion that the expression profile of the target cells modulates the efficacy of T-cell-redirecting antibodies. By combining the antibody treatment with an IMiD, we were able to enhance impaired T-cell responses and observed an improvement in immune synapse formation, supporting the potential use of combinational strategies in future clinical trials.

Supplementary Information The online version contains supplementary material available at https://doi.org/10.1007/s00262-023-03439-x.

Acknowledgements The authors thank Sabine Sandner-Thiede, Marina Leeping, Simone Pentz, Elke Habben, Bianca Kirschbaum, and Ewelina Zientara (University Hospital, LMU Munich) for their excellent technical support. We acknowledge the iFlow Core Facility of the University Hospital, LMU Munich (INST 409/225-1 FUGG) for assistance in generating flow cytometry data and the Core Facility Flow Cytometry at the Biomedical Center, LMU Munich, for providing equipment, services, and expertise.

Author contributions MS, VLB, RK, JRJ and AM: study design and supervision. AM, MS and VLB: manuscript writing and editing. AM, LR, FM, TS, DU, JRJ and GH: Data acquisition and analysis. KS, ST, SK, FM, AM, BB, LR, GH, NP, SML, JRJ, VLB and MS: research design and data interpretation. All authors read and approved the final manuscript.

Funding Open Access funding enabled and organized by Projekt DEAL. The work was supported by the Bavarian Elite Graduate School "i-target" (L.R., F.M., and N.P.), the Else-Kröner-Fresenius Forschungskolleg CSP Cancer Immunotherapy (V.L.B. and S.K.), the Wilhelm-Sander Stiftung (G.H. and M.S.; project no. 2018.087.1), the Deutsche Forschungsgemeinschaft (DFG, German Research Foundation) research Grant provided within the Sonderforschungsbereich SFB 338/1 2021–452881907 (M.S., S.K., and S.T.), DFG research Grant 451580403 (M.S.), DFG research Grant KO5055/3-1 and KO5055-2-1 (S.K.), Marie Sklodowska-Curie Training Network for Optimizing Adoptive T Cell Therapy of Cancer (funded by the Horizon 2020 program of the European Union; grant 955575 to S.K.), German Cancer Aid (S.K.), the Ernst Jung Stiftung (S.K.), Institutional Strategy LMUexcellent of LMU Munich (within the framework of the German Excellence Initiative to S.K.), the Go-Bio-Initiative (S.K.), the m4-Award of the Bavarian Ministry for Economical Aairs (S.K.), Bundesministerium für Bildung und Forschung (S.K.), European Research Council (Starting Grant 756017 and PoC Grant 101100460 to S.K.), Fritz-Bender Foundation (S.K.), Deutsche José Carreras Leukämie Stiftung (S.K.), the Bayerische Forschungsstiftung (BAYCELLator to S.K.), Hector Foundation (S.K.) and research funding from Amgen (M.S.).

Data and materials availability The datasets analyzed during the current study are available from the corresponding author on reasonable request.

Declarations

Conflict of interest M.S. receives industry research support from Amgen, BMS/Celgene, Gilead, Janssen, Miltenyi Biotec, Morphosys, Novartis, Roche, Seattle Genetics and Takeda. She serves as a consultant/advisor to AvenCell, CDR-Life, Ichnos Sciences, Incyte Biosciences, Janssen, Miltenyi Biotec, Molecular Partners, Novartis, Pfizer and Takeda and serves on the speakers' bureau at Amgen, AstraZeneca, BMS/Celgene, Gilead, GSK, Janssen, Novartis, Pfizer, Roche and Takeda. V.L.B. has received research funding from Miltenyi Biotec, Novartis, and Pfizer, and has served as a consultant/advisor to Novartis, Amgen, and Gilead. He serves on the speakers' bureau at Novartis and Pfizer. R.K. is employed at Amgen Research Munich, Germany. S.M.L. (now employed at iOmx Therapeutics AG) received research funding from Roche. S.T. has served as a consultant/advisor to Amgen, BMS, GSK, Janssen, Pfizer, Sanofi, and Takeda. S.K. has received honoraria from TCR2, Inc., Novartis, BMS and GSK. S.K. is inventor of several patents in the field of immunooncology. S.K. received license fees from TCR2, Inc., and Carina Biotech. S.K. received research support from TCR2, Inc., Tabby Therapeutics, Plectonic GmBH and Arcus Bioscience for work unrelated to the paper. A.M., B.B. (now employed at Adivo GmbH), L.R., G.H., F.M., T.S., N.P., K.S., and J.R.J. declare no relevant conflicts of interest.

Consent to participate PB samples from HDs and samples of PB and BM from AML patients were collected with written consent in accordance with the Declaration of Helsinki and with approval from the Institutional Review Board of LMU Munich.

Consent for publication Not applicable.

References

1. DiNardo CD, Jonas BA, Pullarkat V et al (2020) Azacitidine and Venetoclax in previously untreated acute myeloid Leukemia. N Engl J Med 383:617–629. https://doi.org/10.1056/NEJMoa2012971
2. DiNardo CD, Pratz K, Pullarkat V et al (2019) Venetoclax combined with decitabine or azacitidine in treatment-naive, elderly patients with acute myeloid leukemia. Blood 133:7–17. https://doi.org/10.1182/blood-2018-08-868752
3. Stone RM, Mandrekar SJ, Sanford BL et al (2017) Midostaurin plus chemotherapy for Acute myeloid Leukemia with a FLT3 mutation. N Engl J Med 377:454–464. https://doi.org/10.1056/NEJMoa1614359
4. Schmid C, Labopin M, Schaap N et al (2019) Prophylactic donor lymphocyte infusion after allogeneic stem cell transplantation in acute leukaemia – a matched pair analysis by the Acute Leukaemia working party of EBMT. Br J Haematol 184:782–787. https://doi.org/10.1111/bjh.15691
5. Topp MS, Gökbuget N, Stein AS et al (2015) Safety and activity of blinatumomab for adult patients with relapsed or refractory B-precursor acute lymphoblastic leukaemia: a multicentre, single-arm, phase 2 study. Lancet Oncol 16:57–66. https://doi.org/10.1016/S1470-2045(14)71170-2

6. Wu J, Fu J, Zhang M, Liu D (2015) Blinatumomab: a bispecific T cell engager (BiTE) antibody against CD19/CD3 for refractory acute lymphoid leukemia. J Hematol Oncol 8:1–7. https://doi.org/10.1186/s13045-015-0195-4
7. Budde LE, Assouline S, Sehn LH et al (2022) Single-agent Mosunetuzumab shows durable complete responses in patients with relapsed or refractory B-cell lymphomas: phase I dose-escalation study. J Clin Oncol 40:481–491. https://doi.org/10.1200/JCO.21.00931
8. Hutchings M, Mous R, Clausen MR et al (2021) Dose escalation of subcutaneous epcoritamab in patients with relapsed or refractory B-cell non-Hodgkin lymphoma: an open-label, phase 1/2 study. Lancet 398:1157–1169. https://doi.org/10.1016/S0140-6736(21)00889-8
9. Krupka C, Kufer P, Kischel R et al (2014) CD33 target validation and sustained depletion of AML blasts in long-term cultures by the bispecific T-cell-engaging antibody AMG 330. Blood 123:356–365. https://doi.org/10.1182/blood-2013-08-523548
10. Ravandi F, Walter RB, Subklewe M et al (2020) Updated results from phase I dose-escalation study of AMG 330, a bispecific T-cell engager molecule, in patients with relapsed/refractory acute myeloid leukemia (R/R AML). J Clin Oncol 38:7508–7508. https://doi.org/10.1200/jco.2020.38.15_suppl.7508
11. Ravandi F, Stein AS, Kantarjian HM et al (2018) A phase 1 first-in-human study of AMG 330, an anti-CD33 bispecific T-cell engager (BiTE®) antibody construct, in relapsed/refractory acute myeloid Leukemia (R/R AML). Blood 132:25–25. https://doi.org/10.1182/blood-2018-99-109762
12. Brauchle B, Goldstein RL, Karbowski CM et al (2020) Characterization of a novel FLT3 BiTE molecule for the treatment of acute myeloid leukemia. Mol Cancer Ther 19:1875–1888. https://doi.org/10.1158/1535-7163.MCT-19-1093
13. Daver N, Alotaibi AS, Bücklein V, Subklewe M (2021) T-cell-based immunotherapy of acute myeloid leukemia: current concepts and future developments. Leukemia 35:1843–1863
14. Uy GL, Aldoss I, Foster MC et al (2021) Flotetuzumab as salvage immunotherapy for refractory acute myeloid leukemia. Blood 137:751–762. https://doi.org/10.1182/blood.2020007732
15. Augsberger C, Hänel G, Xu W et al (2021) Targeting intracellular WT1 in AML with a novel RMF-peptide-MHC-specific T-cell bispecific antibody. Blood 138:2655–2669. https://doi.org/10.1182/blood.2020010477
16. Mehta NK, Pfluegler M, Meetze K et al (2022) A novel IgG-based FLT3xCD3 bispecific antibody for the treatment of AML and B-ALL. J Immunother Cancer 10:3882. https://doi.org/10.1136/jitc-2021-003882
17. Offner S, Hofmeister R, Romaniuk A et al (2006) Induction of regular cytolytic T cell synapses by bispecific single-chain antibody constructs on MHC class I-negative tumor cells. Mol Immunol 43:763–771. https://doi.org/10.1016/j.molimm.2005.03.007
18. Herrmann M, Krupka C, Deiser K et al (2018) Bifunctional PD-1 x aCD3 x aCD33 fusion protein reverses adaptive immune escape in acute myeloid leukemia. Blood 132:2484–2494. https://doi.org/10.1182/blood-2018-05-849802
19. Feucht J, Kayser S, Gorodezki D et al (2016) T-cell responses against CD19+ pediatric acute lymphoblastic leukemia mediated by bispecific T-cell engager (BiTE) are regulated contrarily by PD-L1 and CD80/CD86 on leukemic blasts. Oncotarget 7:76902–76919. https://doi.org/10.18632/oncotarget.12357
20. Laszlo GS, Gudgeon CJ, Harrington KH, Walter RB (2015) T-cell ligands modulate the cytolytic activity of the CD33/CD3 BiTE antibody construct, AMG 330. Blood Cancer J 5:340. https://doi.org/10.1038/bcj.2015.68
21. Monks CRF, Freiberg BA, Kupfer H et al (1998) Three-dimensional segregation of supramolecular activation clusters in T cells. Nature 395:82–86. https://doi.org/10.1038/25764
22. Li J, Stagg NJ, Johnston J et al (2017) Membrane-proximal epitope facilitates efficient T cell synapse formation by anti-FcRH5/CD3 and Is a requirement for myeloma cell killing. Cancer Cell 31:383–395. https://doi.org/10.1016/j.ccell.2017.02.001
23. James JR, Vale RD (2012) Biophysical mechanism of T-cell receptor triggering in a reconstituted system. Nature 487:64–69. https://doi.org/10.1038/nature11220
24. Li T, Fu J, Zeng Z et al (2020) TIMER2.0 for analysis of tumor-infiltrating immune cells. Nucleic Acids Res 48:W509–W514. https://doi.org/10.1093/NAR/GKAA407
25. Tamura H, Dan K, Tamada K et al (2005) Expression of functional B7–H2 and B7.2 costimulatory molecules and their prognostic implications in de novo acute myeloid Leukemia. Clin Cancer Res 11:5708–5717. https://doi.org/10.1158/1078-0432.CCR-04-2672
26. Patsoukis N, Bardhan K, Chatterjee P et al (2015) PD-1 alters T-cell metabolic reprogramming by inhibiting glycolysis and promoting lipolysis and fatty acid oxidation. Nat Commun 6:6692. https://doi.org/10.1038/ncomms7692
27. Bröske AME, Korfi K, Belousov A et al (2022) Pharmacodynamics and molecular correlates of response to glofitamab in relapsed/refractory non-Hodgkin lymphoma. Blood Adv 6:1025–1037. https://doi.org/10.1182/bloodadvances.2021005954
28. Frances N, Bacac M, Bray-French K et al (2022) Novel in vivo and in vitro pharmacokinetic/pharmacodynamic-based human starting dose selection for Glofitamab. J Pharm Sci 111:1208–1218. https://doi.org/10.1016/j.xphs.2021.12.019
29. Moreau P, Garfall AL, van de Donk NWCJ et al (2022) Teclistamab in relapsed or refractory multiple myeloma. N Engl J Med. https://doi.org/10.1056/nejmoa2203478
30. Nathan P, Hassel JC, Rutkowski P et al (2021) Overall survival benefit with Tebentafusp in metastatic uveal melanoma. N Engl J Med 385:1196–1206. https://doi.org/10.1056/NEJMoa2103485
31. Zugmaier G, Gökbuget N, Klinger M et al (2015) Long-term survival and T-cell kinetics in relapsed/refractory all patients who achieved MRD response after Blinatumomab treatment. Blood 126:2578–2584. https://doi.org/10.1182/blood-2015-06-649111
32. Graf M, Reif S, Hecht K, Pelka-Fleischer R, Kroell T, Pfister K, Schmetzer H (2005) High expression of costimulatory molecules correlates with low relapse-free survival probability in acute myeloid Leukemia (AML). Ann Hematol 84:287–297. https://doi.org/10.1007/s00277-004-0978-0
33. Re F, Arpinati M, Testoni N et al (2002) Expression of CD86 in acute myelogenous leukemia is a marker of dendritic/monocytic lineage. Exp Hematol 30:126–134
34. Maeda A, Yamamoto K, Yamashita K et al (1998) The expression of co-stimulatory molecules and their relationship to the prognosis of human acute myeloid leukaemia: poor prognosis of B7–2-positive leukaemia. Br J Haematol 102:1257–1262. https://doi.org/10.1046/j.1365-2141.1998.00901.x
35. Hosseini BH, Louban I, Djandji D et al (2009) Immune synapse formation determines interaction forces between T cells and antigen-presenting cells measured by atomic force microscopy. Proc Natl Acad Sci 106:17852–17857. https://doi.org/10.1073/pnas.0905384106
36. Cassioli C, Balint S, Compeer EB et al (2021) Increasing LFA-1 expression enhances immune synapse architecture and T cell receptor signaling in jurkat E6.1 Cells. Front Cell Dev Biol 9:1862. https://doi.org/10.3389/fcell.2021.673446
37. Núñez D, Comas L, Lanuza PM et al (2017) A functional analysis on the interspecies interaction between mouse LFA-1 and human intercellular adhesion molecule-1 at the cell level. Front Immunol 8:1817. https://doi.org/10.3389/fimmu.2017.01817
38. Melenhorst JJ, Chen GM, Wang M et al (2022) Decade-long leukaemia remissions with persistence of CD4+ CAR T cells. Nature 602:503–509. https://doi.org/10.1038/s41586-021-04390-6

39. van Leeuwen EMM, Remmerswaal EBM, Vossen MTM et al (2004) Emergence of a CD4+CD28− Granzyme B+, cytomegalovirus-specific T cell subset after recovery of primary cytomegalovirus infection. J Immunol 173:1834–1841. https://doi.org/10.4049/jimmunol.173.3.1834
40. Zaunders JJ, Dyer WB, Wang B et al (2004) Identification of circulating antigen-specific CD4+ T lymphocytes with a CCR5+, cytotoxic phenotype in an HIV-1 long-term nonprogressor and in CMV infection. Blood 103:2238–2247. https://doi.org/10.1182/blood-2003-08-2765
41. Bental M, Deutsch C (1993) Metabolic changes in activated T cells: An NMR study of human peripheral blood lymphocytes. Magn Reson Med 29:317–326. https://doi.org/10.1002/mrm.1910290307
42. Kawalekar OU, O'Connor RS, Fraietta JA et al (2016) Distinct signaling of coreceptors regulates specific metabolism pathways and impacts memory development in CAR T cells. Immunity 44:380–390. https://doi.org/10.1016/j.immuni.2016.01.021
43. Pearce EL, Poffenberger MC, Chang CH (1979) Jones RG (2013) Fueling immunity: Insights into metabolism and lymphocyte function. Science 342:1242454
44. Krupka C, Kufer P, Kischel R et al (2016) Blockade of the PD-1/PD-L1 axis augments lysis of AML cells by the CD33/CD3 BiTE antibody construct AMG 330: reversing a T-cell-induced immune escape mechanism. Leukemia 30:484–491. https://doi.org/10.1038/leu.2015.214
45. Correnti CE, Laszlo GS, de van der Schueren WJ et al (2018) Simultaneous multiple interaction T-cell engaging (SMITE) bispecific antibodies overcome bispecific T-cell engager (BiTE) resistance via CD28 co-stimulation. Leukemia 32:1239–1243. https://doi.org/10.1038/s41375-018-0014-3
46. Ramsay AG, Clear AJ, Fatah R, Gribben JG (2012) Multiple inhibitory ligands induce impaired T-cell immunologic synapse function in chronic lymphocytic leukemia that can be blocked with lenalidomide: establishing a reversible immune evasion mechanism in human cancer. Blood 120:1412–1421. https://doi.org/10.1182/blood-2012-02-411678
47. Ramsay AG, Evans R, Kiaii S et al (2013) Chronic lymphocytic leukemia cells induce defective LFA-1-directed T-cell motility by altering Rho GTPase signaling that is reversible with lenalidomide. Blood 121:2704–2714. https://doi.org/10.1182/blood-2012-08-448332
48. Roas M, Vick B, Kasper M-A et al (2022) Targeting FLT3 by new-generation antibody-drug-conjugate in combination with kinase inhibitors for treatment of AML. Blood. https://doi.org/10.1182/blood.2021015246
49. Zieger N, Kazerani M, Nicholls A et al (2022) T-cell exhaustion induced by continuous bispecific molecule exposure is ameliorated by treatment-free intervals. Blood 140(10):1104–1118. https://doi.org/10.1182/blood.2022015956

Cancer Immunology, Immunotherapy
https://doi.org/10.1007/s00262-023-03457-9

CORRECTION

Correction to: CD33 BiTE® molecule-mediated immune synapse formation and subsequent T-cell activation is determined by the expression profile of activating and inhibitory checkpoint molecules on AML cells

Anetta Marcinek[1,2] · Bettina Brauchle[1,2] · Lisa Rohrbacher[1,2] · Gerulf Hänel[1,2] · Nora Philipp[1,2] · Florian Märkl[6] · Thaddäus Strzalkowski[6] · Sonja M. Lacher[1,2] · Dragica Udiljak[1,2] · Karsten Spiekermann[1,3,4] · Sebastian Theurich[1,3,5] · Sebastian Kobold[3,6] · Roman Kischel[7,8] · John R. James[9] · Veit L. Bücklein[1,2] · Marion Subklewe[1,2,3]

Correction to: Cancer Immunology, Immunotherapy
https://doi.org/10.1007/s00262-023-03439-x

The original version of this article unfortunately contained a mistake. Figure 2D is not displayed correctly. In the "BaF3 CD33+" line no cell images are displayed and it seem that something went wrong with the layers of the figure.

The corrected Fig. 2 is given in the next page.

The original article can be found online at https://doi.org/10.1007/s00262-023-03439-x.

✉ Marion Subklewe
Marion.Subklewe@med.uni-muenchen.de

1 Department of Medicine III, University Hospital, LMU Munich, Munich, Germany

2 Laboratory for Translational Cancer Immunology, LMU Gene Center, Munich, Germany

3 German Cancer Consortium (DKTK) and German Cancer Research Center (DKFZ), Heidelberg, Germany

4 Experimental Leukemia and Lymphoma Research (ELLF), Department of Medicine III, University Hospital, LMU Munich, Munich, Germany

5 Cancer-and Immunometabolism Research Group, LMU Gene Center, Munich, Germany

6 Division of Clinical Pharmacology, Department of Medicine IV; Member of the German Center for Lung Research (DZL), University Hospital, LMU, Munich, Germany

7 AMGEN Research Munich GmbH, Munich, Germany

8 AMGEN Inc., Thousand Oaks, CA, USA

9 Division of Biomedical Sciences, Warwick Medical School, University of Warwick, Coventry, UK

Published online: 08 May 2023

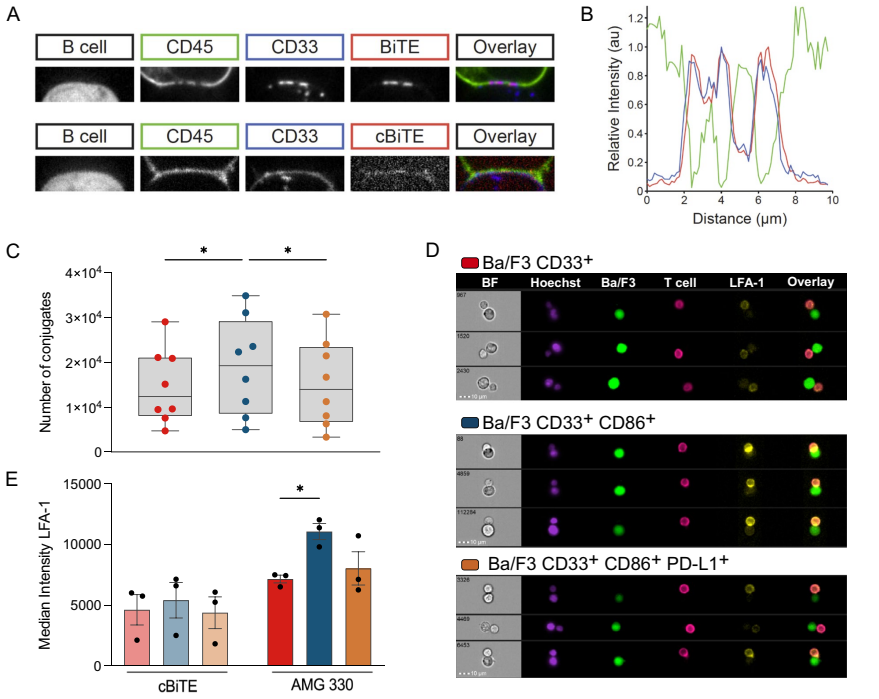

Fig. 2 AMG 330 induces TCR triggering characterized by CD45 exclusion from and CD33 clustering within the synapse. **A** Representative spinning disc confocal microscope images of AMG 330 (BiTE® molecule) and c BiTE molecule-mediated conjugates formed of a CD33-transduced Raji B cell and a reconstituted HEK-T cell. **B** Line profiles of CD45 (green), CD33 (blue), and AMG 330 (red) intensities across a conjugate interface equivalent to that shown in a representative image in panel A. **C** Total number of AMG 330-induced T-cell–CD33$^+$ CD86$^\pm$ PD-L1$^\pm$ Ba/F3 cell conjugates after 20 min, assessed by flow cytometry. **D** Representative imaging flow cytometric analysis of AMG 330-induced T-cell–CD33$^+$ CD86$^\pm$ PD-L1$^\pm$ Ba/F3 cell conjugation: brightfield (BF, gray), Hoechst staining (purple), Ba/F3 cell (GFP$^+$; green), T cell (CD45$^+$; magenta), LFA-1 (yellow), and overlay of Ba/F3, T-cell and LFA-1 channels. **E** Median intensity of LFA-1 accumulation at the interface of AMG 330-and c BiTE molecule-induced T-cell–CD33$^+$ CD86$^\pm$ PD-L1$^\pm$ Ba/F3 cell conjugates. Statistical analysis: One-way ANOVA with Dunnett's multiple comparisons test; ns $p > 0.05$, $^*p \leq 0.05$

2.2 Publication II

Tahk *et al. J Hematol Oncol (2021) 14:155*
https://doi.org/10.1186/s13045-021-01163-6

Journal of Hematology & Oncology

RESEARCH Open Access

SIRPα-αCD123 fusion antibodies targeting CD123 in conjunction with CD47 blockade enhance the clearance of AML-initiating cells

Siret Tahk[1], Binje Vick[2,3], Björn Hiller[1], Saskia Schmitt[1], Anetta Marcinek[4,5], Enrico D. Perini[1], Alexandra Leutbecher[4,5], Christian Augsberger[4,5], Anna Reischer[4,5], Benjamin Tast[4,5], Andreas Humpe[6], Irmela Jeremias[2,3,7], Marion Subklewe[3,4,5], Nadja C. Fenn[1*] and Karl-Peter Hopfner[1*]

Abstract

Background: Acute myeloid leukaemia (AML) stem cells (LSCs) cause disease relapse. The CD47 "don't eat me signal" is upregulated on LSCs and contributes to immune evasion by inhibiting phagocytosis through interacting with myeloid-specific signal regulatory protein alpha (SIRPα). Activation of macrophages by blocking CD47 has been successful, but the ubiquitous expression of CD47 on healthy cells poses potential limitations for such therapies. In contrast, CD123 is a well-known LSC-specific surface marker utilized as a therapeutic target. Here, we report the development of SIRPα-αCD123 fusion antibodies that localize the disruption of CD47/SIRPα signalling to AML while specifically enhancing LSC clearance.

Methods: SIRPα-αCD123 antibodies were generated by fusing the extracellular domain of SIRPα to an αCD123 antibody. The binding properties of the antibodies were analysed by flow cytometry and surface plasmon resonance. The functional characteristics of the fusion antibodies were determined by antibody-dependent cellular phagocytosis and antibody-dependent cellular cytotoxicity assays using primary AML patient cells. Finally, an in vivo engraftment assay was utilized to assess LSC targeting.

Results: SIRPα-αCD123 fusion antibodies exhibited increased binding and preferential targeting of $CD123^+$ $CD47^+$ AML cells even in the presence of $CD47^+$ healthy cells. Furthermore, SIRPα-αCD123 fusion antibodies confined disruption of the CD47-SIRPα axis locally to AML cells. In vitro experiments demonstrated that SIRPα-αCD123 antibodies greatly enhanced AML cell phagocytosis mediated by allogeneic and autologous macrophages. Moreover, SIRPα-αCD123 fusion antibodies efficiently targeted LSCs with in vivo engraftment potential.

Conclusions: SIRPα-αCD123 antibodies combine local CD47 blockade with specific LSC targeting in a single molecule, minimize the risk of targeting healthy cells and efficiently eliminate AML LSCs. These results validate SIRPα-αCD123 antibodies as promising therapeutic interventions for AML.

Keywords: CD47, Acute myeloid leukaemia, CD123, Leukemic stem cells, Phagocytosis, Immunotherapy

Background

Therapeutic options for acute myeloid leukaemia (AML) are limited, and the majority of patients relapse due to persistent chemorefractory LSCs [1–3]. Targeting and eradicating the leukemic stem cell (LSC) population is therefore a prerequisite for sustained

*Correspondence: nfenn@genzentrum.lmu.de; hopfner@genzentrum.lmu.de
[1] Gene Center and Department of Biochemistry, Ludwig-Maximilians-Universität München, Feodor-Lynen-Straße 25, 81377 Munich, Germany
Full list of author information is available at the end of the article

remission. CD47 is an innate immune checkpoint upregulated on LSCs, where it functions as a "don't eat me" signal by interacting with SIRPα on myeloid cells [4–6]. The first in class CD47-blocking antibody, magrolimab (Hu5F9-G4), was evaluated as a monotherapy in AML in a phase 1 trial (NCT02678338) [7, 8]. However, preclinical data support the combination of magrolimab with pro-phagocytic signals, such as activation of Fcγ receptors (FcγR) on macrophages or expression of calreticulin on target cells [8–12]. Magrolimab has consequently been combined with calreticulin-inducing azacytidine in a phase 1b trial including untreated AML patients unfit for chemotherapy and patients with intermediate to very high-risk myelodysplastic syndrome (MDS) [8, 13]. The combination demonstrated encouraging results; 64% of AML patients achieved an objective response (OR), while 56% achieved complete remission (CR) or CR with incomplete haematological recovery. In patients with high-risk MDS, 91% had an OR, and 42% had a CR (NCT03248479).

Nevertheless, CD47 is ubiquitously expressed on healthy cells as well, which generates an antigen sink lowering the effective dose and comprising a potential site of toxicity for αCD47 therapies [14, 15]. Combining the CD47 blocking domain, such as endogenous SIRPα, with a cancer-specific antibody in a single molecule can restrict the blockade of CD47 locally on antigen-expressing cells [16–18].

Similar to CD47, the interleukin-3 receptor alpha chain (CD123) is upregulated on AML LSCs and is associated with increased proliferation of AML cells and a poor prognosis [19–21]. Furthermore, high CD47 and CD123 coexpression has been demonstrated to correlate with AML chemoresistance [22]. These studies suggest that dual targeting of CD123 and CD47 could reduce the LSC count and enhance the rate and duration of response in AML patients.

To improve AML LSC targeting and clearance, we fused an αCD123 antibody with the endogenous N-terminal SIRPα immunoglobulin V-like domains and generated 1 × SIRPα-αCD123 and 2 × SIRPα-αCD123 fusion antibodies. Both of our antibodies exhibited improved binding to $CD123^+$ $CD47^+$ cells and stimulated efficient natural killer (NK) cell-mediated lysis of AML compared to the conventional αCD123 antibody in vitro. Importantly, SIRPα-αCD123 fusion antibodies blocked CD47 locally on $CD123^+$ cells and induced phagocytosis of primary AML cells by allogeneic and autologous macrophages in vitro. Finally, the 2 × SIRPα-αCD123 antibody targeted LSCs that are capable of engrafting and reinitiating AML in an in vivo model.

Materials and methods

Expression and purification of the antibodies

αCD123 antibody light and heavy chain plasmids were generated by cloning the αCD123 variable light (V_L) and variable heavy (V_H) sequences of talacotuzumab [23] into the respective pFUSE2-CLIg-hK and pFUSE-CHIg-hG1 vectors (InvivoGen). For 1 × SIRPα-αCD123 and 2 × SIRPα-αCD123, one or two N-terminal SIRPα variant 1 immunoglobulin V-like domains (amino acids 31-149) were subcloned from a previously described construct [18] into the N-terminus of the αCD123 V_L using a $(Gly_4Ser)_4$ linker. The αCD19 V_L and V_H plasmids (clone 4G7) were cloned to generate the control molecules. The αCD47 (clone Hu5F9) V_L and V_H sequences [24] were subcloned into pFUSE2-CLIg-hK and pFUSE-CHIg-hG4, respectively. The SIRPα-Fc fusion construct (similar to TTI-621) [25] was generated by fusing the N-terminal V domain of human SIRPα variant 2 [26] to the human IgG1 Fc region of a pFUSE-CHIg-hG1 vector (InvivoGen). The plasmids were transfected into Expi293F cells (Thermo Fisher Scientific) according to the manufacturer's protocol. After five to seven days, the supernatant was harvested, and antibodies were purified by protein A affinity chromatography followed by size exclusion chromatography using a Superdex 200 increase 10/300 GL column (GE Healthcare). Antibodies were analysed by sodium dodecyl sulphate (SDS) polyacrylamide gel electrophoresis, and stability was measured using a Tycho NT.6 (NanoTemper Technologies). The coding sequence for the CD123 extracellular domain was amplified by PCR from complementary DNA of L-428 cells and subcloned into pSecTag2/HygroC containing a His_6-tag (Thermo Fisher Scientific). CD123 was expressed in Expi293F cells and purified by nickel affinity chromatography and size exclusion chromatography.

Surface plasmon resonance analysis

Binding of the αCD123 antibodies to CD123 was measured using a Biacore X100 (Biacore). Antibodies were captured on a CM5 sensor chip using the Human Antibody Capture Kit (both GE Healthcare). CD123 was used at concentrations of 3.91–1000 nM, and equilibrium dissociation constants (K_D) were calculated from the ratio of the rate constants (k_{off}/k_{on}) of the multicycle kinetics measurements using Biacore Evaluation software.

Cell lines

All cell lines were cultured under standard conditions. MOLM-13 and Raji cells were purchased from the Deutsche Sammlung von Mikroorganismen und Zellkulturen (DSMZ). Chinese hamster ovary (CHO) cells stably overexpressing human CD47 were previously generated [18]. Expi293F cells were obtained from Thermo Fisher

Scientific. Cell lines were routinely screened for mycoplasma contamination.

Patient and healthy donor material

At initial diagnosis or relapse, AML patient samples were characterized at the Laboratory for Leukemia Diagnostics of the Klinikum der Universität München as previously described [27–29]. Peripheral blood mononuclear cells (PBMCs) were isolated from healthy donor (HD) blood or residual cells of leukoreduction chambers by Biocoll (Biochrom). RBCs were collected from HD peripheral blood. Platelet-rich plasma (PRP) was isolated from HD peripheral blood by centrifugation at 200×*g* for 20 min at 25 °C. In the binding studies, platelets were isolated from PRP in the presence of prostaglandin E1 (Merck). For patient-derived xenograft (PDX) cells, AML patient cells were serially transplanted into NOD/SCID gamma null mice (NOD.Cg-Prkdc^{scid} IL2rg^{tm1Wjl}/SzJ, NSG). PDX cells were transduced with luciferase and mCherry lentiviral constructs for bioluminescence imaging [23]. For ex vivo experiments, PDX cells were grown in StemPro-34 medium with 2% FBS, L-glutamine and penicillin–streptomycin (all Gibco) supplemented with rhIL3, rhTPO, rhSCF (all Peprotech) and rhFLT3-ligand (R&D Systems). Patient characteristics are summarized in Table 1 and Additional file 1: Table S1.

Antibodies and flow cytometry

Commercial antibodies were from Biolegend (San Diego) unless otherwise stated. Human IgG1 isotype control (QA16A12) and αCD47 (B6H12, eBioscience) were used in binding, CD47 blocking and functional experiments. FITC or APC α human IgG (αhIgG, HP6017) was used for binding, and FITC αCD47 (B6H12, eBioscience) was used in CD47 blocking experiments for secondary staining. APC and FITC isotype (MOPC-21), APC αCD123 (6H6) and FITC αCD47 (B6H12) were used for surface expression analysis. Surface antigen density was evaluated using QIFIKIT (Agilent Technologies). Flow cytometry was performed using the Guava easyCyte 6HT (Merck Millipore), the Cytoflex LX (Beckman Coulter) or the BD LSRFortessa (Becton Dickinson). As a measure

Table 1 Patient characteristics

Patient	Age	Sex	Disease status	Karyotype	ELN genetic group	*FLT3*-ITD	*NPM1*
0276	29	F	ID	Aberrant	Adverse	wt	wt
2562	52	M	ID	Intermediate aberrant	n.a.	wt	wt
3140	74	M	ID	Normal	Intermediate	wt	wt
3073	54	M	R	Normal	Favourable	wt	wt
1233	49	F	ID	Complex aberrant	Adverse	mut	mut
3826	85	M	ID	Aberrant	Adverse	wt	wt
2449	30	F	ID	Aberrant	Favourable	wt	wt
4169	20	M	ID	Aberrant	Intermediate	wt	wt
0178	56	F	ID	Complex aberrant	Favourable	wt	wt
3386	52	M	ID	Normal	Favourable	wt	mut
3776	35	F	ID	Normal	Favourable	wt	wt
3221	59	M	ID	Normal	Favourable	wt	mut
3495	58	M	ID	Normal	Favourable	mut	wt
0885	74	F	ID	Normal	Intermediate	mut	mut
4321	50	F	ID	Normal	Intermediate	mut	mut
6789	68	M	ID	Normal	Favourable	mut	wt
0252	84	F	ID	Aberrant	Favourable	mut	mut
1421	66	F	ID	Aberrant/normal	Adverse	wt	wt
0682	56	F	ID	Complex aberrant	Adverse	wt	wt
7782	76	M	ID	Complex aberrant	Adverse	wt	wt
5964	87	F	ID	Complex aberrant	Adverse	wt	wt
AML-491 [3]	53	F	R	del(7)(q21)	Adverse	wt	wt
AML-579 [3]	51	M	R	Normal	Adverse	mut, LOH	mut
AML-640	79	M	R	t(11;15)	Intermediate	mut	mut
AML-979	56	F	R	Normal	n.a.	wt + mut subclone	mut

European LeukemiaNet (ELN), initial diagnosis (ID), relapse (R), not available (n.a.), wild type (wt), mutated (mut), loss of heterozygosity (LOH), female (F), male (M)

of antibody binding, the median fluorescence intensity (MFI) ratio was calculated by dividing the MFI of the tested antibody by the MFI of the corresponding isotype. Antibodies were considered to bind the cells if the intensity exceeded an MFI ratio of 1.5.

Competitive binding assays

PKH26 (Sigma-Aldrich)-labelled MOLM-13 was incubated with a 20-fold excess of red blood cells (RBCs) and antibodies. APC αhIgG (HP6017) or APC αmIgG (Poly4053) was used for secondary labelling. For assays with PBMCs, calcein AM (Thermo Fisher Scientific) or CellTrace™ calcein red-orange AM (Thermo Fisher Scientific)-labelled MOLM-13 cells were incubated with a fivefold excess of PBMCs and antibodies. APC or FITC αhIgG (HP6017) was used for secondary antibody labelling.

Platelet aggregation

PRP was centrifuged at 15,000×*g* for 2 min to obtain platelet-poor plasma (PPP). PRP was incubated in the presence of 100 nM antibodies, and absorbance was measured at 595 nm using an Infinite M100 plate reader (TECAN) for 16 min. The percentage of aggregation was calculated as $(\text{platelet aggregation}[\%] = 100 \times \frac{(\text{OD PRP - OD sample})}{(\text{OD PRP - OD PPP})})$ [30].

Antibody-dependent cellular phagocytosis (ADCP) assay

Monocytes were enriched using a classical monocyte isolation kit (Miltenyi) and were differentiated into macrophages in the presence of 100 ng/ml MCSF (Biolegend) for 5–7 days. Macrophages were labelled with calcein AM and incubated with CellTrace™ calcein red-orange AM-labelled target cells and antibodies at 50 pM or 50 nM for 3 h at 37 °C at a 1:1 effector-to-target (E:T) ratio.

Antibody-dependent cellular cytotoxicity (ADCC) assays

NK cells were enriched using a NK cell isolation kit (Miltenyi). MOLM-13 cells were labelled with calcein AM and incubated with NK cells and antibodies for 4 h at 37 °C at a 5:1 E:T ratio. In the competitive ADCC assay, NK cells were incubated with labelled MOLM-13 or Raji cells mixed with unlabelled Raji or MOLM-13 cells, respectively, at a 5:1:1 E:T:T ratio. Triton X-100 (2.5%, Sigma-Aldrich) was used for maximum lysis. Fluorescence intensity (FI) from calcein AM release was measured using an Infinite M100 plate reader, and lysis was calculated as $(\text{specific lysis}[\%] = 100 \times \frac{\text{FI}(\text{antibody stimulation}) - \text{FI}(\text{untreated})}{\text{FI}(\text{max}) - \text{FI}(\text{target})})$. Data were fitted to a four-parameter dose–response curve.

ADCC assays of AML patient samples were performed in α-MEM (Thermo Fisher Scientific) supplemented with 12.5% foetal calf serum, 12.5% horse serum, 1% penicillin, 1% streptomycin, 1% glutamine (Invitrogen) and a distinct cytokine cocktail on irradiated MS-5 cells in a long-term culture as described elsewhere [31, 32]. AML cells were incubated with HD NK cells and 10 nM antibodies for 20 h at 37 °C at a 5:1 E:T ratio. Dead cells were excluded as 7-AAD (BioLegend) or LIVE/DEAD™ Fixable Aqua (Thermo Fisher Scientific)-positive cells. $CD33^+$ or $CD123^+$ AML cells were determined by BV421, APC αhCD33 (WM53) or PE αhCD123 (6H6) labelling, respectively. Additionally, APC-Cy7 or FITC αhCD69 (FN50) and the corresponding isotype control (MOPC-21) were used to determine the percentage of $CD69^+$ cells. In some experiments, NK cells were labelled with CellTrace™ CFSE or CellTrace™ Far Red (both Thermo Fisher Scientific) according to the manufacturer's recommendations. Cell populations were assessed by flow cytometry, and the percentage of viable $CD33^+$ or $CD123^+$ AML cells was normalized to the human IgG1 isotype control sample. The percentage of $CD69^+$ cells was normalized to the human IgG1 isotype control sample.

In the AML PDX ADCC, AML-491, AML-979, and AML-640 were incubated with NK cells and 100 nM antibodies for 20 h at 37 °C at a 5:1 E:T ratio. Cells were labelled with LIVE/DEAD Fixable Aqua, and the proportion of live $mCherry^+$ cells was determined by flow cytometry and normalized to the isotype control.

In vivo engraftment experiments

To evaluate the targeting of AML cells with leukaemia-initiating properties, ex vivo NK cell-mediated ADCC was performed using the αCD123 antibody, the 2 × SIRPα-αCD123 fusion antibody or isotype antibody as a control, and surviving cells were used in an in vivo engraftment experiment. To this end, PDXs AML-491 and AML-579 [33, 34] were incubated with HD NK cells at an E:T ratio of 5:1 and antibodies for 20 h. After ADCC, residual $mCherry^+$ PDX cells were separated from NK cells and quantified by fluorescence-activated cell sorting (FACS) using a FACSAria III (BD Biosciences). According to previous data [34] and assuming that the isotype control antibody did not alter LIC frequency, we injected cell numbers corresponding to 10 leukaemia-initiating cells (10 × LIC, $n = 5$) and 100 × LIC ($n = 5$) for AML-491 or 14 × LIC ($n = 4$) and 140 × LIC ($n = 2$) for AML-579 by counting and diluting sorted cells of the isotype control suspensions. To enable comparison between the groups, equal volumes of αCD123 and 2 × SIRPα-αCD123 antibody ex vivo cell suspensions were sorted and injected intravenously into 10- to 12-week-old male (AML-491) or female (AML-579) NSG mice. Positive AML engraftment was analysed by in vivo

bioluminescence imaging (BLI), and total flux was quantified as previously described [33]. Mice exhibiting a total flux greater than 5×10^7 photons per second were classified as exhibiting positive engraftment; mice displaying no positive imaging signal within 28 weeks after transplantation were classified as negative for engraftment. To evaluate the percentage of human $CD33^+$ cells in peripheral blood, PE anti-human CD33 (WM53, BD Biosciences) and PE isotype control (MOPC-21, BD Biosciences) were used. Mice exhibiting any clinical signs of illness or end-stage leukaemia (total flux > 2×10^{10} photons/s; $hCD33^+$ cells in peripheral blood > 50%) were euthanized. Three mice died in narcosis during imaging and were counted as positive according to the last imaging signal or were excluded if not engrafted.

Data analysis

Statistical evaluation was performed using GraphPad Prism versions 6.07 and 8.1.2 (GraphPad). Datasets were analysed using one-way analysis of variance (ANOVA) including a test to determine equal variances within the groups and correction for multiple testing using Holm-Sidak's test. Chi-squared test was used to determine whether there is a statistically significant difference in the growth of engrafted AML PDX cells. A Kaplan–Meier plot was generated to depict AML engraftment and survival by treatment group, and significance was assessed using the log-rank Mantel-Cox test. Extreme limiting dilution analysis was performed using the injected cell number and number of AML engrafted mice as inputs as previously described [35] (Figure 7; Additional file 1: Table S2). The results were considered statistically significant at the following values and are marked in the figures as follows: p value < 0.05 (*), < 0.01 (**), < 0.001 (***), < 0.0001 (****).

Results

Generation and characterization of SIRPα-αCD123 fusion antibodies

The 1 × SIRPα-αCD123 recombinant antibody was generated by fusing the N-terminal SIRPα immunoglobulin V-like domain to the αCD123 antibody light chain via a flexible polypeptide linker (Fig. 1A). Likewise, for 2 × SIRPα-αCD123, a second SIRPα domain was connected to the N-terminus of 1 × SIRPα-αCD123 (Fig. 1A). Antibodies were produced in Expi293F cells, purified from cell culture supernatants and analysed by size exclusion chromatography and SDS–polyacrylamide gel electrophoresis (Additional file 1: Figure S1A-B). Thermal stability was assessed by measuring changes in the intrinsic fluorescence of the proteins using Tycho NT.6 (Additional file 1: Figure S1C). To investigate whether the N-terminal fusion of the SIRPα domains alters the binding to CD123, we determined the K_D values using a Biacore assay. The K_D values were in the low nanomolar range for all constructs, indicating that the high affinity for CD123 was not affected by the fusion of the SIRPα domains (Fig. 1B). We further evaluated binding of the antibodies to CHO cells stably overexpressing human CD47 (hCD47) by flow cytometry (Table 2). As expected, 1 × SIRPα-αCD123 and 2 × SIRPα-αCD123 bound to $^+$CHO_$hCD47^+$ cells but not to $^-$CHO_$hCD47^-$ cells (Fig. 1C). These binding experiments indicate that the αCD123 and SIRPα domains can bind to their respective targets in the fusion antibody.

SIRPα-αCD123 fusion antibodies specifically bind to $CD123^+CD47^+$ AML cells

Next, we used the $CD123^+$ $CD47^+$ AML cell line MOLM-13 in a flow cytometry-based binding assay to study the dual targeting properties of the antibody constructs (Fig. 2A, Table 2). The binding of 1 × SIRPα-αCD123 and 2 × SIRPα-αCD123 to MOLM-13 cells was stronger than that of the αCD123 antibody, indicating a contribution by the SIRPα domain. The αCD19 SIRPα fusion antibodies mediated only weak binding to $CD19^-$ MOLM-13 cells due to some low binding of the SIRPα domains (Fig. 2A, Table 2). In summary, we hypothesize that the strong binding of the SIRPα-αCD123 antibodies to MOLM-13 cells is due to avidity-dependent binding to both CD123 and CD47.

The physiological interaction of the SIRPα domain and CD47 is approximately 100-fold weaker than the affinity of the αCD123 antibody for CD123 [26, 36]. Therefore, we postulated that the high affinity αCD123 drives the preferential binding of SIRPα-αCD123 fusion antibodies onto $CD123^+CD47^+$ leukemic cells over $CD123^-CD47^+$ healthy cells. To test this hypothesis, we first utilized RBCs as highly abundant healthy cells expressing CD47 (Fig. 2B, Table 2).

We observed selective binding to MOLM-13 cells using the 1 × SIRPα-αCD123 antibody even in the presence of a 20-fold excess of RBCs (Fig. 2B, C). 2 × SIRPα-αCD123, on the other hand, was also detected on the surface of RBCs, indicating that the additional SIRPα domains can increase the competition between $CD47^+$ MOLM-13 cells and RBCs (Fig. 2B, C). Nevertheless, the RBC targeting observed for 2 × SIRPα-αCD123 was very weak, with a binding intensity far below an MFI ratio of 1.5 (Fig. 2D). In contrast, the high affinity αCD47 B6H12 antibody demonstrated a substantial on-target off-leukaemia effect, as it primarily bound to RBCs with a high MFI ratio (Fig. 2B–D). We concluded that despite carrying the SIRPα domains, the SIRPα-αCD123 fusion antibodies target MOLM-13 cells more than the high affinity αCD47 and avoid the antigen sink generated by the RBCs.

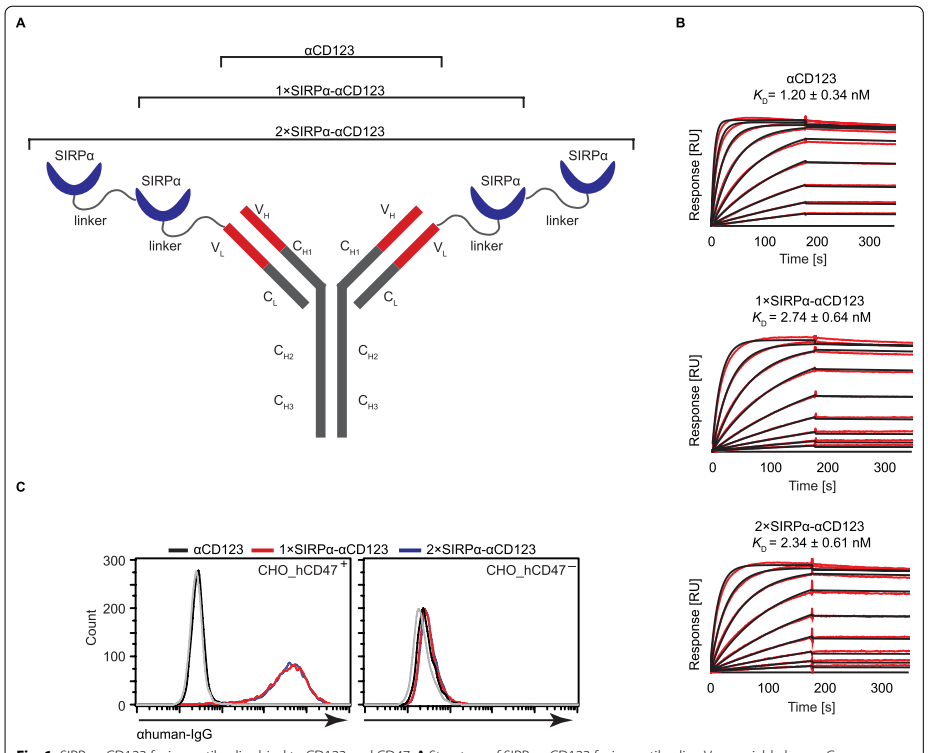

Fig. 1 SIRPα-αCD123 fusion antibodies bind to CD123 and CD47. **A** Structure of SIRPα-αCD123 fusion antibodies. V_H—variable heavy, C_L—constant light, C_{H1}—constant heavy 1, C_{H2}—constant heavy 2, C_{H3}—constant heavy 3. **B** Different CD123 concentrations binding to the antibody constructs measured using SPR. Raw data are shown in red; black curves were fitted to a 1:1 interaction. K_D values represent mean values from $n = 3$ independent experiments ± standard error of the mean (SEM). **C** Binding of antibodies to CHO_hCD47$^+$ and CHO_hCD47$^-$ cells at 100 nM concentration measured by flow cytometry. The grey line indicates nonspecific staining of the isotype control and secondary antibody. Histograms show 1 of 3 experiments with similar results

Table 2 Antigen expression levels

Cell type	CD123	CD47	CD19
MOLM-13	13 723 ± 1 108	67 703 ± 3 784	30 ± 2
Raji	94 ± 95	170 868 ± 37 029	141 688 ± 19 997
CHO^{CD47+}	104 ± 68	1 424 894 ± 329 869	n. d.
CHO^{CD47-}	159 ± 50	532 ± 35	n. d.
RBC	106 ± 33	33 841 ± 2 221	n. d.

Determined using QIFIKIT. Data are shown as the means ± SEM ($n = 2$–3). Not determined (n. d.)

In another set of experiments, we investigated the selective binding of our antibodies to MOLM-13 cells in the presence of HD PBMCs (Fig. 2E). From PBMCs, plasmacytoid dendritic cells express CD123 and are targeted by the αCD123 antibody CSL362 [37]. We also found that some of our αCD123 binds to PBMCs; however, the majority of the antibodies still bound to MOLM-13 cells (Fig. 2E). The 1 × SIRPα-αCD123 antibody bound PBMCs to a considerable extent, but higher selective binding to MOLM-13 cells was observed compared to the αCD47 Hu5F9-G4 clone. 2 × SIRPα-αCD123 targeted MOLM-13 cells similarly to αCD47 Hu5F9-G4. However, when we analysed binding of the antibodies to PBMCs

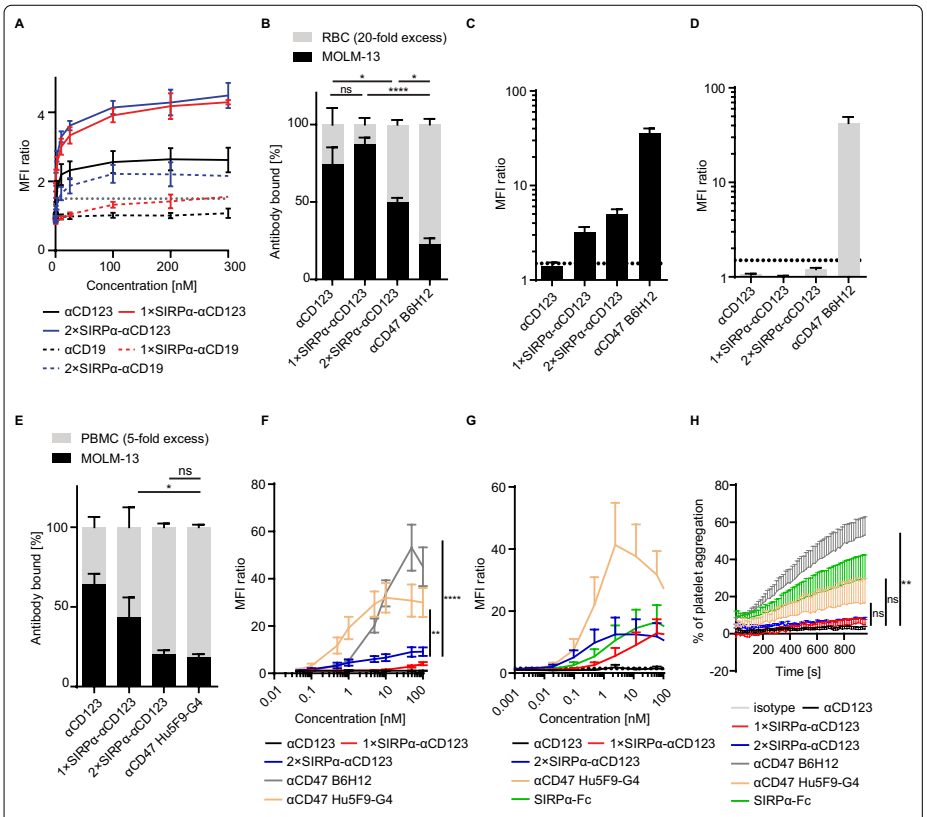

Fig. 2 SIRPα-αCD123 fusion antibodies preferentially bind to MOLM-13 cells in the presence of RBCs. **A** Binding of SIRPα-αCD123 fusion antibodies to MOLM-13 cells assessed by flow cytometry-based MFI ratio. The dotted line indicates an MFI ratio of 1.5 as the cut-off for positivity. Shown are the mean values from $n = 2$–3 independent experiments ± SEM. **B** Percentage of 100 nM antibodies targeting MOLM-13 cells or RBCs measured by flow cytometry at a 20-fold excess of RBCs. **C** MFI ratios of antibody binding to MOLM-13 cells in the presence of a 20-fold excess of RBCs. **D** MFI ratios of antibody binding to RBCs in the presence of MOLM-13 cells. The results of independent experiments with 4 different RBC donors represented as the mean ± SEM are shown. **E** Percentage of 100 nM antibodies targeting MOLM-13 cells or PBMCs measured by flow cytometry at a fivefold excess of PBMCs. Shown are mean values from $n = 6$ donors ± SEM. **F** Binding of SIRPα-αCD123 fusion antibodies to PBMCs assessed by flow cytometry-based MFI ratio. Shown are mean values from $n = 5$ donors ± SEM. **G** Binding of SIRPα-αCD123 fusion antibodies to platelets assessed by flow cytometry-based MFI ratio. Mean values from $n = 4$ donors ± SEM are shown. **H** Platelet aggregation induced by 100 nM antibody over time. Mean values from $n = 4$ donors ± SEM are shown. **F** and **H** p values are the same for both SIRPα-αCD123 fusion antibodies. Statistical differences were determined by one-way ANOVA using Holm–Sidak's post hoc test. *$p < 0.05$, **$p < 0.01$, ***$p < 0.001$, ****$p < 0.0001$

alone, we observed that our fusion antibodies bound PBMCs significantly less than the αCD47 Hu5F9-G4 and B6H12 antibodies (Fig. 2F). These data indicate that although our fusion antibodies seem to target PBMCs more than RBCs, they bind to PBMCs to a lesser extent than the high affinity αCD47 antibodies.

In addition to binding to RBCs, CD47-targeting agents have been reported to bind platelets and interfere with their function [38, 39]. We therefore investigated whether our SIRPα-αCD123 fusion antibodies target platelets and induce their aggregation (Fig. 2G–H). Indeed, SIRPα-αCD123 fusion antibodies bound to platelets similarly to

the SIRPα-Fc construct but less than the αCD47 Hu5F9-G4 control (Fig. 2G). However, SIRPα-αCD123 antibodies did not induce aggregation of platelets, unlike SIRPα-Fc, αCD47 Hu5F9-G4 and especially αCD47 B6H12 antibodies (Fig. 2H). These experiments suggest that binding of the constructs does not directly correlate with a functional effect and indicate that our SIRPα-αCD123 fusion antibodies do not stimulate platelet aggregation.

SIRPα-αCD123 fusion antibodies block CD47 and induce phagocytosis of MOLM-13 cells in vitro

SIRPα-αCD123 fusion antibodies were designed to inhibit the CD47-SIRPα axis locally on $CD123^{+}$ cells. To examine this, we performed a blocking assay using labelled αCD47 antibodies that interfere with the binding of SIRPα. Despite the weak affinities of the SIRPα domains, 1 × SIRPα-αCD123 and 2 × SIRPα-αCD123 were able to block CD47 molecules on MOLM-13 cells. Not surprisingly, maximum blockade was observed with the high affinity αCD47 antibody. In comparison, 1 × SIRPα-αCD123 did not block CD47 on $CD123^{-}$ Raji cells, and 2 × SIRPα-αCD123 minimally blocked CD47 (Additional file 1: Figure S2A), indicating that binding of the αCD123 moiety to target cells is required for efficient disruption of the CD47-SIRPα axis.

We next examined whether CD47 blockade with concomitant engagement of FcγRs stimulates the ADCP of MOLM-13 cells by HD-derived macrophages (Fig. 3B). Indeed, phagocytosis was significantly boosted by 1 × SIRPα-αCD123 compared to αCD123. 2 × SIRPα-αCD123 also induced elevated phagocytosis, but this was not statistically significant. In contrast, αCD47 did not stimulate phagocytosis either alone or in combination with αCD123 in this setting. The respective αCD19 controls did not have an effect on phagocytosis. In summary, SIRPα-αCD123 fusion antibodies boost ADCP in MOLM-13 cells, whereas αCD123 and αCD47 antibodies alone lack this ability.

SIRPα-αCD123 fusion antibodies induce enhanced phagocytosis of patient-derived AML cells by allogeneic and autologous macrophages in vitro

We further investigated the stimulation of phagocytosis by SIRPα-αCD123 antibodies using primary AML patient-derived blasts as targets and allogeneic or autologous monocyte-derived macrophages as effector cells (Fig. 4A, B). We observed enhanced overall phagocytosis by primary AML cells compared to MOLM-13 cells. Allogeneic macrophages from HDs mediated significantly higher ADCP with the 1 × SIRPα-αCD123 fusion antibody compared to αCD123. The 2 × SIRPα-αCD123 had a similar effect (Fig. 4A). More importantly, these results were confirmed in the autologous setting (Fig. 4B). Phagocytosis mediated by 1 × SIRPα-αCD123 and 2 × SIRPα-CD123 was significantly higher than that mediated by αCD123. αCD47 antibodies B6H12 and Hu5F9-G4 alone or in combination with αCD123 antibody induced similar ADCP as SIRPα-αCD123 fusion antibodies. When comparing SIRPα-CD123 fusion antibodies to similar αCD33-based constructs [18], we did not observe significant differences in the ability to induce phagocytosis of AML cells (Fig. 4B). Taken together, these data reveal that SIRPα-αCD123 fusion antibodies

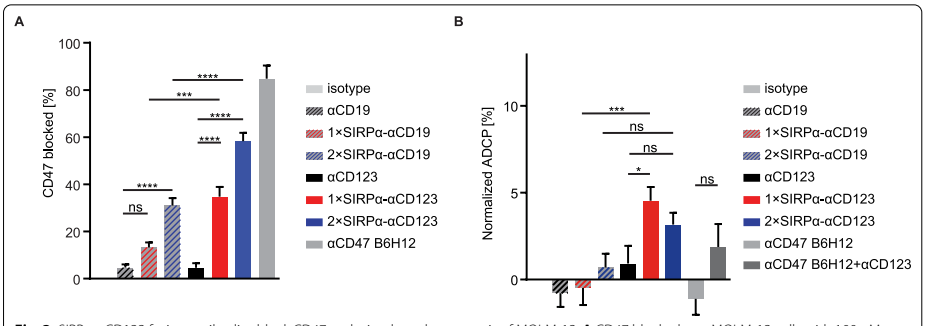

Fig. 3 SIRPα-αCD123 fusion antibodies block CD47 and stimulate phagocytosis of MOLM-13. **A** CD47 blockade on MOLM-13 cells with 100 nM antibodies determined by FITC αCD47 binding using flow cytometry. Background fluorescence was subtracted from the FITC αCD47 signal and normalized to isotype to calculate the CD47 blockade. Mean ± SEM of $n = 4$ independent experiments. **B** ADCP of MOLM-13 cells at a 50 pM concentration of antibodies after 3 h at an E:T ratio of 1:1. ADCP was measured as the percentage of double-positive cells from macrophages and normalized to the isotype control. Bar charts represent the mean ± SEM from $n = 7$ different donors. Statistical differences were determined by one-way ANOVA using Holm-Sidak's post hoc test. *$p < 0.05$, ***$p < 0.001$, ****$p < 0.0001$, not significant (ns)

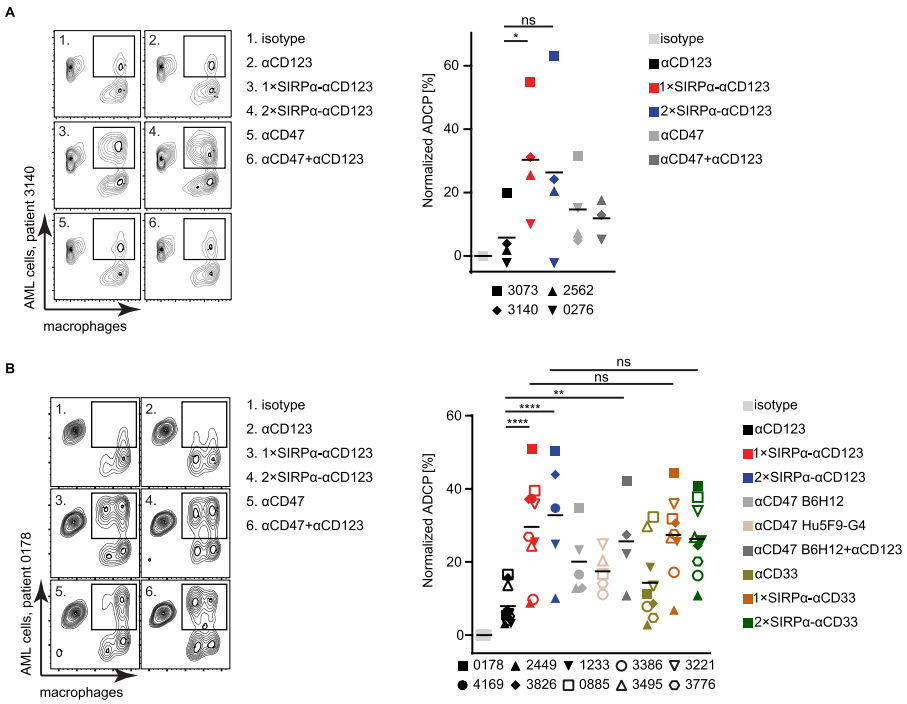

Fig. 4 SIRPα-αCD123 fusion antibodies stimulate phagocytosis of AML patient cells by allogeneic and autologous macrophages. AML target cells and macrophages were incubated with 50 nM antibody for 3 h at an E:T ratio of 1:1. ADCP was measured as the percentage of double-positive cells (gated) from all macrophages. Each symbol represents one patient (Table 1). **A** Phagocytosis of AML patient cells by allogeneic macrophages ($n = 4$). **B** Phagocytosis of AML patient cells by autologous macrophages ($n = 10$). Statistical differences were determined by one-way ANOVA using Holm-Sidak's post hoc test. *$p < 0.05$, ****$p < 0.0001$, not significant (ns)

represent an effective tool to overcome the CD47-mediated inhibition of phagocytosis in AML.

SIRPα-αCD123 fusion antibodies induce NK cell-mediated specific lysis of AML cells in vitro

ADCC by NK cells is one of the primary mechanisms by which IgG1 antibodies induce the elimination of antibody-bound cells in addition to macrophage-mediated ADCP [40]. Therefore, we analysed specific lysis of MOLM-13 cells by HD-derived NK cells (Fig. 5A). αCD123 induced moderate dose-dependent lysis of MOLM-13, whereas 1 × SIRPα-αCD123 and 2 × SIRPα-αCD123 were more potent. We postulated that SIRPα-αCD123 fusion antibodies are more efficient due to the avidity-dependent targeting of both CD123 and CD47. The respective αCD19 controls induced lysis of MOLM-13 cells only at high concentrations, which can be attributed to autonomous targeting of CD47 by the fused SIRPα domain. Nevertheless, the half maximal effective concentration (EC_{50}) was considerably lower for 2 × SIRPα-αCD123 (19.1 pM) than for the 2 × SIRPα αCD19 analogue (192.1 pM), demonstrating target antigen-specific cytotoxicity. This was further demonstrated in a competitive ADCC assay in which $CD123^{+}$ MOLM-13 cells were mixed with $CD123^{-}$ Raji cells (Additional file 1: Figure S2B). In this setting, Raji cells were not lysed by 1 × SIRPα-αCD123 and 2 × SIRPα-αCD123 only exerted an effect at high concentrations. In summary, although independent binding of the SIRPα domains can cause some lysis of target cells at high concentrations, we

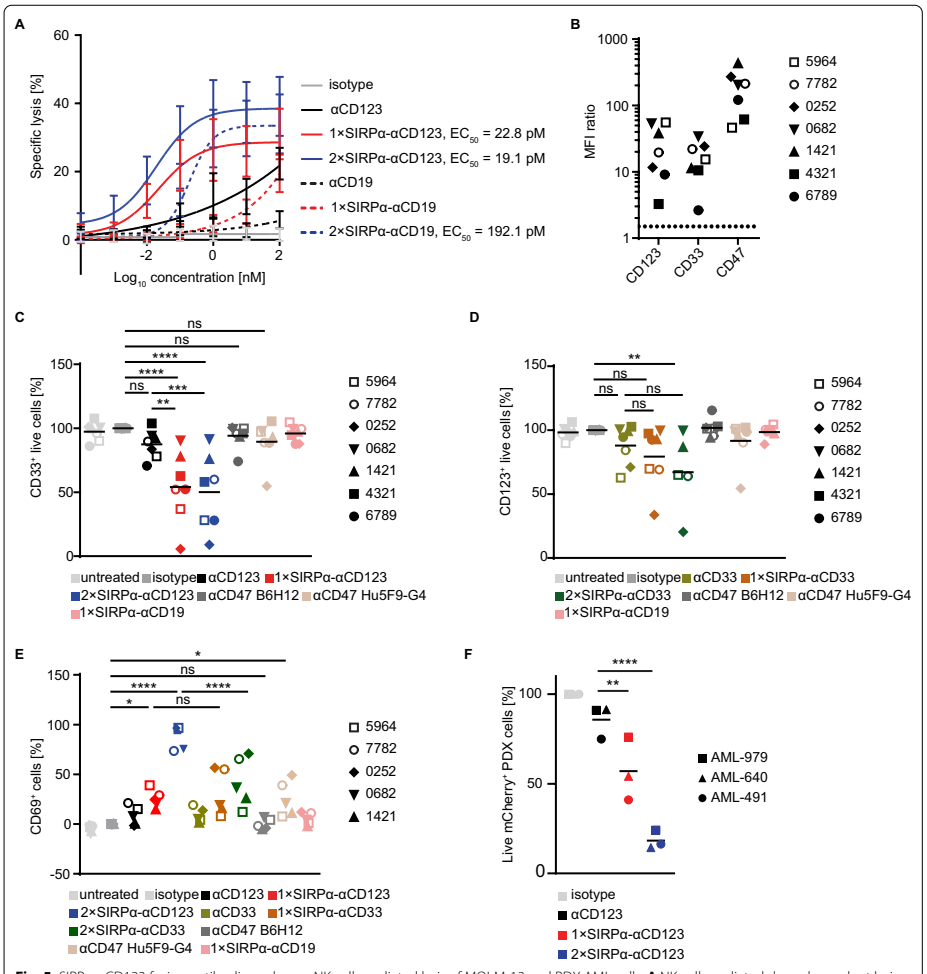

Fig. 5 SIRPα-αCD123 fusion antibodies enhance NK cell-mediated lysis of MOLM-13 and PDX AML cells. **A** NK cell-mediated dose-dependent lysis of MOLM-13 cells after 4 h at an E:T ratio of 5:1 measured by calcein AM release. Mean values ± SEM for $n = 6$ different NK cell donors are shown. EC_{50} values were calculated where possible. **B** Expression of CD123, CD33 and CD47 in primary AML samples assessed by flow cytometry. **C**, **D** NK cell-mediated lysis of AML cells in long-term culture at a 10 nM antibody concentration after 20 h at an E:T ratio of 5:1 measured by flow cytometry. The results from $n = 7$ different AML patient samples are represented as different symbols, and their mean values are shown. **E** Percentage of $CD69^+$ cells measured by flow cytometry. **F** NK cell-mediated lysis of PDX cells at 100 nM antibody concentration after 20 h at an E:T ratio of 5:1 measured by flow cytometry. The results from $n = 3$ different AML patient samples are represented as different symbols, and their mean values are shown. Statistical differences were determined by one-way ANOVA using Holm-Sidak's post hoc test. *$p < 0.05$, **$p < 0.01$, ***$p < 0.001$, ****$p < 0.0001$

consider high affinity αCD123 binding to be a prerequisite for targeting by SIRPα-αCD123 fusion antibodies.

The ability of SIRPα-αCD123 fusion antibodies to activate NK cells was further investigated using AML patient cells. First, we used blasts from primary AML patients (Fig. 5B) in a long-term culture system with HD-derived NK cells as effectors [31]. Compared to isotype controls and αCD123, 1 × SIRPα-αCD123 and 2 × SIRPα-αCD123 antibodies significantly boosted the cytotoxicity by NK cells, leading to reduced numbers of AML cells (Fig. 5C). As expected, the αCD47 antibodies B6H12 and Hu5F9-G4 and the 1 × SIRPα αCD19 control molecule did not stimulate lysis of AML cells (Fig. 5C). From the αCD33 constructs, only the 2 × SIRPα αCD33 analogue induced significant lysis of AML cells compared to the isotype control (Fig. 5D). When analysing the NK cell population of the ADCC samples, we observed a significant upregulation of the activation marker CD69 with 1 ×- and 2 × SIRPα-αCD123 (Fig. 5E). Treatment with 2 × SIRPα-αCD123 induced especially potent CD69 upregulation, which was also significantly greater than that induced by the 2 × SIRPα αCD33 analogue (Fig. 5E). Interestingly, the αCD47 antibody Hu5F9-G4 induced slight upregulation of CD69 (Fig. 5E). Together, these results demonstrate that in addition to highly effective FcγR-dependent ADCC stimulation, SIRPα-αCD123 antibodies might further activate NK cells via mechanisms related to CD47 blockade.

Next, we used AML PDX cells as target cells. Here, we observed that 1 × SIRPα-αCD123 and 2 × SIRPα-αCD123 both dramatically increased the lysis of AML PDX cells compared to αCD123 (Fig. 5E). This again highlights that our fusion antibodies enhance NK cell-mediated lysis of patient-derived AML cells.

SIRPα-αCD123 fusion antibodies have the potential to target AML stem cells

Specific targeting of AML LSCs is needed to prevent relapse and enhance the rate and duration of response to therapy in patients. We hypothesized that SIRPα-αCD123 fusion antibodies would efficiently eliminate $CD123^{high}$ $CD47^{high}$ LSCs due to the avidity-dependent binding of the αCD123 and SIRPα moieties. Xenograft mouse models have been widely used to investigate leukaemia-initiating cells (LICs) as surrogates for LSCs [41, 42]. To evaluate the impact of HD NK cell-dependent cytotoxicity of our antibodies on LICs, we performed an in vivo engraftment assay using residual AML PDX cells that survived an ex vivo ADCC assay (Fig. 6A). We expect that LICs are killed more efficiently with SIRPα-αCD123 fusion antibodies than with αCD123 antibodies in the ex vivo ADCC assay and thus lead to reduced engraftment of AML cells. To this end, PDX cells from two AML patients were incubated with NK cells and isotype control, αCD123 or 2 × SIRPα-αCD123 (Additional file 1: Figure S3). Only the 2 × SIRPα-αCD123 fusion antibody was used as it showed superior killing of AML PDX cells (Fig. 5F). After this ADCC, surviving PDX cells were sorted and injected into NSG mice at two doses corresponding to 10 leukaemia-initiating cells (10 × LIC) or 100 × LIC. AML engraftment was analysed by in vivo BLI and peripheral blood analysis.

As expected, all mice that received residual cells from isotype control-treated AML-491 ADCC culture exhibited PDX cell engraftment soon after transplantation [10 × LIC: 28–49 days post injection (dpi), $n = 5$; 100 × LIC: 33 dpi, $n = 5$], whereas treatment with the αCD123 antibody slightly delayed the time to positive engraftment (10 × LIC: 62–91 dpi, $n = 5$; AML-491 100 × LIC: 49 dpi, $n = 4$) (Fig. 6B–F). Importantly, residual cells from 2 × SIRPα-αCD123 ADCC cultures exhibited a dramatically reduced engraftment capacity, with only one animal in the 10 × LIC group (114 dpi) and none in the 100 × LIC group showing positive engraftment (Fig. 6B–F). All mice with positive engraftment reached end-stage leukaemia with high BLI signals and $hCD33^{+}$ cells in peripheral blood (Fig. 6; Additional file 1: Figure S5). AML-579 cells were injected at slightly higher doses of 14 × LIC and 140 × LIC, but the results were similar to those observed for AML-491 (Additional file 1: Figures S4 and S5).

We used the extreme limiting dilution analysis algorithm to determine whether the nearly absent engraftment in the 2 × SIRPα-αCD123 condition was due to specific LIC targeting or a lower number of injected residual cells [35]. Even though all mice in the isotype and αCD123 treatment groups exhibited engraftment, a significant difference in the estimated LIC frequencies was detected between αCD123 and 2 × SIRPα-αCD123 for AML-491 (Fig. 7A, B; Additional file 1: Table S2). We concluded that while 2 × SIRPα-αCD123 markedly reduces the number of bulk AML cells, it targets leukemic stem cells with an even higher preference.

Discussion

The ubiquitously expressed surface marker CD47 interacts with the SIRPα receptor to inhibit myeloid cell-mediated phagocytosis of autologous cells [4, 14, 15]. Blocking the CD47-SIRPα checkpoint as an anticancer therapy is under intense investigation since CD47 is overexpressed on AML as well as on various other cancer types [5, 10, 43]. However, ubiquitous expression of CD47 creates an antigen sink that can sequester CD47-targeting agents and reduce the effective dose. Moreover, nonspecific targeting can cause toxicities to healthy cells, as CD47 has various roles in physiological tissue homeostasis [44]. For

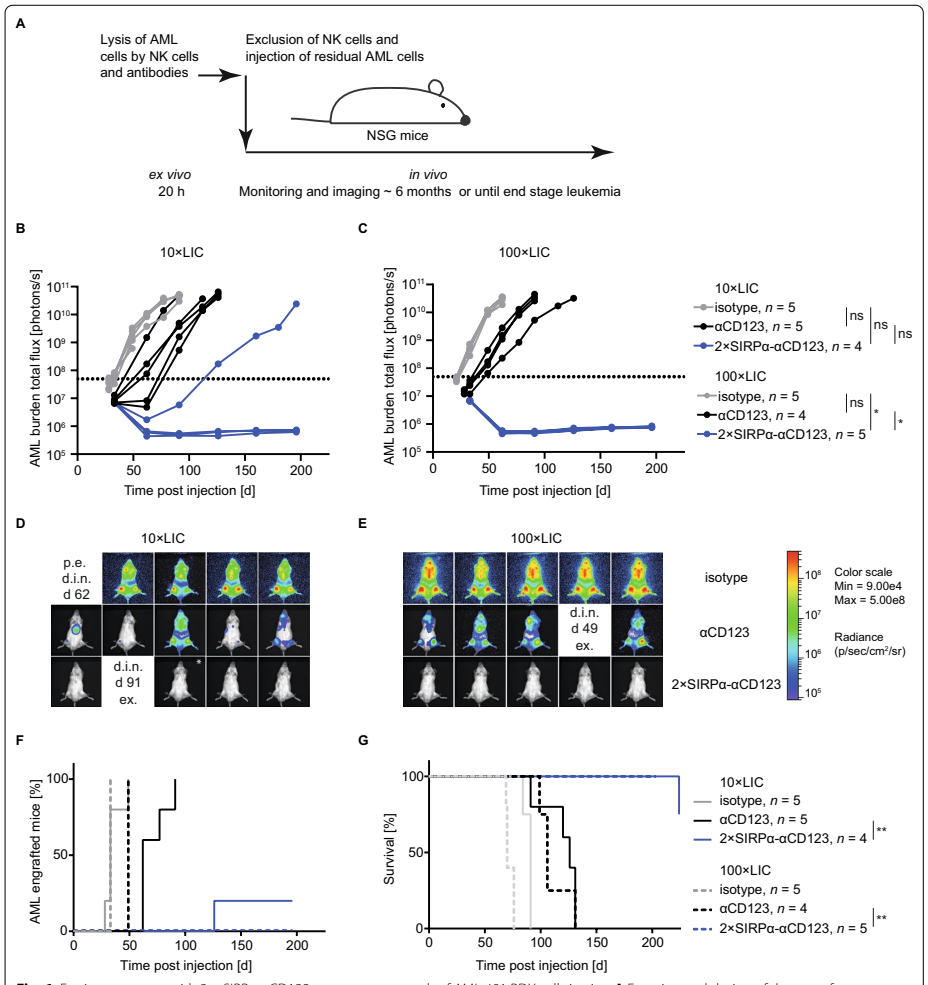

Fig. 6 Ex vivo treatment with 2 × SIRPα-αCD123 prevents outgrowth of AML-491 PDX cells in vivo. **A** Experimental design of the engraftment assay. Residual AML cell from ADCC in (Additional file 1: Figure 3A, B) was FACS sorted, and equal volumes were injected intravenously into NSG mice. Mice were monitored using in vivo BLI. **B**, **C** AML burden in individual mice of the 10 × LIC and 100 × LIC groups measured by BLI. The dotted line indicates a total flux of 5×10^7 photons/s as the cut-off for evaluating positive AML engraftment. Statistical analysis was performed using Chi-squared test. Representative images of mice injected with 10 × LIC (**D**) and 100 × LIC (**E**) on day (d) 62. Mice that died in narcosis during imaging (d.i.n.) were counted as positive if the last imaging signal showed positive engraftment (p. e.) or were excluded from analysis (ex.) if not engrafted. **F** Kaplan–Meier curve of AML-491 engraftment analysed by BLI. (**G**) Kaplan–Meier curves showing survival of mice. Statistical significance was calculated using the log-rank test. $*p < 0.05$, $**p < 0.01$, not significant (ns)

A

	Injected cells	Mice injected / engrafted	Estimated LIC frequency (95% confidence interval)
isotype	180 000	5 / 5	1/1 (1/1-1/22 575)
	18 000	5 / 5	
αCD123	26 000	4 / 4	1 / 1 (1/1-1/3 261)
	2 600	5 / 5	
2×SIRPα-αCD123	4 000	5 / 0	1 / 21 399 (1/2 786-1/164 397)
	400	4 / 1	

B

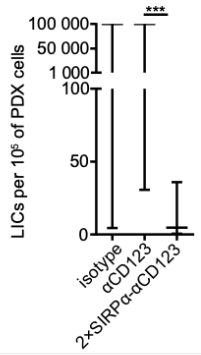

Fig. 7 LIC frequencies of AML-491 after NK cell-mediated lysis with the 2 × SIRPα-αCD123 fusion antibody. **A** Engraftment at each injected cell dose for each antibody. Residual AML cells were counted during cell sorting before injection. **B** LIC frequencies were estimated using extreme limiting dilution analysis software [35]. Horizontal lines indicate the estimated LIC frequencies, and the bars indicate 95% confidence intervals

example, the CD47 ligand SIRPγ is expressed on human T cells, and targeting CD47 with a mAb has been shown to affect human T cell responses [45].

The most serious side effects reported from CD47-targeting agents in clinical trials are anaemia and thrombocytopenia [39, 46–49]. The SIRPα-αCD123 antibodies presented here specifically bind to the AML cell line MOLM-13 in the presence of excess RBCs, in contrast to the high-affinity CD47-targeting antibody B6H12. These results agree with previous reports where similar constructs targeting CD33 and CD20 avoid the CD47 sink generated by RBCs [17, 18]. We also observed that SIRPα-αCD123 antibodies targeted PBMCs more than RBCs. The low-affinity SIRPα-dependent binding to PBMCs might, however, not lead to activation of macrophages or NK cells based on our results with SIRPα-αCD19 control molecules in experiments with MOLM-13 cells and primary AML cells. Importantly, although the SIRPα-αCD123 fusion antibodies also bind platelets, they do not induce any aggregation, unlike other CD47-targeting molecules tested herein. The underlying reason for this might be a combination of relatively low-affinity binding of the SIRPα domain to CD47 as well as different steric features of the antibody constructs.

Despite the low-affinity binding of the SIRPα domains, SIRPα-αCD123 fusion antibodies were able to induce the same or even higher phagocytosis than high affinity αCD47 either alone or in combination with αCD123. This is in line with the well-known synergy between CD47-SIRPa axis disruption and prophagocytic signals [8, 10, 50–52] and supports the rationale of combining CD47 blockade and FcγR stimulation into one molecule.

AML LSCs reside in specific niches in the bone marrow [53]. Antibodies can freely access the bone marrow through sinusoidal clefts and therefore represent a promising therapeutic strategy for targeting LSCs in their microenvironment [54]. CD33-targeting gemtuzumab ozogamicin is currently the only antibody-based therapy approved for AML [55]. Unfortunately, only some patients are likely to benefit from gemtuzumab ozogamicin [56, 57]. CD33/CD47 cotargeting has been previously preclinically investigated [18, 58]. However, bivalent mAbs against CD33 have been shown to internalize upon cross-linking, which can compromise the immune response [59, 60]. Expression of CD33 on LSCs is also associated with variability, which might affect therapeutic outcomes [20, 61]. Our results indicate that the SIRPα-αCD123 constructs are comparable to αCD33-based fusion antibodies in inducing autologous ADCP or allogenic ADCC. Interestingly, we observed much higher activation of NK cells in response to 2 × SIRPα-αCD123 than with the αCD33 analogue. Whether this was due to CD33-related internalization effects or other reasons remains to be investigated, but we consider αCD123-based constructs promising candidates next to αCD33-targeting antibodies.

Because chemorefractory LSCs build a reservoir for relapse, elimination of these cells is essential for AML treatment [1, 2]. In younger adults, a lower percentage of $CD123^{+}$ LSCs at diagnosis is correlated with a better response to treatment and survival [62]. Similarly, in

older patients who are fit for intensive chemotherapy, survival was higher in those who displayed lower levels of $CD123^+$ LSCs [63]. Therefore, eliminating or reducing the numbers of $CD123^+$ LSCs might lead to more durable responses and prolonged survival. We show here that compared to αCD123, SIRPα-αCD123 antibodies exhibit increased targeting efficacy of $CD123^+$ $CD47^+$ AML cells due to avidity-dependent binding to both antigens. Our fusion antibodies could take advantage of the high expression of both CD123 and CD47 on LSCs and effectively address this population. Indeed, we observed an extreme reduction in the engraftment of AML after an ex vivo ADCC assay with the 2 × SIRPα-αCD123 antibody, as our antibodies stimulated NK cell-mediated cytotoxic lysis of AML LSCs. The increased avidity of SIRPα-αCD123 antibodies thus provides the opportunity to preferentially target and eliminate AML LSCs.

Because of avidity-dependent binding to CD123 and CD47, SIRPα-αCD123 antibodies could further target malignant LSCs cells over healthy haematopoietic stem cells, which express low levels of CD47 and minimal amounts of CD123 [5, 19, 21, 64]. The 2 × SIRPα-αCD123 fusion antibody facilitated the most potent NK cell activation in our assays, and only this antibody was evaluated in LSC targeting experiments. To further analyse the safety and efficacy of the molecules and to determine whether the 1 ×- or 2 × SIRPα-αCD123 fusion format would be favourable in future clinical trials, assessing competitive targeting of patient-derived LSCs and healthy haematopoietic stem cells would be very pertinent.

While we are the first to combine CD123 and CD47 targeting, other therapeutic molecules have been developed against CD123 alone [65–67]. Talacotuzumab is an αCD123 antibody with a modified Fc region for enhanced ADCC [37, 68]. Unfortunately, talacotuzumab showed limited in vivo efficacy in clinical studies, which has been associated with the compromised NK cell activity in MDS and AML [69–71]. This suggests that recruiting other immune cells, such as macrophages, could stimulate a broader response to antibody-based CD123-targeting therapies. The benefit of activating macrophages in AML has been demonstrated by the αCD47 antibody magrolimab in combination with azacytidine [8]. Recent data additionally suggest that upon activation, NK cells can upregulate SIRPα, which leads to strong inhibition of cytotoxicity when interacting with CD47 on the surface of target cells [72]. An effective blockade of CD47 signalling could therefore be the reason we observed an extremely potent upregulation of CD69 on NK cells in response to 2 × SIRPα-αCD123 treatment. This was also indicated by the slight increase in the percentage of $CD69^+$ cells when the αCD47 antibody Hu5F9-G4 was used. A growing body of evidence indicates that adaptive immunity, especially the activation of $CD8^+$ T cells, further contributes to the effects observed in response to CD47-SIRPα inhibition [73–75]. As SIRPα-αCD123 fusion antibodies improve phagocytosis of AML patient cells compared to αCD123 while still initiating strong NK cell activation, we propose that SIRPα-αCD123 fusion antibodies stimulate a much broader immune response, including a long-lasting T-cell response.

Conclusions

In summary, we demonstrated that SIRPα-αCD123 antibodies specifically target LSCs, mediate their efficient clearance and stimulate phagocytosis of AML while restricting CD47-related on-target off-leukaemia toxicity. These encouraging results establish SIRPα-αCD123 antibodies as a promising approach for LSC targeting for prolonged remission in AML patients. Future in vivo studies using an appropriate AML mouse model are necessary for the translation of this approach into a clinical setting.

Abbreviations

AML: Acute myeloid leukaemia; LSC: Leukemic stem cell; SIRPα: Signal regulatory protein alpha; FcγR: Fcγ receptor; MDS: Myelodysplastic syndrome; OR: Objective response; CR: Complete remission; NK: Natural killer; V_L: Variable light; V_H: And variable heavy; SDS: Sodium dodecyl sulphate; EC_{50}: Half maximal effective concentration; PCR: Polymerase chain reaction; K_D: Equilibrium dissociation constant; CHO: Chinese hamster ovary; PBMC: Peripheral blood mononuclear cells; PDX: Patient-derived xenograft; NSG: NOD/SCID gamma null mice; MFI: Median fluorescence intensity; RBC: Red blood cells; E:T: Effector-to-target; LIC: Leukaemia-initiating cell; BLI: Bioluminescence imaging; ANOVA: Analysis of variance; ADCP: Antibody-dependent cellular phagocytosis; ADCC: Antibody-dependent cellular cytotoxicity; HD: Healthy donor; FACS: Fluorescence-activated cell sorting.

Supplementary Information

The online version contains supplementary material available at https://doi.org/10.1186/s13045-021-01163-6.

Additional file 1. Supplementary tables and figures.

Acknowledgements

The authors are grateful to Bettina Brauchle for help with the AML patient material and to Manuel Albanese, Marcel Stern and Oliver Keppler for help with the leukoreduction chamber material. We thank Maike Fritschle and Fabian Klein for technical assistance in the in vivo experiment, Daniel Bergér for help with the assay setup and Vindi Jurinovic for advice on statistical analysis. We acknowledge the iFlow Core Facility of the university hospital Munich (INST 409/225-1 FUGG) for assistance with the generation of flow cytometry data.

Authors' contributions

BV, BH, SS contributed equally to this work. ST, NCF and KPH designed the experiments and interpreted the data. ST generated and characterized the molecules and performed functional assays with cell lines and patient materials and data analysis. SS contributed to ADCP and SPR analysis and helped with interpreting the data. BV and IJ provided PDX cells, designed the in vivo engraftment assay and performed the experiments after ex vivo ADCC. BV

analysed the results of the in vivo engraftment experiment. BH performed experiments with PBMCs and platelets and contributed to autologous ADCP results. AM performed the AML long-term ADCC experiments. EP generated molecules. AR, CA, BT and MS provided AML patient material. AL performed PBMC binding studies. AH provided the leukoreduction chamber material. MS interpreted the data and provided critical feedback and support. ST and NCF wrote the manuscript with input from BV, MS and KPH. KPH supervised the project. All authors approved the final version of the manuscript. All authors read and approved the final manuscript

Funding
Open Access funding enabled and organized by Projekt DEAL. This study was supported by the Marie-Sklodowska-Curie Training Network "Immutrain" funded by the H2020 Program of the European Union (Grant 641549, KPH), the International Doctoral Program "i-Target" funded by the Elite Network of Bavaria (MS and KPH), the Collaborative Research Center 1243 "Cancer Evolution" of the Deutsche Forschungsgemeinschaft (IJ, MS and KPH), the Deutsche Forschungsgemeinschaft grants HO2489/10-1 and SU197/3-1 (KPH and MS), and the Exist Transfer of Research I grant (NCF).

Availability of data and materials
All data generated or analysed during this study are included in this published article [and its supplementary information files].

Declarations

Ethics approval and consent to participate
After obtaining written informed consent in accordance with the Declaration of Helsinki and approval by the Institutional Review Board of the Ludwig-Maximilians-Universität, peripheral blood, bone marrow or leukoreduction material was collected from AML patients and healthy donors. All animal studies were performed in accordance with the current ethical standards of the official committee on animal experimentation (written approval by Regierung von Oberbayern, ROB-55.2Vet-2532. Vet_02-16–7 and ROB-55.2Vet-2532. Vet_03-16–56).

Consent for publication
Not applicable.

Competing interests
KPH, MS and NCF are inventors of a patent application regarding the SIRPα-antibody fusion proteins.

Author details
[1]Gene Center and Department of Biochemistry, Ludwig-Maximilians-Universität München, Feodor-Lynen-Straße 25, 81377 Munich, Germany. [2]Research Unit Apoptosis in Hematopoietic Stem Cells, Helmholtz Zentrum München, German Research Center for Environmental Health (HMGU), Neuherberg, Germany. [3]German Cancer Consortium (DKTK), Partner Site Munich, Munich, Germany. [4]Laboratory for Translational Cancer Immunology, Gene Center, LMU Munich, Munich, Germany. [5]Department of Hematology and Oncology, Department of Medicine III, University Hospital, LMU Munich, Munich, Germany. [6]Department of Transfusion Medicine, Cellular Therapeutics and Hemostaseology, University Hospital, LMU Munich, Munich, Germany. [7]Department of Pediatrics, Dr. von Hauner Children's Hospital, LMU Munich, Munich, Germany.

Received: 5 March 2021 Accepted: 7 September 2021
Published online: 27 September 2021

References

1. Shlush LI, Mitchell A, Heisler L, Abelson S, Ng SWK, Trotman-Grant A, et al. Tracing the origins of relapse in acute myeloid leukaemia to stem cells. Nature. 2017;547(7661):104–8.
2. Wulf GG, Wang RY, Kuehnle I, Weidner D, Marini F, Brenner MK, et al. A leukemic stem cell with intrinsic drug efflux capacity in acute myeloid leukemia. Blood. 2001;98(4):1166–73.
3. Dohner H, Estey E, Grimwade D, Amadori S, Appelbaum FR, Buchner T, et al. Diagnosis and management of AML in adults: 2017 ELN recommendations from an international expert panel. Blood. 2017;129(4):424–47.
4. Tsai RK, Discher DE. Inhibition of "self" engulfment through deactivation of myosin-II at the phagocytic synapse between human cells. J Cell Biol. 2008;180(5):989–1003.
5. Majeti R, Chao MP, Alizadeh AA, Pang WW, Jaiswal S, Gibbs KD Jr, et al. CD47 is an adverse prognostic factor and therapeutic antibody target on human acute myeloid leukemia stem cells. Cell. 2009;138(2):286–99.
6. Jaiswal S, Jamieson CH, Pang WW, Park CY, Chao MP, Majeti R, et al. CD47 is upregulated on circulating hematopoietic stem cells and leukemia cells to avoid phagocytosis. Cell. 2009;138(2):271–85.
7. Vyas P, Knapper S, Kelly R, Salim R, Lubowiecki M, Royston D, et al. Initial phase 1 results of the first-in-class anti-CD47 antibody Hu5F9-G4 in relapsed/refractory acute myeloid leukemia patients. European Hematology Association Annual Meeting, Stockholm. 2018: (*Abstract PF232*).
8. Chao MP, Takimoto CH, Feng DD, McKenna K, Gip P, Liu J, et al. Therapeutic targeting of the macrophage immune checkpoint CD47 in myeloid malignancies. Front Oncol. 2019;9:1380.
9. Ring NG, Herndler-Brandstetter D, Weiskopf K, Shan L, Volkmer JP, George BM, et al. Anti-SIRPalpha antibody immunotherapy enhances neutrophil and macrophage antitumor activity. Proc Natl Acad Sci U S A. 2017;114(49):E10578–85.
10. Chao MP, Alizadeh AA, Tang C, Myklebust JH, Varghese B, Gill S, et al. Anti-CD47 antibody synergizes with rituximab to promote phagocytosis and eradicate non-Hodgkin lymphoma. Cell. 2010;142(5):699–713.
11. Weiskopf K, Jahchan NS, Schnorr PJ, Cristea S, Ring AM, Maute RL, et al. CD47-blocking immunotherapies stimulate macrophage-mediated destruction of small-cell lung cancer. J Clin Investig. 2016;126(7):2610–20.
12. Jain S, Van Scoyk A, Morgan EA, Matthews A, Stevenson K, Newton G, et al. Targeted inhibition of CD47-SIRPalpha requires Fc-Fcgam-maR interactions to maximize activity in T-cell lymphomas. Blood. 2019;134(17):1430–40.
13. Sallman DA, Asch AS, Malki MMA, Lee DJ, Donnellan WB, Marcucci G, et al. The first-in-class anti-CD47 antibody magrolimab (5F9) in combination with azacitidine is effective in MDS and AML patients: ongoing phase 1b results. Blood. 2019;134(Supplement_1):569 (**Abstract**).
14. Reinhold MI, Lindberg FP, Plas D, Reynolds S, Peters MG, Brown EJ. In vivo expression of alternatively spliced forms of integrin-associated protein (CD47). J Cell Sci. 1995;108:3419–25.
15. Oldenborg PA, Zheleznyak A, Fang YF, Lagenaur CF, Gresham HD, Lindberg FP. Role of CD47 as a marker of self on red blood cells. Science. 2000;288(5473):2051–4.
16. Piccione EC, Juarez S, Liu J, Tseng S, Ryan CE, Narayanan C, et al. A bispecific antibody targeting CD47 and CD20 selectively binds and eliminates dual antigen expressing lymphoma cells. MAbs. 2015;7(5):946–56.
17. Piccione EC, Juarez S, Tseng S, Liu J, Stafford M, Narayanan C, et al. SIRPalpha-antibody fusion proteins selectively bind and eliminate dual antigen-expressing tumor cells. Clin Cancer Res. 2016;22(20):5109–19.
18. Ponce LP, Fenn NC, Moritz N, Krupka C, Kozik JH, Lauber K, et al. SIRPalpha-antibody fusion proteins stimulate phagocytosis and promote elimination of acute myeloid leukemia cells. Oncotarget. 2017;8(7):11284–301.
19. Jordan CT, Upchurch D, Szilvassy SJ, Guzman ML, Howard DS, Pettigrew AL, et al. The interleukin-3 receptor alpha chain is a unique marker for human acute myelogenous leukemia stem cells. Leukemia. 2000;14(10):1777–84.
20. Taussig DC, Pearce DJ, Simpson C, Rohatiner AZ, Lister TA, Kelly G, et al. Hematopoietic stem cells express multiple myeloid markers: implications for the origin and targeted therapy of acute myeloid leukemia. Blood. 2005;106(13):4086–92.
21. Haubner S, Perna F, Kohnke T, Schmidt C, Berman S, Augsberger C, et al. Coexpression profile of leukemic stem cell markers for combinatorial targeted therapy in AML. Leukemia. 2019;33(1):64–74.
22. Yan B, Chen Q, Shimada K, Tang M, Li H, Gurumurthy A, et al. Histone deacetylase inhibitor targets CD123/CD47-positive cells and reverse chemoresistance phenotype in acute myeloid leukemia. Leukemia. 2019;33(4):931–44.
23. Broughton SE, Hercus TR, Nero TL, Dhagat U, Owczarek CM, Hardy MP, et al. Crystallization and preliminary X-ray diffraction analysis of the interleukin-3 alpha receptor bound to the Fab fragment of antibody CSL362. Acta Crystallogr F Struct Biol Commun. 2014;70(Pt 3):358–61.

24. Liu J, Wang L, Zhao F, Tseng S, Narayanan C, Shura L, et al. Pre-Clinical Development of a Humanized Anti-CD47 Antibody with Anti-Cancer Therapeutic Potential. PLoS ONE. 2015;10(9):e0137345.
25. Petrova PS, Viller NN, Wong M, Pang X, Lin GH, Dodge K, et al. TTI-621 (SIRPalphaFc): A CD47-blocking innate immune checkpoint inhibitor with broad antitumor activity and minimal erythrocyte binding. Clin Cancer Res. 2017;23(4):1068–79.
26. Hatherley D, Lea SM, Johnson S, Barclay AN. Polymorphisms in the human inhibitory signal-regulatory protein alpha do not affect binding to its ligand CD47. J Biol Chem. 2014;289(14):10024–8.
27. Dufour A, Schneider F, Metzeler KH, Hoster E, Schneider S, Zellmeier E, et al. Acute myeloid leukemia with biallelic CEBPA gene mutations and normal karyotype represents a distinct genetic entity associated with a favorable clinical outcome. J Clin Oncol. 2010;28(4):570–7.
28. Benthaus T, Schneider F, Mellert G, Zellmeier E, Schneider S, Kakadia PM, et al. Rapid and sensitive screening for CEBPA mutations in acute myeloid leukaemia. Br J Haematol. 2008;143(2):230–9.
29. Büchner T, Hiddemann W, Wörmann B, Löffler H, Gassmann W, Haferlach T, et al. Double induction strategy for acute myeloid leukemia: the effect of high-dose cytarabine with mitoxantrone instead of standard-dose cytarabine with daunorubicin and 6-thioguanine: a randomized trial by the German AML Cooperative Group. Blood. 1999;93(12):4116–24.
30. Vinholt PJ, Nybo M, Nielsen CB, Hvas A-M. Light transmission aggregometry using pre-coated microtiter plates and a Victor X5 plate reader. PLoS ONE. 2017;12(10):e0185675.
31. Krupka C, Kufer P, Kischel R, Zugmaier G, Bögeholz J, Köhnke T, et al. CD33 target validation and sustained depletion of AML blasts in long-term cultures by the bispecific T-cell–engaging antibody AMG 330. Blood. 2014;123(3):356–65.
32. Krupka C, Kufer P, Kischel R, Zugmaier G, Lichtenegger FS, Kohnke T, et al. Blockade of the PD-1/PD-L1 axis augments lysis of AML cells by the CD33/CD3 BiTE antibody construct AMG 330: reversing a T-cell-induced immune escape mechanism. Leukemia. 2016;30(2):484–91.
33. Vick B, Rothenberg M, Sandhofer N, Carlet M, Finkenzeller C, Krupka C, et al. An advanced preclinical mouse model for acute myeloid leukemia using patients' cells of various genetic subgroups and in vivo bioluminescence imaging. PLoS ONE. 2015;10(3):e0120925.
34. Ebinger S, Zeller C, Carlet M, Senft D, Bagnoli JW, Liu WH, et al. Plasticity in growth behavior of patients' acute myeloid leukemia stem cells growing in mice. Haematologica. 2020;32:939.
35. Hu Y, Smyth GK. ELDA: extreme limiting dilution analysis for comparing depleted and enriched populations in stem cell and other assays. J Immunol Methods. 2009;347(1–2):70–8.
36. Kwong LS, Brown MH, Barclay AN, Hatherley D. Signal-regulatory protein alpha from the NOD mouse binds human CD47 with an exceptionally high affinity—implications for engraftment of human cells. Immunology. 2014;143(1):61–7.
37. Busfield SJ, Biondo M, Wong M, Ramshaw HS, Lee EM, Ghosh S, et al. Targeting of acute myeloid leukemia in vitro and in vivo with an anti-CD123 mAb engineered for optimal ADCC. Leukemia. 2014;28(11):2213–21.
38. Pietsch EC, Dong J, Cardoso R, Zhang X, Chin D, Hawkins R, et al. Anti-leukemic activity and tolerability of anti-human CD47 monoclonal antibodies. Blood Cancer J. 2017;7(2):e536.
39. Ansell SM, Maris M, Lesokhin AM, Chen R, Flinn IW, Sawas A, et al. Phase 1 study of the CD47 blocker TTI-621 in patients with relapsed or refractory hematologic malignancies. Clin Cancer Res. 2021;27:2190–9.
40. Bakema JE, van Egmond M. Fc receptor-dependent mechanisms of monoclonal antibody therapy of cancer. Curr Top Microbiol Immunol. 2014;382:373–92.
41. Lapidot T, Sirard C, Vormoor J, Murdoch B, Hoang T, Caceres-Cortes J, et al. A cell initiating human acute myeloid leukaemia after transplantation into SCID mice. Nature. 1994;367(6464):645–8.
42. Sarry JE, Murphy K, Perry R, Sanchez PV, Secreto A, Keefer C, et al. Human acute myelogenous leukemia stem cells are rare and heterogeneous when assayed in NOD/SCID/IL2Rgammac-deficient mice. J Clin Investig. 2011;121(1):384–95.
43. Willingham SB, Volkmer JP, Gentles AJ, Sahoo D, Dalerba P, Mitra SS, et al. The CD47-signal regulatory protein alpha (SIRPa) interaction is a therapeutic target for human solid tumors. Proc Natl Acad Sci U S A. 2012;109(17):6662–7.
44. Logtenberg MEW, Scheeren FA, Schumacher TN. The CD47-SIRPalpha immune checkpoint. Immunity. 2020;52(5):742–52.
45. Brooke G, Holbrook JD, Brown MH, Barclay AN. Human lymphocytes interact directly with CD47 through a novel member of the signal regulatory protein (SIRP) family. J Immunol. 2004;173(4):2562–70.
46. Advani R, Bartlett N, Smith S, Roschewski M, Popplewell L, Flinn I, et al. The first in class anti CD47 antibody HU5FY G4 + rituximab induces durable responses in relapsed/refractory dlbcl and indolent lymphoma: interim phase 1B/2 results. Hematol Oncol. 2019;37:89–90.
47. Sallman DA, Asch AS, Kambhampati S, Al Malki MM, Zeidner JF, Donnellan W, Lee DJ, Vyas P, Jeyakumar D, Mannis GN, Tanaka TN, Chai-Ho W, Larson RA, Whiteley AR, Marcucci G, Komrokji RS, Garcia-Manero G, Van Elk J, Lin M, Maute R, Volkmer J-P, Takimoto CH, Chao MP, Daver N. The first-in-class anti-CD47 antibody magrolimab combined with azacitidine is well-tolerated and effective in AML patients: phase 1b results. Blood. 2020;21(Supplement_1):S213.
48. Zeidan AM, DeAngelo DJ, Palmer JM, Seet CS, Tallman MS, Wei X, et al. A phase I study of CC-90002, a monoclonal antibody targeting CD47, in patients with relapsed and/or refractory (R/R) acute myeloid leukemia (AML) and high-risk myelodysplastic syndromes (MDS): final results. Blood. 2019;134(1):1320.
49. Qi J, Li J, Jiang B, Jiang B, Liu H, Cao X, et al. A phase I/IIa study of lemzoparlimab, a monoclonal antibody targeting CD47, in patients with relapsed and/or refractory acute myeloid leukemia (AML) and myelodysplastic syndrome (MDS): initial phase I results. Blood. 2020;136(Supplement 1):30–1.
50. Weiskopf K, Ring AM, Ho CC, Volkmer JP, Levin AM, Volkmer AK, et al. Engineered SIRPalpha variants as immunotherapeutic adjuvants to anticancer antibodies. Science. 2013;341(6141):88–91.
51. Zhao XW, van Beek EM, Schornagel K, Van der Maaden H, Van Houdt M, Otten MA, et al. CD47-signal regulatory protein-alpha (SIRPalpha) interactions form a barrier for antibody-mediated tumor cell destruction. Proc Natl Acad Sci U S A. 2011;108(45):18342–7.
52. Advani R, Flinn I, Popplewell L, Forero A, Bartlett NL, Ghosh N, et al. CD47 blockade by Hu5F9-G4 and rituximab in non-Hodgkin's lymphoma. N Engl J Med. 2018;379(18):1711–21.
53. Ishikawa F, Yoshida S, Saito Y, Hijikata A, Kitamura H, Tanaka S, et al. Chemotherapy-resistant human AML stem cells home to and engraft within the bone-marrow endosteal region. Nat Biotechnol. 2007;25(11):1315–21.
54. Weinstein JN, van Osdol W. The macroscopic and microscopic pharmacology of monoclonal antibodies. Int J Immunopharmacol. 1992;14(3):457–63.
55. Godwin CD, Gale RP, Walter RB. Gemtuzumab ozogamicin in acute myeloid leukemia. Leukemia. 2017;31(9):1855–68.
56. Fournier E, Duployez N, Ducourneau B, Raffoux E, Turlure P, Caillot D, et al. Mutational profile and benefit of gemtuzumab ozogamicin in acute myeloid leukemia. Blood. 2020;135(8):542–6.
57. Fenwarth L, Fournier E, Cheok M, Boyer T, Gonzales F, Castaigne S, et al. Biomarkers of gemtuzumab ozogamicin response for acute myeloid leukemia treatment. Int J Mol Sci. 2020;21(16):5626.
58. Boyd-Kirkup J, Thakkar D, Brauer P, Zhou J, Chng W-J, Ingram PJ. HMBD004, a novel anti-CD47xCD33 bispecific antibody displays potent anti-tumor effects in pre-clinical models of AML. Blood. 2017;130(Supplement 1):1378.
59. van der Velden VHJ, te Marvelde JG, Hoogeveen PG, Bernstein ID, Houtsmuller AB, Berger MS, et al. Targeting of the CD33-calicheamicin immunoconjugate Mylotarg (CMA-676) in acute myeloid leukemia: in vivo and in vitro saturation and internalization by leukemic and normal myeloid cells. Blood. 2001;97(10):3197–204.
60. van der Jagt RHC, Badger CC, Appelbaum FR, Press OW, Matthews DC, Eary JF, et al. Localization of radiolabeled antimyeloid antibodies in a human acute leukemia xenograft tumor model. Can Res. 1992;52(1):89–94.
61. Walter RB, Appelbaum FR, Estey EH, Bernstein ID. Acute myeloid leukemia stem cells and CD33-targeted immunotherapy. Blood. 2012;119(26):6198–208.
62. Vergez F, Green AS, Tamburini J, Sarry JE, Gaillard B, Cornillet-Lefebvre P, et al. High levels of CD34+CD38low/-CD123+ blasts are predictive of an adverse outcome in acute myeloid leukemia: a Groupe Ouest-Est des

Leucemies Aigues et Maladies du Sang (GOELAMS) study. Haematologica. 2011;96(12):1792–8.
63. Vergez F, Nicolau-Travers ML, Bertoli S, Rieu JB, Tavitian S, Bories P, et al. CD34(+)CD38(-)CD123(+) leukemic stem cell frequency predicts outcome in older acute myeloid leukemia patients treated by intensive chemotherapy but not hypomethylating agents. Cancers (Basel). 2020;12(5):1174.
64. Perna F, Berman SH, Soni RK, Mansilla-Soto J, Eyquem J, Hamieh M, et al. Integrating proteomics and transcriptomics for systematic combinatorial chimeric antigen receptor therapy of AML. Cancer Cell. 2017;32(4):506-19.e5.
65. Testa U, Pelosi E, Castelli G. CD123 as a therapeutic target in the treatment of hematological malignancies. Cancers (Basel). 2019;11(9):1358.
66. Jen EY, Gao X, Li L, Zhuang L, Simpson NE, Aryal B, et al. FDA approval summary: tagraxofusp-erzs for treatment of blastic plasmacytoid dendritic cell neoplasm. Clin Cancer Res. 2020;26(3):532–6.
67. Uy GL, Aldoss I, Foster MC, Sayre PH, Wieduwilt MJ, Advani AS, et al. Flotetuzumab as salvage immunotherapy for refractory acute myeloid leukemia. Blood. 2020;137:751–62.
68. Smith BD, Roboz GJ, Walter RB, Altman JK, Ferguson A, Curcio TJ, et al. First-in man, phase 1 study of CSL362 (anti-IL3Rα/anti-CD123 monoclonal antibody) in patients with CD123+ acute myeloid leukemia (AML) in CR at high risk for early relapse. Blood. 2014;124(21):120.
69. Epling-Burnette PK, Bai F, Painter JS, Rollison DE, Salih HR, Krusch M, et al. Reduced natural killer (NK) function associated with high-risk myelodysplastic syndrome (MDS) and reduced expression of activating NK receptors. Blood. 2007;109(11):4816–24.
70. Kubasch AS, Schulze F, Giagounidis A, Gotze KS, Kronke J, Sockel K, et al. Single agent talacotuzumab demonstrates limited efficacy but considerable toxicity in elderly high-risk MDS or AML patients failing hypomethylating agents. Leukemia. 2020;34(4):1182–6.
71. Montesinos P, Roboz GJ, Bulabois CE, Subklewe M, Platzbecker U, Ofran Y, et al. Safety and efficacy of talacotuzumab plus decitabine or decitabine alone in patients with acute myeloid leukemia not eligible for chemotherapy: results from a multicenter, randomized, phase 2/3 study. Leukemia. 2020;35:62–74.
72. Deuse T, Hu X, Agbor-Enoh S, Jang MK, Alawi M, Saygi C, et al. The SIRPα–CD47 immune checkpoint in NK cells. J Exp Med. 2021. https://doi.org/10.1084/jem.20200839.
73. Tseng D, Volkmer JP, Willingham SB, Contreras-Trujillo H, Fathman JW, Fernhoff NB, et al. Anti-CD47 antibody-mediated phagocytosis of cancer by macrophages primes an effective antitumor T-cell response. Proc Natl Acad Sci U S A. 2013;110(27):11103–8.
74. Li Y, Zhang M, Wang X, Liu W, Wang H, Yang YG. Vaccination with CD47 deficient tumor cells elicits an antitumor immune response in mice. Nat Commun. 2020;11(1):581.
75. Liu X, Pu Y, Cron K, Deng L, Kline J, Frazier WA, et al. CD47 blockade triggers T cell-mediated destruction of immunogenic tumors. Nat Med. 2015;21(10):1209–15.

Publisher's Note

References

1. Döhner H, Weisdorf DJ, Bloomfield CD (2015) Acute Myeloid Leukemia. New England Journal of Medicine 373:1136–1152. https://doi.org/10.1056/NEJMra1406184

2. Döhner H, Estey E, Grimwade D, et al (2017) Diagnosis and management of AML in adults: 2017 ELN recommendations from an international expert panel. Blood 129:424–447

3. Döhner H, Wei AH, Appelbaum FR, et al (2022) Diagnosis and management of AML in adults: 2022 recommendations from an international expert panel on behalf of the ELN. Blood 140:1345–1377. https://doi.org/10.1182/blood.2022016867

4. Castaigne S, Pautas C, Terré C, et al (2012) Effect of gemtuzumab ozogamicin on survival of adult patients with de-novo acute myeloid leukaemia (ALFA-0701): A randomised, open-label, phase 3 study. The Lancet 379:1508–1516. https://doi.org/10.1016/S0140-6736(12)60485-1

5. Lambert J, Pautas C, Terré C, et al (2019) Gemtuzumab ozogamicin for de novo acute myeloid leukemia: Final efficacy and safety updates from the open-label, phase III ALFA-0701 trial. Haematologica 104:113–119. https://doi.org/10.3324/haematol.2018.188888

6. Oran B, Weisdorf DJ (2012) Survival for older patients with acute myeloid leukemia: A population-based study. Haematologica 97:1916–1924. https://doi.org/10.3324/haematol.2012.066100

7. Short NJ, Rytting ME, Cortes JE (2018) Acute myeloid leukaemia. The Lancet 392:593–606

8. Cashen AF, Schiller GJ, O'Donnell MR, DiPersio JF (2010) Multicenter, phase II study of decitabine for the first-line treatment of older patients with Acute Myeloid Leukemia. Journal of Clinical Oncology 28:556–561. https://doi.org/10.1200/JCO.2009.23.9178

9. Al-Ali HK, Jaekel N, Junghanss C, et al (2012) Azacitidine in patients with acute myeloid leukemia medically unfit for or resistant to chemotherapy: A multicenter phase I/II study. Leuk Lymphoma 53:110–117. https://doi.org/10.3109/10428194.2011.606382

10. DiNardo CD, Pratz K, Pullarkat V, et al (2019) Venetoclax combined with decitabine or azacitidine in treatment-naive, elderly patients with acute myeloid leukemia. Blood 133:7–17. https://doi.org/10.1182/blood-2018-08-868752

11. DiNardo CD, Jonas BA, Pullarkat V, et al (2020) Azacitidine and Venetoclax in Previously Untreated Acute Myeloid Leukemia. N Engl J Med 383:617–629. https://doi.org/10.1056/NEJMoa2012971

12. Schmid C, Labopin M, Schaap N, et al (2019) Prophylactic donor lymphocyte infusion after allogeneic stem cell transplantation in acute leukaemia – a matched pair analysis by the Acute Leukaemia Working Party of EBMT. Br J Haematol 184:782–787. https://doi.org/10.1111/bjh.15691

13. Sweeney C, Vyas P (2019) The Graft-Versus-Leukemia Effect in AML. Front Oncol 9

14. Vago L, Gojo I (2020) Immune escape and immunotherapy of acute myeloid leukemia. Journal of Clinical Investigation 130:1552–1564. https://doi.org/10.1172/JCI129204

15. Abaza Y, Fathi AT (2022) Monoclonal Antibodies in Acute Myeloid Leukemia-Are We There Yet? Cancer Journal (United States) 28:37–42

16. Daver N, Alotaibi AS, Bücklein V, Subklewe M (2021) T-cell-based immunotherapy of acute myeloid leukemia: current concepts and future developments. Leukemia 35:1843–1863

17. Haubner S, Perna F, Köhnke T, et al (2019) Coexpression profile of leukemic stem cell markers for combinatorial targeted therapy in AML. Leukemia 33:64–74. https://doi.org/10.1038/s41375-018-0180-3

18. Perna F, Berman SH, Soni RK, et al (2017) Integrating Proteomics and Transcriptomics for Systematic Combinatorial Chimeric Antigen Receptor Therapy of AML. Cancer Cell 32:506-519.e5. https://doi.org/10.1016/j.ccell.2017.09.004

19. Casucci M, Di Robilant BN, Falcone L, et al (2013) CD44v6-targeted T cells mediate potent antitumor effects against acute myeloid leukemia and multiple myeloma. Blood 122:3461–3472. https://doi.org/10.1182/blood-2013-04-493361

20. Neu S, Geiselhart A, Sproll M, et al (1997) Expression of CD44 isoforms by highly enriched CD34-positive cells in cord blood, bone marrow and leukaphereses. Bone Marrow Transplant 20:593–598. https://doi.org/10.1038/sj.bmt.1700940

21. Bendall LJ, Bradstock KF, Gottlieb DJ (2000) Expression of CD44 variant exons in acute myeloid leukemia is more common and more complex than that observed in normal blood, bone marrow or CD34+ cells. Leukemia 14:1239–1246. https://doi.org/10.1038/sj.leu.2401830

22. Stroopinsky D, Rajabi H, Nahas M, et al (2018) MUC1-C drives myeloid leukaemogenesis and resistance to treatment by a survivin-mediated mechanism. J Cell Mol Med 22:3887–3898. https://doi.org/10.1111/jcmm.13662

23. Stroopinsky D, Rosenblatt J, Ito K, et al (2013) MUC1 is a potential target for the treatment of acute myeloid leukemia stem cells. Cancer Res 73:5569–5579. https://doi.org/10.1158/0008-5472.CAN-13-0677

24. Greiner J, Schmitt M, Li L, et al (2006) Expression of tumor-associated antigens in acute myeloid leukemia: Implications for specific immunotherapeutic approaches. Blood 108:4109–4117. https://doi.org/10.1182/blood-2006-01-023127

25. Scheibenbogen C, Letsch A, Thiel E, et al (2002) CD8 T-cell responses to Wilms tumor gene product WT1 and proteinase 3 in patients with acute myeloid leukemia. Blood 100:2132–2137. https://doi.org/10.1182/blood-2002-01-0163

26. Rezvani K, Yong ASM, Tawab A, et al (2009) Ex vivo characterization of polyclonal memory CD8+ T-cell responses to PRAME-specific peptides in patients with acute lymphoblastic leukemia and acute and chronic myeloid leukemia. Blood 113:2245–2255. https://doi.org/10.1182/blood-2008-03-144071

27. Nathan P, Hassel JC, Rutkowski P, et al (2021) Overall Survival Benefit with Tebentafusp in Metastatic Uveal Melanoma. New England Journal of Medicine 385:1196–1206. https://doi.org/10.1056/NEJMoa2103485

28. Augsberger C, Hänel G, Xu W, et al (2021) Targeting intracellular WT1 in AML with a novel RMF-peptide-MHC-specific T-cell bispecific antibody. Blood 138:2655–2669. https://doi.org/10.1182/blood.2020010477

29. Hofmann S, Schubert ML, Wang L, et al (2019) Chimeric antigen receptor (CAR) t cell therapy in acute myeloid leukemia (AML). J Clin Med 8:. https://doi.org/10.3390/jcm8020200

30. Graf C, Heidel F, Tenzer S, et al (2007) A neoepitope generated by an FLT3 internal tandem duplication (FLT3-ITD) is recognized by leukemia-reactive autologous CD8+ T cells. Blood 109:2985–2988. https://doi.org/10.1182/blood-2006-07-032839

31. Van Der Lee DI, Reijmers RM, Honders MW, et al (2019) Mutated nucleophosmin 1 as immunotherapy target in acute myeloid leukemia. Journal of Clinical Investigation 129:774–785. https://doi.org/10.1172/JCI97482

32. Greiner J, Ono Y, Hofmann S, et al (2012) Mutated regions of nucleophosmin 1 elicit both CD4+ and CD8 + T-cell responses in patients with acute myeloid leukemia. Blood 120:1282–1289. https://doi.org/10.1182/blood-2011-11-394395

33. Scott AM, Allison JP, Wolchok JD (2012) Monoclonal antibodies in cancer therapy. Cancer Immun 12:14

34. Reff ME, Carner K, Chambers KS, et al (1994) Depletion of B cells in vivo by a chimeric mouse human monoclonal antibody to CD20. Blood 83:435–445. https://doi.org/10.1182/blood.v83.2.435.435

35. McLaughlin P, Grillo-López AJ, Link BK, et al (1998) Rituximab chimeric anti-CD20 monoclonal antibody therapy for relapsed indolent lymphoma: Half of patients respond to a four-dose treatment program. Journal of Clinical Oncology 16:2825–2833. https://doi.org/10.1200/JCO.1998.16.8.2825

36. Feldman E, Moore JO, Feldman EJ, et al (2005) Phase III Randomized Multicenter Study of a Humanized Anti-CD33 Monoclonal Antibody, Lintuzumab, in Combination With Chemotherapy, Versus Chemotherapy Alone in Patients With Refrac Phase III Randomized Multicenter Study of a Humanized Anti-CD33 Monoclonal Antibody, Lintuzumab, in Combination With Chemotherapy, Versus Chemotherapy Alone in Patients With Refractory or First-Relapsed Acute Myeloid Leukemia. Article in Journal of Clinical Oncology 23:4110–4116. https://doi.org/10.1200/JCO.2005.09.133

37. Sekeres MA, Lancet JE, Wood BL, et al (2013) Randomized, phase IIb study of low-dose cytarabine and lintuzumab versus low-dose cytarabine and placebo in older adults with untreated acute myeloid leukemia. Haematologica 98:119–128. https://doi.org/10.3324/haematol.2012.066613

38. Montesinos P, Roboz GJ, Bulabois CE, et al (2021) Safety and efficacy of talacotuzumab plus decitabine or decitabine alone in patients with acute myeloid leukemia not eligible for chemotherapy: results from a multicenter, randomized, phase 2/3 study. Leukemia 35:62–74. https://doi.org/10.1038/s41375-020-0773-5

39. Kubasch AS, Schulze F, Götze KS, et al (2018) Anti-CD123 Targeted Therapy with Talacotuzumab in Advanced MDS and AML after Failing Hypomethylating Agents - Final Results of the Samba Trial. Blood 132:4045–4045. https://doi.org/10.1182/blood-2018-99-113112

40. Sanford D, Blum WG, Ravandi F, et al (2015) Efficacy and safety of an anti-FLT3 antibody (LY3012218) in patients with relapsed acute myeloid leukemia. Journal of Clinical Oncology 33:7059–7059. https://doi.org/10.1200/jco.2015.33.15_suppl.7059

41. Riether C, Pabst T, Höpner S, et al (2020) Targeting CD70 with cusatuzumab eliminates acute myeloid leukemia stem cells in patients treated with hypomethylating agents. Nat Med 26:1459–1467. https://doi.org/10.1038/s41591-020-0910-8

42. Trudel GC, Howes AJ, Jeste N, et al (2020) CULMINATE: A phase II study of cusatuzumab + azacitidine in patients with newly diagnosed AML, ineligible for intensive chemotherapy. Journal of Clinical Oncology 38:TPS7565–TPS7565. https://doi.org/10.1200/jco.2020.38.15_suppl.tps7565

43. Ochsenbein AF, Riether C, Bacher U, et al (2018) Argx-110 Targeting CD70, in Combination with Azacitidine, Shows Favorable Safety Profile and Promising Anti-Leukemia Activity in Newly Diagnosed AML Patients in an Ongoing Phase 1/2 Clinical Trial. Blood 132:2680–2680. https://doi.org/10.1182/blood-2018-99-118302

44. Chao MP, Weissman IL, Majeti R (2012) The CD47-SIRPα pathway in cancer immune evasion and potential therapeutic implications. Curr Opin Immunol 24:225–232

45. Jaiswal S, Jamieson CHM, Pang WW, et al (2009) CD47 Is Upregulated on Circulating Hematopoietic Stem Cells and Leukemia Cells to Avoid Phagocytosis. Cell 138:271–285. https://doi.org/10.1016/j.cell.2009.05.046

46. Majeti R, Chao MP, Alizadeh AA, et al (2009) CD47 Is an Adverse Prognostic Factor and Therapeutic Antibody Target on Human Acute Myeloid Leukemia Stem Cells. Cell 138:286–299. https://doi.org/10.1016/j.cell.2009.05.045

47. Daver NG, Vyas P, Kambhampati S, et al (2022) Tolerability and efficacy of the first-in-class anti-CD47 antibody magrolimab combined with azacitidine in frontline TP53m AML patients: Phase 1b results. Journal of Clinical Oncology 40:7020–7020. https://doi.org/10.1200/jco.2022.40.16_suppl.7020

48. Sallman DA, Asch AS, Al Malki MM, et al (2019) The First-in-Class Anti-CD47 Antibody Magrolimab (5F9) in Combination with Azacitidine Is Effective in MDS and AML Patients: Ongoing Phase 1b Results. Blood 134:569–569. https://doi.org/10.1182/blood-2019-126271

49. Appelbaum FR, Bernstein ID (2017) Gemtuzumab ozogamicin for acute myeloid leukemia. Blood 130:2373–2376

50. Jen EY, Ko CW, Eun Lee J, et al (2018) FDA approval: Gemtuzumab ozogamicin for the treatment of adults with newly diagnosed cd33-positive acute myeloid leukemia. Clinical Cancer Research 24:3242–3246. https://doi.org/10.1158/1078-0432.CCR-17-3179

51. Norsworthy KJ, Ko C-W, Lee JE, et al (2018) FDA Approval Summary: Mylotarg for Treatment of Patients with Relapsed or Refractory CD33-Positive Acute Myeloid Leukemia. Oncologist 23:1103–1108. https://doi.org/10.1634/theoncologist.2017-0604

52. Daver N, Sweet KL, Montesinos P, et al (2020) A Phase 1b/2 Study of IMGN632, a CD123-Targeting Antibody-Drug Conjugate (ADC), As Monotherapy or in Combination with Venetoclax and/or Azacitidine for Patients with CD123-Positive Acute Myeloid Leukemia. Blood 136:50–51. https://doi.org/10.1182/blood-2020-139884

53. Cortes JE, DeAngelo DJ, Erba HP, et al (2018) Maturing Clinical Profile of IMGN779, a Next-Generation CD33-Targeting Antibody-Drug Conjugate, in Patients with Relapsed or Refractory Acute Myeloid Leukemia. Blood 132:26–26. https://doi.org/10.1182/blood-2018-99-112891

54. Wu J, Fu J, Zhang M, Liu D (2015) Blinatumomab: a bispecific T cell engager (BiTE) antibody against CD19/CD3 for refractory acute lymphoid leukemia. J Hematol Oncol 8:. https://doi.org/10.1186/s13045-015-0195-4

55. Kantarjian H, Stein A, Gökbuget N, et al (2017) Blinatumomab versus Chemotherapy for Advanced Acute Lymphoblastic Leukemia. New England Journal of Medicine 376:836–847. https://doi.org/10.1056/nejmoa1609783

56. Gökbuget N, Dombret H, Bonifacio M, et al (2018) Blinatumomab for minimal residual disease in adults with B-cell precursor acute lymphoblastic leukemia. Blood 131:1522–1531. https://doi.org/10.1182/blood-2017-08-798322

57. Zugmaier G, Gökbuget N, Klinger M, et al (2015) Long-term survival and T-cell kinetics in relapsed/refractory ALL patients who achieved MRD response after blinatumomab treatment. Blood 126:2578–2584. https://doi.org/10.1182/blood-2015-06-649111

58. Topp MS, Gökbuget N, Stein AS, et al (2015) Safety and activity of blinatumomab for adult patients with relapsed or refractory B-precursor acute lymphoblastic

leukaemia: A multicentre, single-arm, phase 2 study. Lancet Oncol 16:57–66. https://doi.org/10.1016/S1470-2045(14)71170-2

59. Budde LE, Assouline S, Sehn LH, et al (2022) Single-Agent Mosunetuzumab Shows Durable Complete Responses in Patients with Relapsed or Refractory B-Cell Lymphomas: Phase I Dose-Escalation Study. J Clin Oncol 40:481–491. https://doi.org/10.1200/JCO.21.00931

60. Moreau P, Garfall AL, van de Donk NWCJ, et al (2022) Teclistamab in Relapsed or Refractory Multiple Myeloma. New England Journal of Medicine. https://doi.org/10.1056/nejmoa2203478

61. Clark MC, Stein A (2020) CD33 directed bispecific antibodies in acute myeloid leukemia. Best Pract Res Clin Haematol 33

62. Krupka C, Kufer P, Kischel R, et al (2014) CD33 target validation and sustained depletion of AML blasts in long-term cultures by the bispecific T-cell-engaging antibody AMG 330. Blood 123:356–365. https://doi.org/10.1182/blood-2013-08-523548

63. Subklewe M, Stein A, Walter RB, et al (2019) Preliminary Results from a Phase 1 First-in-Human Study of AMG 673, a Novel Half-Life Extended (HLE) Anti-CD33/CD3 BiTE® (Bispecific T-Cell Engager) in Patients with Relapsed/Refractory (R/R) Acute Myeloid Leukemia (AML). Blood 134:833–833. https://doi.org/10.1182/blood-2019-127977

64. Ravandi F, Walter RB, Subklewe M, et al (2020) Updated results from phase I dose-escalation study of AMG 330, a bispecific T-cell engager molecule, in patients with relapsed/refractory acute myeloid leukemia (R/R AML). J Clin Oncol 38:7508–7508. https://doi.org/10.1200/jco.2020.38.15_suppl.7508

65. Ravandi F, Stein AS, Kantarjian HM, et al (2018) A Phase 1 First-in-Human Study of AMG 330, an Anti-CD33 Bispecific T-Cell Engager (BiTE®) Antibody Construct, in Relapsed/Refractory Acute Myeloid Leukemia (R/R AML). Blood 132:25–25. https://doi.org/10.1182/blood-2018-99-109762

66. Westervelt P, Cortes JE, Altman JK, et al (2019) Phase 1 First-in-Human Trial of AMV564, a Bivalent Bispecific (2:2) CD33/CD3 T-Cell Engager, in Patients with Relapsed/Refractory Acute Myeloid Leukemia (AML). Blood 134:834–834. https://doi.org/10.1182/blood-2019-129042

67. Nair-Gupta P, Diem M, Reeves D, et al (2020) Abstract 5662: JNJ-67571244: A novel anti-CD33 C2 domain binding bispecific antibody with potent T cell

redirection activity. Cancer Res 80:5662–5662. https://doi.org/10.1158/1538-7445.am2020-5662

68. Nair-Gupta P, Diem M, Reeves D, et al (2020) A novel C2 domain binding CD33xCD3 bispecific antibody with potent T-cell redirection activity against acute myeloid leukemia. Blood Adv 4:906–919. https://doi.org/10.1182/bloodadvances.2019001188

69. Jordan CT, Upchurch D, Szilvassy SJ, et al (2000) The interleukin-3 receptor alpha chain is a unique marker for human acute myelogenous leukemia stems cells. Leukemia 14:1777–1784. https://doi.org/10.1038/sj.leu.2401903

70. Vergez F, Green AS, Tamburini J, et al (2011) High levels of CD34 +CD38 low/-CD123 + blasts are predictive of an adverse outcome in acute myeloid leukemia: A groupe ouest-est des leucémies aiguës et maladies du sang (GOELAMS) study. Haematologica 96:1792–1798. https://doi.org/10.3324/haematol.2011.047894

71. Lamble AJ, Brodersen LE, Alonzo TA, et al (2022) CD123 Expression Is Associated With High-Risk Disease Characteristics in Childhood Acute Myeloid Leukemia: A Report From the Children's Oncology Group. Journal of Clinical Oncology 40:252–261. https://doi.org/10.1200/JCO.21.01595

72. Ehninger A, Kramer M, Röllig C, et al (2014) Distribution and levels of cell surface expression of CD33 and CD123 in acute myeloid leukemia. Blood Cancer J 4:. https://doi.org/10.1038/bcj.2014.39

73. Uy GL, Aldoss I, Foster MC, et al (2021) Flotetuzumab as salvage immunotherapy for refractory acute myeloid leukemia. Blood 137:751–762. https://doi.org/10.1182/blood.2020007732

74. Brauchle B, Goldstein RL, Karbowski CM, et al (2020) Characterization of a novel FLT3 BiTE molecule for the treatment of acute myeloid leukemia. Mol Cancer Ther 19:1875–1888. https://doi.org/10.1158/1535-7163.MCT-19-1093

75. Mehta NK, Pfluegler M, Meetze K, et al (2022) A novel IgG-based FLT3xCD3 bispecific antibody for the treatment of AML and B-ALL. J Immunother Cancer 10:3882. https://doi.org/10.1136/jitc-2021-003882

76. van Loo PF, Hangalapura BN, Thordardottir S, et al (2019) MCLA-117, a CLEC12AxCD3 bispecific antibody targeting a leukaemic stem cell antigen, induces T cell-mediated AML blast lysis. Expert Opin Biol Ther 19:721–733. https://doi.org/10.1080/14712598.2019.1623200

77. Tettamanti S, Pievani A, Biondi A, et al (2022) Catch me if you can: how AML and its niche escape immunotherapy. Leukemia 36:13–22

78. Vago L, Perna SK, Zanussi M, et al (2009) Loss of Mismatched HLA in Leukemia after Stem-Cell Transplantation. New England Journal of Medicine 361:478–488. https://doi.org/10.1056/nejmoa0811036

79. Stölzel F, Hackmann K, Kuithan F, et al (2012) Clonal evolution including partial loss of human leukocyte antigen genes favoring extramedullary acute myeloid leukemia relapse after matched related allogeneic hematopoietic stem cell transplantation. Transplantation 93:744–749. https://doi.org/10.1097/TP.0b013e3182481113

80. Jan M, Leventhal MJ, Morgan EA, et al (2019) Recurrent genetic HLA loss in AML relapsed after matched unrelated allogeneic hematopoietic cell transplantation. Blood Adv 3:2199–2204. https://doi.org/10.1182/bloodadvances.2019000445

81. Vasold J, Wagner M, Drolle H, et al (2015) The bone marrow microenvironment is a critical player in the NK cell response against acute myeloid leukaemia in vitro. Leuk Res 39:257–262. https://doi.org/10.1016/j.leukres.2014.12.001

82. Tohumeken S, Baur R, Bottcher M, et al (2020) Palmitoylated proteins on AML-derived extracellular vesicles promote myeloid-derived suppressor cell differentiation via TLR2/Akt/mTOR signaling. Cancer Res 80:3663–3676. https://doi.org/10.1158/0008-5472.CAN-20-0024

83. Wang L, Jia B, Claxton DF, et al (2018) VISTA is highly expressed on MDSCs and mediates an inhibition of T cell response in patients with AML. Oncoimmunology 7:. https://doi.org/10.1080/2162402X.2018.1469594

84. Pyzer AR, Stroopinsky D, Rajabi H, et al (2017) MUC1-mediated induction of myeloid-derived suppressor cells in patients with acute myeloid leukemia. Blood 129:1791–1801. https://doi.org/10.1182/blood-2016-07-730614

85. Yang Y, Li C, Liu T, et al (2020) Myeloid-Derived Suppressor Cells in Tumors: From Mechanisms to Antigen Specificity and Microenvironmental Regulation. Front Immunol 11

86. Al-Matary YS, Botezatu L, Opalka B, et al (2016) Acute myeloid leukemia cells polarize macrophages towards a leukemia supporting state in a growth factor independence 1 dependent manner. Haematologica 101:1216–1227. https://doi.org/10.3324/haematol.2016.143180

87. Mussai F, De Santo C, Abu-Dayyeh I, et al (2013) Acute myeloid leukemia creates an arginase-dependent immunosuppressive microenvironment. Blood 122:749–758. https://doi.org/10.1182/blood-2013-01-480129

88. Curti A, Pandolfi S, Valzasina B, et al (2007) Modulation of tryptophan catabolism by human leukemic cells results in the conversion of CD25- into CD25+ T regulatory cells. Blood 109:2871–2877. https://doi.org/10.1182/blood-2006-07-036863

89. Szczepanski MJ, Szajnik M, Czystowska M, et al (2009) Increased frequency and suppression by regulatory T cells in patients with acute myelogenous leukemia. Clinical Cancer Research 15:3325–3332. https://doi.org/10.1158/1078-0432.CCR-08-3010

90. Delia M, Carluccio P, Mestice A, et al (2018) Impact of bone marrow aspirate tregs on the response rate of younger newly diagnosed acute myeloid leukemia patients. J Immunol Res 2018:1–7. https://doi.org/10.1155/2018/9325261

91. Shenghui Z, Yixiang H, Jianbo W, et al (2011) Elevated frequencies of CD4+CD25+CD127lo regulatory T cells is associated to poor prognosis in patients with acute myeloid leukemia. Int J Cancer 129:1373–1381. https://doi.org/10.1002/ijc.25791

92. Zajac M, Zaleska J, Dolnik A, et al (2018) Expression of CD274 (PD-L1) is associated with unfavourable recurrent mutations in AML. Br J Haematol 183:822–825. https://doi.org/10.1111/bjh.15040

93. Norde WJ, Maas F, Hobo W, et al (2011) PD-1/PD-L1 interactions contribute to functional T-cell impairment in patients who relapse with cancer after allogeneic stem cell transplantation. Cancer Res 71:5111–5122. https://doi.org/10.1158/0008-5472.CAN-11-0108

94. Toffalori C, Zito L, Gambacorta V, et al (2019) Immune signature drives leukemia escape and relapse after hematopoietic cell transplantation. Nat Med 25:603–611. https://doi.org/10.1038/s41591-019-0400-z

95. Williams P, Basu S, Garcia-Manero G, et al (2019) The distribution of T-cell subsets and the expression of immune checkpoint receptors and ligands in patients with newly diagnosed and relapsed acute myeloid leukemia. Cancer 125:1470–1481. https://doi.org/10.1002/cncr.31896

96. Knaus HA, Berglund S, Hackl H, et al (2018) Signatures of CD8+ T cell dysfunction in AML patients and their reversibility with response to chemotherapy. JCI Insight 3:. https://doi.org/10.1172/jci.insight.120974

97. Le Dieu R, Taussig DC, Ramsay AG, et al (2009) Peripheral blood T cells in acute myeloid leukemia (AML) patients at diagnosis have abnormal phenotype and genotype and form defective immune synapses with AML blasts. Blood 114:3909–3916. https://doi.org/10.1182/blood-2009-02-206946

98. Kong Y, Zhang J, Claxton DF, et al (2015) PD-1hiTIM-3+ T cells associate with and predict leukemia relapse in AML patients post allogeneic stem cell transplantation. Blood Cancer J 5:330. https://doi.org/10.1038/bcj.2015.58

99. Rutella S, Vadakekolathu J, Mazziotta F, et al (2022) Immune dysfunction signatures predict outcomes and define checkpoint blockade–unresponsive microenvironments in acute myeloid leukemia. Journal of Clinical Investigation 132:. https://doi.org/10.1172/JCI159579

100. Krupka C, Kufer P, Kischel R, et al (2016) Blockade of the PD-1/PD-L1 axis augments lysis of AML cells by the CD33/CD3 BiTE antibody construct AMG 330: Reversing a T-cell-induced immune escape mechanism. Leukemia 30:484–491. https://doi.org/10.1038/leu.2015.214

101. Herrmann M, Krupka C, Deiser K, et al (2018) Bifunctional PD-1 x aCD3 x aCD33 fusion protein reverses adaptive immune escape in acute myeloid leukemia. Blood 132:2484–2494. https://doi.org/10.1182/blood-2018-05-849802

102. Tahk S, Vick B, Hiller B, et al (2021) SIRPα-αCD123 fusion antibodies targeting CD123 in conjunction with CD47 blockade enhance the clearance of AML-initiating cells. J Hematol Oncol 14:155. https://doi.org/10.1186/s13045-021-01163-6

103. Offner S, Hofmeister R, Romaniuk A, et al (2006) Induction of regular cytolytic T cell synapses by bispecific single-chain antibody constructs on MHC class I-negative tumor cells. Mol Immunol 43:763–771. https://doi.org/10.1016/j.molimm.2005.03.007

104. Li J, Stagg NJ, Johnston J, et al (2017) Membrane-Proximal Epitope Facilitates Efficient T Cell Synapse Formation by Anti-FcRH5/CD3 and Is a Requirement for Myeloma Cell Killing. Cancer Cell 31:383–395. https://doi.org/10.1016/j.ccell.2017.02.001

105. Ramsay AG, Clear AJ, Fatah R, Gribben JG (2012) Multiple inhibitory ligands induce impaired T-cell immunologic synapse function in chronic lymphocytic leukemia that can be blocked with lenalidomide: Establishing a reversible immune evasion mechanism in human cancer. Blood 120:1412–1421. https://doi.org/10.1182/blood-2012-02-411678

106. Ramsay AG, Evans R, Kiaii S, et al (2013) Chronic lymphocytic leukemia cells induce defective LFA-1-directed T-cell motility by altering Rho GTPase signaling that is reversible with lenalidomide. Blood 121:2704–2714. https://doi.org/10.1182/blood-2012-08-448332

107. Ramsay AG, Gribben JG (2009) Immune dysfunction in chronic lymphocytic leukemia T cells and lenalidomide as an immunomodulatory drug. Haematologica 94:1198–1202

108. Görgün G, Samur MK, Cowens KB, et al (2015) Lenalidomide enhances immune checkpoint blockade-induced immune response in multiple myeloma. Clinical Cancer Research 21:4617–4618. https://doi.org/10.1158/1078-0432.CCR-15-0200

109. Mcdaniel JM, Pinilla-Ibarz J, Epling-Burnette PK (2012) Molecular Action of Lenalidomide in Lymphocytes and Hematologic Malignancies. Adv Hematol 2012:. https://doi.org/10.1155/2012/513702

110. Rajkumar SV (2022) Multiple myeloma: 2022 update on diagnosis, risk stratification, and management. Am J Hematol 97:1086–1107. https://doi.org/10.1002/ajh.26590

111. Leonard JP, Trneny M, Izutsu K, et al (2019) AUGMENT: A Phase III study of lenalidomide plus rituximab versus placebo plus rituximab in relapsed or refractory indolent lymphoma. In: Journal of Clinical Oncology. American Society of Clinical Oncology, pp 1188–1199

Acknowledgements

“With a little help from a friend”- Mit ein bisschen Hilfe von Freunden.

Der Titel meiner Doktorarbeit beschreibt recht gut, dass ich ohne die Unterstützung von gewissen Menschen, wahrscheinlich nicht dort angekommen wäre, wo ich jetzt bin. Und genau dafür möchte ich mich gerne bedanken.

Mein erster Dank geht an Marion Subklewe, die mir als Doktormutter einen Platz in ihrer Forschungsgruppe gegeben hat und ich somit an einem der für mich spannendsten und interessantesten Forschungsgebiete mitwirken durfte. Danke auch, für die vielen Möglichkeiten, meine Arbeit auf (internationalen) Kongressen präsentieren zu dürfen und dass der Kontakt und Austausch mit anderen Wissenschaftler:innen immer groß geschrieben wurde.

Auch möchte ich all meinen Arbeitskolleg:innen danken. Ihr habt eine Arbeitsatmosphäre geschaffen, welche über das rein berufliche hinausgeht. Die Team-Events, Weinproben, Isarausflüge, Kongressreisen und Weihnachtsfeiern haben einfach viel Spaß und Abwechslung in den Arbeitsalltag gebracht.

Lisa, Nora, Daniel Gerulf und Bettina: Die Zeit mit euch hat mir gezeigt, wie wertvoll es ist, in einem Team zu sein, das während dem PhD gemeinsam an einem Strang zieht. Ihr seid weitaus mehr als nur Arbeitskolleg:innen für mich und ich schätze jede:n Einzelne:n von euch sehr. Danke für die vielen gemeinsamen Stunden in der Boulderhalle, die unzähligen Stunden an Brettspieleabenden, die unvergesslichen Urlaube in Norwegen, Kalifornien, Stockholm, Amsterdam und New York, die Besuche in den vielen Museen mit all den Kunstwerken, die mir sonst verborgen geblieben wären, die gemeinsamen Feierabendbiere und vor allem dafür, dass ich mich immer auf euch verlassen kann. Darauf erstmal eine Berliner Luft!

Dank geht auch an A. Sch., die mir geholfen hat ein Band der Freundschaft mit meiner Doktorarbeit zu knüpfen.

Unendlich viel Dank auch an Konstantin, der mit Tito (und Rita) während meiner Doktorarbeit in mein Leben getreten ist, dort ganz viel Konfetti verstreut, Karussell mit mir fährt und zu einem meiner größten Unterstützer geworden ist.

Der größte Dank geht an meine Eltern Gerhard und Aleksandra, sowie an meine Schwestern Aldona, Alina, Anna und Agnes. Danke für eure bedingungslose Unterstützung in allen Phasen meines Lebens.